"Vertically generated and horizontally acquired variation could be viewed as the yin and the yang of the evolutionary process"

- Carl R.Woese

University of Alberta

Characterization of Plasmid-Encoded Proteins that Mediate or Inhibit R27 Conjugative Transfer

by

James Eric Gunton ©

A thesis submitted to the Faculty of Graduate studies and Research in partial fulfillment
of the requirements for the degree of Doctor of Philosophy

in

Bacteriology

Department of Medical Microbiology and Immunology

Edmonton, Alberta
Spring, 2006

Library and
Archives Canada

Published Heritage
Branch

395 Wellington Street
Ottawa ON K1A 0N4
Canada

Bibliothèque et
Archives Canada

Direction du
Patrimoine de l'édition

395, rue Wellington
Ottawa ON K1A 0N4
Canada

Your file Votre référence
ISBN: 0-494-13980-3
Our file Notre référence
ISBN: 0-494-13980-3

NOTICE:
The author has granted a non-exclusive license allowing Library and Archives Canada to reproduce, publish, archive, preserve, conserve, communicate to the public by telecommunication or on the Internet, loan, distribute and sell theses worldwide, for commercial or non-commercial purposes, in microform, paper, electronic and/or any other formats.

The author retains copyright ownership and moral rights in this thesis. Neither the thesis nor substantial extracts from it may be printed or otherwise reproduced without the author's permission.

AVIS:
L'auteur a accordé une licence non exclusive permettant à la Bibliothèque et Archives Canada de reproduire, publier, archiver, sauvegarder, conserver, transmettre au public par télécommunication ou par l'Internet, prêter, distribuer et vendre des thèses partout dans le monde, à des fins commerciales ou autres, sur support microforme, papier, électronique et/ou autres formats.

L'auteur conserve la propriété du droit d'auteur et des droits moraux qui protège cette thèse. Ni la thèse ni des extraits substantiels de celle-ci ne doivent être imprimés ou autrement reproduits sans son autorisation.

In compliance with the Canadian Privacy Act some supporting forms may have been removed from this thesis.

While these forms may be included in the document page count, their removal does not represent any loss of content from the thesis.

Conformément à la loi canadienne sur la protection de la vie privée, quelques formulaires secondaires ont été enlevés de cette thèse.

Bien que ces formulaires aient inclus dans la pagination, il n'y aura aucun contenu manquant.

Canada

University of Alberta

Faculty of Graduate Studies and Research

The undersigned certify that they have read, and recommended to the Faculty of Graduate Studies and Research for acceptance, a thesis entitled Characterization of Plasmid-Encoded Proteins which Mediate or Inhibit R27 Conjugative Transfer by James Eric Gunton in partial fulfillment of the requirements for the degree of Doctor of Philosophy in Bacteriology.

____

Dr. Diane Taylor

____

Dr. Laura Frost

____

Dr. Bart Hazes

____

Dr. Phil Silverman

____

Dr. Mark Peppler

____

Date

For my beautiful wife Karen, my daughter Ella,
and my parents, John and Pat Gunton.

ABSTRACT

Bacterial conjugation is a mechanism of horizontal gene transfer that requires the intimate association of donor and recipient cells. There are three multiprotein complexes which mediate the transfer of plasmid DNA into neighbouring bacteria: a membrane-spanning Mpf complex, the cytoplasmic-associated relaxosome and a hexameric coupling protein. The link between the Mpf complex and the relaxosome is provided by the coupling protein. An interaction between the IncHI1 plasmid R27 Mpf complex and coupling protein has been previously identified through bacterial two-hybrid and immunoprecipitation studies. Using these techniques, an interaction was detected between the R27 coupling protein TraG and TraJ, an essential conjugative protein that was originally classified as a relaxosome component. A module encoding TraG and TraJ has been found to be co-inherited in a number of plasmid and chromosomal genomes. Homologues of TraG and TraJ from a variety of these genomic sources were found to interact. Furthermore, limited homology has been identified between the transmembrane and nucleotide binding domains of the SpoIIIE/FtsK family of DNA translocases and TraJ and TraG, respectively. TraJ has been reclassified as an accessory protein to the R27 coupling protein TraG.

Site specific mutagenesis and immunofluorescent (IMF) microscopic studies on the R27 coupling protein have identified functional domains and cellular localization of this conjugative protein. Essential residues of TraG within the nucleotide binding domain were determined and the periplasmic domain of the coupling protein was found to mediate an interaction with the Mpf protein TrhB. The R27 coupling protein was visualized within discrete, membrane-associated foci using IMF microscopy. The number and position of these foci were comparable to the fluorescent foci produced by the GFP-labeled R27 Mpf complex.

The R27 proteins EexH and TrhZ have been found to prevent the redundant transfer of IncH plasmid into recipient cells harbouring the isogenic or closely-related IncH plasmids. The two R27 Entry exclusion proteins EexH and TrhZ were determined to localize to the outer and inner membrane, respectively. Mutational analyses of the R27 exclusion genes have indicated that a functional exclusion protein is required in the donor cell to elicit an exclusion process. In conclusion, this thesis has characterized proteins which mediate or inhibit R27 conjugative transfer.

ACKNOWLEDGEMENTS

I would like to extend my deepest gratitude to my PhD supervisor Dr. Diane Taylor who has been a source of constant support over the past five years. Dr. Taylor was recommended to me upon completion of my studies at the University of Victoria, and I am thankful to Dr. Nano for the advice. The method of supervision that Dr. Taylor utilizes with her graduate students encourages independent thinking and self-motivation. These are skills I will carry with me in future academic endeavors.

I thank my graduate committee of Dr. Laura Frost and Dr. Bart Hazes. Our meetings were insightful and I was always treated as a peer. Each committee member extended an open-door policy to me and these individual sessions were instrumental in shaping my experimental design. I would like to thank the additional members of my examination committee Dr. Philip Silverman and Dr. Mark Peppler. I would also like to thank the Alberta Heritage Foundation for Medical Research (AHFMR), Alberta Learning Ministry, and the University of Alberta for funding my research.

To the members (current and former) of Dr. Taylor's laboratory, you have made coming into work each day an enjoyable experience. Dr. Taylor carefully selects technicians and I have reaped the benefits of working in a well-run laboratory over the past five years. My summer students John Ussher and Dan Kobewka offered me new perspective on old scientific problems. The re-emergence of IncH into current plasmid literature is a direct result of the collaborative efforts of the H plasmid boys- Trevor Lawley, Matt Gilmour, Dobryan Tracz and I. It is my hope that we maintain contact outside the world of science.

Inherent in completing a PhD thesis are weekly trials and tribulations- it is friends and family which ensure that life is bearable when these problems seem insurmountable. I owe a great deal to my Edmonton friends: Sebastien and Carmen Gittens, Marc Couturier, JP Bacik, Jennifer Horton, Bing Ma, Matt and Sue Gilmour, Trevor and Bronwyn Lawley, Aaron and Angela Millar, Adam Hrdlicka, Dan Kobewka and John Ussher. I must also thank my adopted Edmonton family: Ken and Leanne Haltiner, Grandma and Grandpa Dutka, Larry, Shelley and Hordo Yuskow, Nancy Dutka, Ray and Janice Little, Glen, Lana, Evan and Jaron Haltiner.

I have been blessed with a close family who provide unconditional support. My parents John and Pat Gunton have instilled in me a love of science and learning which is necessary when an experiment fails for the third time. My brothers Sean and Matt, we find ourselves separated around the globe but spatial proximity means little with family.

Finally, I wish to thank my wife and closest friend Karen, and my baby daughter Ella. You both had to listen to hours of scientific problems, wait in cars as plates were pulled, or watch as cultures were inoculated. The completion of this PhD is a testament to the strength of our growing family.

TABLE OF CONTENTS

1. General Introduction....2
   - 1.1 Tree of life....2
   - 1.2 Horizontal Gene Transfer....2
     - 1.2.1 Transformation....5
     - 1.2.2 Transduction....7
     - 1.2..3 Conjugation....8
   - 1.3 Plasmids....8
     - 1.3.1 IncF1....9
     - 1.3.2 IncW....10
     - 1.3.3 IncPα....11
     - 1.3.4 IncH....12
   - 1.4 Type IV Secretion System....13
     - 1.4.1 T4SS and bacterial pathogenesis....16
     - 1.4.2 Mating pair formation complex....18
     - 1.4.3 T4SS ATPases....19
   - 1.5 Coupling proteins....21
     - 1.5.1 Coupling protein structural and sequence similarities....22
     - 1.5.2 Nucleotide/ATPase Activity....25
     - 1.5.3 Coupling protein Interactions....25
   - 1.6 Relaxosome/Accessory proteins....26
   - 1.7 Plasmid encoded barriers to HGT....27
     - 1.7.1 Entry exclusion....28
   - 1.8 Objectives....29

2. An accessory protein, TraJ, associated with the coupling protein is unique to the H plasmid-type conjugative DNA transfer system....31
   - 2.1 Introduction....32
   - 2.2 Experimental Procedures....36
     - 2.2.1 Bacterial Strains and Growth Conditions....36
     - 2.2.2 DNA Manipulation and Cloning....36
     - 2.2.3 Protein Expression of Coupling Proteins Homologs....36
     - 2.2.4 Conjugation Assay....41

2.2.5 Bacterial Two-Hybrid (BTH) ... 41

2.2.6 Immunoprecipitation ... 42

2.2.7 Phylogenetic analysis ... 42

2.2.8 Web-based computer programs ... 43

2.3 Results ... 44

2.3.1 *In vivo* Detection of the R27 TraG and TraJ Interaction ... 44

2.3.2 Immunoprecipitation of a TraG and TraJ complex ... 47

2.3.3 Coupling Proteins Determine the Specificity of Interactions with T4SS and Relaxosome/Accessory Components. ... 50

2.3.4 Functional Co-Inheritance of TraJ and TraG Homologs ... 54

2.4 Discussion ... 65

3. Subcellular localization and functional domains of the coupling protein, TraG, from Incompatibility H1 plasmid ... 74

3.1 Introduction ... 75

3.2 Experimental Procedures ... 77

3.2.1 Bacterial strains, growth conditions and plasmids ... 77

3.2.2 RNA extraction. ... 79

3.2.3 Reverse transcriptase-Polymerase chain reaction (RT-PCR) ... 79

3.2.4 Site-directed mutagenesis of Walker A and B motifs of TraG ... 81

3.2.5 Insertional mutagenesis of traG on drR27 ... 81

3.2.6 Conjugation ... 82

3.2.7 Immunofluorescence (IMF) microscopy ... 82

3.2.8 Bacterial Two-Hybrid System ... 83

3.2.9 Immunoprecipitation ... 83

3.2.10 Web-based computer programs ... 84

3.3 Results ... 84

3.3.1 Temperature-dependent transcription of *traG* ... 84

3.3.2 Generation of NTP-binding motif mutations in *traG* ... 85

3.3.3 Mutations in the NTP-binding motifs of TraG inhibit plasmid transfer ... 88

3.3.4. Production and stability of TraG$_{His6}$ containing mutations within the Walker A and B regions ... 92

3.3.5. The TraG periplasmic residues are essential for an interaction with TrhB......93
3.3.6 The R27 coupling protein forms membrane-associated fluorescent foci......101
3.4 Discussion......109

4. Entry exclusion in the IncHI1 plasmid R27 is mediated by TrhZ and EexH......116
4.1 Introduction......117
4.2 Experimental Procedures......119
4.2.1 Bacterial strains, growth conditions, and plasmids......119
4.2.2 Reverse transcriptase PCR (RT-PCR)......119
4.2.3 Entry Exclusion (EEX) Studies......119
4.2.4 DNA Manipulations and Mutagenesis......122
4.2.5 Bacterial Fractionation......123
4.2.6 Electron Microscopy......124
4.2.7 Web-based computer programs......124
4.3 Results......124
4.3.1 EexH and TrhZ mediate entry exclusion activity of the R27 plasmid......124
4.3.2 Temperature-dependent transcription of Z operon......127
4.3.3 Effect of R27 entry exclusion proteins on the transfer of related and non-related conjugative plasmids......132
4.3.4 Localization of TrhZ and EexH in the bacterial cell......133
4.3.5 Do the R27 entry exclusion proteins interact with themselves?.139
4.4 Discussion......141

5. General Discussion......153
5.1 Bacterial Conjugation......154
5.2 Mediators of R27 HGT......155
5.2.1 Future Studies on the R27 Conjugative Apparatus......162
5.3 Inhibitors of R27 HGT......166

5.3.1 Future Studies on R27 Eex proteins....171

Bibliography....173

List of Tables

Table 1-1. Summary of conjugative proteins from IncP, IncW, InF, IncH plasmids..20

Table 2-1. Bacteria and Plasmids Used in This Study..........37
Table 2-2. Primers Used in This Study..........39
Table 2-3. Conjugation results from complementation experiments of coupling protein mutations with cognate and non-cognate coupling proteins........57

Table 3-1. Bacteria and plasmids used in this study..........78
Table 3-2. Primers used for RT-PCR analysis of the transcriptional profile and mutational analyses of the *traG* gene of R27..........80
Table 3-3. Complementation of pDT3152 with pJEG217 or Walker A or B mutant derivatives of pJEG217..........91
Table 3-4. Complementation of pDT3152 with pJEG217 and a TraG:S4 construct, pMWG385..........104
Table 3-5. Immunofluorescence data representing the effect of temperature and additional R27 proteins on the subcellular localization of $\text{TraG}_{\text{His6}}$.........108

Table 4-1. Bacterial Strains and Plasmids used in this study..........120
Table 4-2. Primers used in this study to clone the genes of the Eex operon and for transcriptional analysis of the Eex operon..........121
Table 4-3. R27 Cosmid library screen for entry exclusion activity..........126
Table 4-4. Specificity of the Entry Exclusion process mediated by TrhZ and EexH..........134
Table 4-5. Summary of entry and surface exclusion genes from Gram-negative plasmids..........135
Table 4-6. Entry exclusion by TrhZ and EexH require that donor cells contain R27 exclusion protein for exclusion activity..........140

List of Figures

Figure 1-1. Circular map of the IncHI1 plasmid R27 (180 401bp) representing each ORF......15
Figure 1-2. The coupling protein phylogeny......24

Figure 2-1. *In vivo* bacterial two-hybrid interactions between the R27 coupling protein, TraG, and R27 transfer proteins TraJ and TrhB......46
Figure 2-2. Co-immunoprecipitation of an IncH R27 TraJ-TraG complex......49
Figure 2-3. Bacterial-two hybrid interaction data demonstrating the diversity and specificity of coupling protein interactions......52
Figure 2-4. Expression profile of coupling proteins from the R27, RP4, R388 and F plasmids from the IncH, IncP, IncW and IncF families, respectively......56
Figure 2-5. Summary of protein interactions between VirB10-homolog TrhB, coupling proteins, relaxosome proteins, and the coupling protein accessory protein......59
Figure 2-6. The TraJ protein phylogeny......61
Figure 2-7. Bacterial two-hybrid data demonstrating the conservation of the interaction between TraJ and TraG homologs......64
Figure 2-8. Genetic organization of the *traJ* and *traG* homologous sequences from five plasmids, one conjugative, and eight chromosomes......69

Figure 3-1. RT-PCR analysis of the co-transcription of R27 *traG* gene with the adjacent genes, *traI* and ORF 118......87
Figure 3-2. Alignment of Walker A and Walker B boxes from coupling proteins from R27......90
Figure 3-3. Production and stability of pJEG217 and pJEG217 constructs containing mutations within the Walker A or Walker B regions, expressed from DY330R harbouring pDT3152......95
Figure 3-4. The N terminus of the coupling proteins from R27 (TraG), R388 (TrwB), F(TraD) and RP4 (TraG)......97
Figure 3-5. *In vivo* bacterial two-hybrid interaction data......100
Figure 3-6. Co-immunoprecipitation of TraG and not a TraG:S4 construct by the R27 Mpf protein, TrhB......103

Figure 3-7. Subcellular localization of TraG$_{\text{His6}}$ from R27 107

Figure 4-1. Open reading frame map of the Tra2 region of R27, with an enlarged map of the operon encoding the entry exclusion proteins TrhZ and EexH of R27 129
Figure 4-2. Transcriptional analysis of the Z operon 131
Figure 4-3. TrhZ and EexH localize to the inner and outer membrane, Respectively 138
Figure 4-4 Electron microscopic images of RG11 transconjugant cells expressing TrhZ 143
Figure 4-5 Electron microscopic images of RG11 transconjugant cells 145
Figure 4-6. Alignment of the R27 entry exclusion protein 150

Figure 5-1. Model for the structural arrangement of the R27 conjugative apparatus 159
Figure 5-2. Alignment of the Walker B motifs from coupling proteins from R27 (TraG), R478 (TraG), R391 (TraD), SXT (TraD), Ti (VirD4), R388 (TrwB), F (TraD), and RP4 (TraG) 165
Figure 5-3. Schematic representation of the entry exclusion phenomenon in the R27 plasmid 170

List of Abbreviations

ABC	ATP-binding cassette
Ap	ampicillin
ATP	adenosine triphosphate
BLAST	basic local alignment search tool
Bp	base pair
BSA	bovine serum albumin
BTH	bacterial two-hybrid
C	carboxy
Cm	chloramphenicol
DNA	deoxyribonucleic acid
Dr	derepressed
DTT	dithiothreitol
EDTA	ethylene-diaminetetra-acetic acid
Eex	entry exclusion
GFP	green fluorescent protein
HRP	horseradish peroxidase
ICE	integrative chromosomal element
IMF	immunofluorescence
IPTG	isopropyl-β-D-thiogalactoside
Inc	incompatibility group
Km	kanamycin
LB	Luria Bertani
Mpf	Mating pair formation
N	amino
Nal	nalidixic acid
NTP	nucleotide triphosphate
NCBI	National Centre for Biotechnology Information
OD	optical density
ORF	open reading frame
PBS	phosphate buffered saline
PCR	polymerase chain reaction
Rif	rifampicin

RNA	ribonucleic acid
SDS-PAGE	sodium dodecyl sulfate polyacrylamide gel ectrophoresis
Sm	streptomycin
T2SS	type two secretion system
T3SS	type three secretion system
T4SS	type four secretion system
TM	transmembrane
Tp	trimethoprim
Tra1	transfer region 1
Tra2	transfer region 2
UV	ultraviolet
WT	wild type
X-gal	5-bromo-4-chloro-3-indoyl-β-D-galactopyranoside

Chapter 1

General Introduction

1. Introduction

1.1 Tree of Life

The three domains of life are the Eucarya, the Bacteria and the Archaea (216). The method by which these major domains evolved remains a contentious issue with three hypotheses proposed to explain the divergence. One proposal suggests that pre-eucarya were formed through the acquisition of a cytoskeleton, thus diverging from the Bacteria and Archaea (collectively called prokaryotes). Subsequently, phagocytosis of a prokaryote by the pre-eucarya resulted in the formation of Eucarya (48, 86). A second hypothesis also involves a phagocytic event, but this evolutionary model contends that the inclusion of the Archaea within the Bacteria resulted in the formation of a nucleus, thereby creating the Eucarya (93). A final hypothesis suggests that from the "ancestral chaos" three different cell types, representing the three domains of life, evolved in communal fashion as a result of extensive gene sharing. (215). With the ever-increasing access to whole genome information of organisms representing each domain of life, a solution to determining the root of the phylogenetic relationship may be on the horizon (47). Ultimately, tracing the tree of life back to its origin should theoretically identify a common ancestral cell type. A major impediment to determining this origin is the "blurring" of the phylogenetic lines by horizontal (or lateral) gene transfer (HGT or LGT) (47). The influence of HGT on phylogenetic classification has led to a proposal for a switch from the Tree of Life to the Synthesis of Life, which accounts for both vertical and horizontal genetic inheritance (15).

1.2 Horizontal Gene transfer (HGT)

Within prokaryotes, HGT has been proposed to be so common that this process is a major force in the evolution of the Archaea and Bacteria domains (49). A recent genomic comparison of uropathogenic *Escherichia coli* revealed 20-30% variation in genomic content due to HGT (209). The boundaries between prokaryotic species have been classified as "fuzzy", when compared to eukaryotes, therefore HGT in combination with homologueous recombination has been proposed to emulate the role that sexual reproduction plays for eukaryotic organisms (70, 113). Bacteria and Archaea reproduce by binary fission, a process in which a mother cell separates into two daughter cells with faithful segregation of genetic material to each progeny. In comparison to the diploid, obligately sexual eukaryotic organisms, gene exchange in prokaryotic organisms is extremely limited (113). As a result, the expectation would be generations of clonally proliferated cells with any significant genetic differences in these prokaryote organisms arising from point mutations, or random insertions or deletions. Early genomic investigation into *E. coli* chromosomes seemed to confirm this expectation (148, 149), however, in the 1980's with the expanded databank of nucleotide sequence information becoming available, the true impact of HGT was fully realized. In 2003, Doolitte *et. al.* described a variety of anecdotal HGT examples and posed the question, are these cases just the tip of the iceberg with respect to the role that HGT has in evolution? (49). Interestingly, an answer to this question has been provided by systematic studies of entire genome sequences; phylogenetic anomalies that were found in genomic screens were attributed to deletions and biased mutation rates and not HGT (for review see (105)).

Whereas the evolutionary role that HGT may have is under debate, the impact of HGT on the medical community is indisputable. From a medical perspective, the implications of HGT were first realized with the dissemination of antibiotic resistance determinants (42). The first recorded case of gene exchange resulting in the development of antibiotic resistance was in 1959. Through "infective heredity" genes encoding multiple drug resistance were exchanged between Shigella and *E.coli* (204). In addition to multiple drug resistance genes, HGT has also resulted in the transmission of gene clusters or operons that encode entire biodegradation pathways for xenobiotics (for review, see (43)). A third medically relevant HGT event is the transmission of pathogenicity islands (PAI). The acquisition of large genomic fragments such as a PAI can represent an evolutionary leap when compared to the slow evolutionary result of point mutations. The presence of a PAI within the chromosome of a bacterial organism is usually the primary difference between non-pathogenic bacteria of the same species (82). Pathogenicity islands can range up to 200 kb in size and the G + C content of this region is usual markedly different than the nucleotide composition of the host genome Other characteristics of PAIs include terminal inverted repeats and mobility genes such as transposases or integrases (82).

An interesting field in the study of HGT is the investigation into genetic exchange *in situ*. A number of environmental factors such as pH, moisture content and soil type have been cited as influencing the rate of HGT in terrestrial environments (162, 163). In addition to the difficulty of determining the influence of environmental factors on genetic exchange, an added difficulty in ascertaining the levels of HGT within the environment is the presence of non-culturable organisms. In one particular study, the percentage of culturable organisms within the terrestrial environment was determined to be <1% (196). The presence of numerous viable organisms within the environment which are unable to be grown under laboratory conditions makes the study of HGT *in situ* increasingly complex.

One of the most significant hotspots for HGT to occur within nature are biofilms (180). Biofilms are highly-populated bacterial communities that are encased in a self-produced matrix that confers resistance to antimicrobials and host defense mechanisms (22, 62, 64). The extra-cellular polymeric substance (EPS) that forms a barrier around the surface-attached microbial communities is composed of exopolysaccharides, proteins and DNA (183, 184). Interestingly, the presence of DNA within these biofilms not only increases the chance of an HGT event, but the extra-cellular DNA was also found to play a structural role in biofilm formation (211). Biofilms are reported to be present in more than 60% of infections requiring antibiotic treatment in the developed world (36). A further complication associated with these biofilms is that antimicrobial treatment with aminoglycosides has been demonstrated to induce the formation of biofilms in *E.coli* and *Pseudomonas aeruginosa* (91).

HGT has been elegantly demonstrated within biofilms using confocal laser scanning microscopy to visualize gene transfer in strains labeled with green fluorescent protein (GFP) (64, 89, 219). In a landmark study (65) the presence of conjugative plasmids, mobile genetic elements that mediate HGT, within the laboratory *E.coli* strain K-12 were found to enhance biofilm formation (65, 161). These results suggest that mobile genetic elements are able to induce a phenotypic change (the formation of a biofilm) in host cells, which increases the probability of an HGT event.

There are three mechanisms of HGT; transformation, transduction, and conjugation.

1.2.1 Transformation

Natural transformation is the uptake of naked DNA from the extracellular environment by competent bacteria (for a review, see (31)). Whereas it is possible to induce competence in an organism by electroporation or chemical treatment, natural transformation is conferred by bacteria that express a specific set of 20-50 competence proteins (193). Currently, there are over 40 bacterial species that are naturally transformable (125). The earliest recorded example of HGT was a landmark study in which avirulent *Streptococcus pneumoniae* were transformed by DNA encoding a virulence determinant thereby conferring a virulent phenotype to recipient cells; these studies enabled the identification of DNA as a bearer of genetic information (12).

The first step in the natural transformation process is the binding of extracellular DNA which initiates the transport of foreign DNA across the cellular envelope. The majority of competent bacteria are able to bind DNA non-specifically; however two exceptions are *Haemophilus influenza* and *Neisseria gonorrhoeae*. These two Gram negative organisms are only able to take up DNA containing DNA uptake sequences (74, 177). The multiprotein complex that mediates the transport of foreign DNA across the membranes of the bacterial cell is part of either the type II or type IV secretion systems (T2SS or T4SS). A common feature of the majority of Gram negative and Gram positive competent bacteria is the requirement for the T2SS and the Type IV pilus (50, 197). Notably, the only known organisms that encode a T4SS to mediate natural transformation are *Helicobacter pylori* and *Campylobacter jejuni* (13, 92).

Upon translocation of foreign DNA across the bacterial envelope of Gram positive organisms, one strand of the DNA gets degraded and released into the exterior milieu (50). A similar process is thought to occur within Gram negative organisms however the DNA nuclease which results in a single-strand of foreign DNA entering the cytosol has not been identified (50).

The advantage that competence confers to a bacterial organism is currently a matter of debate. Natural transformation potentially results in genetic variability within competent bacteria which may lead to increased genomic fitness (50). Conversely, the uptake of foreign DNA has been proposed as a method employed by bacteria to acquire a valuable nutrient source (160). A recent transcriptional study on the operon of *H. influenzae* that encodes for competence proteins has indicated that alteration of *H. influenzae* energy supply signals had a significant impact on the expression of competence genes (159). These data support the proposed role of natural transformation in the acquisition of nutrients.

1.2.2 Transduction

Transduction is a mechanism of HGT mediated by bacteriophages (or phages). Bacteriophages are viral parasites that can exist outside the bacterial cell as a virion, but are obligate intracellular parasites that require host cell machinery for replication. During replication and packaging within the protein capsid, accidental incorporation of host DNA fragments can result in the potential for a gene transfer event (generalized transduction). Conversely, a prophage is able to insert within the host genome thereby introducing the possibility of incorporating host DNA adjacent to the phage insertion site (specialized transduction) (60, 147). There are limitations on the amount of foreign DNA that can be packaged into the capsid, however certain phage capsids can contain upwards of 100kb of DNA (147). Bacteriophage initiate the infection of a bacterial cell with a specific interaction to a receptor structure on the cell surface; the receptor structure is frequently a host or plasmid-encoded pilus (76, 132). The specificity of the phage-cell structure interaction enables the typing of phage. Phage specificity has also been used as a tool by diagnostic laboratories to identify bacterial species within mixed bacterial populations (210).

The sheer number of viruses within the environment, in combination with the aforementioned virus-encoded HGT mechanism, suggests that these "life forms" have played a role in shaping microbial evolution (207). Within the ocean, the population of viruses is thought to exceed 10^{29} (213). A prime example of the impact of viruses on bacterial diversity is the drastic phenotypic change elicited by infection of *Vibrio cholera* with the well-characterized filamentous phage CTXφ. The CTXφ genome encodes the cholera toxin, which is the causative agent of the diarrhea commonly associated with *V. cholera* infection (132). The *V. cholera*-encoded type IV bundle forming pilus is the receptor to which CTXφ binds, thus initiating the infection (132). The CTXφ virion interacts with the TolQRA complex located in the periplasm and inner membrane (90). A replicative form of the virus, pCTXφ, is formed when a complementary copy is produced by host-encoded replication machinery. Although pCTXφ can exist outside the *V. cholera* chromosome, host-encoded integration proteins mediate the integration into a specific site in the chromosome in most *V. cholera* strains (95). The phage enters into a lysogenic state upon integration, and virion production is induced with DNA damaging agents such as UV light (201). Interestingly, secretion of CTXφ virions does not induce cell lysis and also requires host-encoded proteins for export into the exterior milieu. This dynamic interplay between bacteria and phage has resulted in the conversion of *V. cholera* into a pathogenic organism that causes morbidity and mortality in developing countries (53).

1.2.3 Conjugation

Conjugation was first described as a cell fusion event that enabled the transfer of genetic information between donor and recipient cells. These first conjugation experiments, performed in 1946 by Joshua Lederberg and Edward Tatum, utilized donor and recipient cells containing double mutants in essential nutritional genes (114). Successful gene exchange allowed for the selection of transconjugants that had no nutrient requirements (114). Conjugation is mediated by transmissible plasmids or by integrative and conjugative elements (ICE) which are transmissible by conjugation and are chromosomally-associated (24). Conjugative plasmids and plasmid-encoded multiprotein complexes that mediate the conjugative event are discussed in greater detail in the following sections.

1.3. Plasmids

Mobile genetic elements are pieces of DNA that encode proteins that facilitate the genetic transfer between bacterial cells (for review see (60)). There are numerous examples of mobile DNA elements such as bacteriophages, transposons, integrated conjugative elements and plasmids. Plasmids have been discovered in Gram negative and Gram positive members of the bacterial domain. Whereas there have been recent advances in the study of Gram positive bacterial plasmids (for review see (77)), the majority of the research on plasmid biology has been performed on Gram negative plasmids. The focus of this thesis will be on Gram negative plasmids, with a specific emphasis on the IncH plasmid R27. Plasmids are extra-chromosomal genomes that are commonly double stranded and can encode transfer proteins that mediate HGT to neighbouring bacteria. Conjugative plasmids range in size from 30 to 300 kb and, a common core of genes, the plasmid backbone, is shared among all to ensure plasmid survival within the host (195). The plasmid backbone is composed of replication, conjugation and partitioning determinants (192, 195). This core set of backbone genes encode proteins required for the lifecycle of the conjugative plasmid; the concept of a conjugative lifecycle incorporates both vertical and horizontal inheritance in the bacterial population (107).

Plasmids have been classified into groups on the basis of incompatibility (Inc). Incompatibility is defined as the inability of two related plasmids to co-exist in the same host cel in the absence of selective pressurel (144). Incompatibility between two plasmids is mediated by shared replication functions (144) and/or partitioning modules (11). There are 26 incompatibility groups within Enterobacteriaceae plasmids, ~ 14 incompatibility groups within Pseudomonad plasmids, and ~18 incompatibility groups within Gram positive plasmids (60). Throughout this thesis, references are made to Gram negative conjugative plasmids from a number of Inc groups. Therefore, a brief description of these plasmid families is included below.

1.3.2 IncF1

The F plasmid is a paradigm for the conjugative transfer of Gram negative plasmid (110). As bacterial conjugation was initially identified as a function of the F plasmid, study of the IncF1 plasmid has been instrumental in identifying the mechanistic process of replication and HGT with the conjugative plasmid (59). As the F plasmid is only able to replicate in *Enterobacteriaceae*, the IncF plasmid is considered a narrow host-range mobile element (40). The F plasmid is 100 kb in size and this genetic element contains a single transfer region 33.3 kb in size, which codes for all essential transfer proteins (59). Within the F transfer region 19 of the 40 genes have been determined to be required for conjugative transfer.

Studies carried out in the 1970 to 1980's on the F plasmid were the first to identify the role of conjugative pili in this mechanism of HGT (for a review see (214)). Conjugative F pili encoded by the F plasmid have been determined to be essential for making initial contact with recipient cells and mediating a retraction event that brings the donor and recipient cells into close proximity (214).

1.3.3 IncW

Unlike the host range of the IncF plasmid, the IncW plasmids have a broad host range and are able to replicate within a number of Gram negative organisms (121). The prototypical IncW plasmid is R388. This 33 kb conjugative plasmid contains a small transfer region of 14.9 kb, of which a 5.2 kb segment was found to identify the three DNA mobilization proteins, TrwA, TrwB and TrwC (18, 121). The R388-encoded proteins required for pilus formation have not been characterized, but the three aforementioned DNA mobilization proteins have been extensively characterized.

The TrwB protein is the coupling protein of the R388 conjugative apparatus, and purification of the cytoplasmic domain of this protein enabled crystallization and biochemical analyses, which represent significant advancements in the field of plasmid biology (see 1.5 Coupling proteins).

TrwC is the nickase-helicase that binds to the R388 origin of transfer (*oriT*) and TrwA enhances this relaxase activity. Homology between TrwA and DNA binding proteins belonging to the Ribbon-Helix-Helix (RHH) family has been recently identified, which may suggest a mechanism by which TrwA elicits the relaxase enhancement activity (138). Structural information on the N-terminal region of the R388 nickase protein has enabled the identification of domains that enable relaxase function (9).

1.3.4 IncPα

The IncP plasmid family has a very broad host range with documented cases of transfer between Gram negative and Gram positive organisms, as well as with eukaryotic cells (153, 205). The ability of IncP plasmids to mobilize between bacterial species has been exploited in the development of vectors (81). In the study of conjugation, the prototypical IncPα plasmid is RP4, a 60.1 kbp genetic element containing two separate transfer regions (153). The Tra1 and Tra2 regions of RP4 comprise 15.7 kb of the plasmid and contain 19 genes (118). These two regions encode 12 proteins essential for pilus formation, a coupling protein, and three relaxosomal proteins (118).

Localization studies on the RP4 essential transfer proteins have indicated that the T4SS structural proteins localize to an "intermediate" fraction with a density in between that of the inner and outer membrane (75). These data suggest that the T4SS form a complex which binds the inner and outer membrane together which may be instrumental for the delivery of DNA to recipient cells. As in the study of the IncW R388 plasmid, there has been extensive research on the RP4 coupling protein, TraG, and relaxosomal proteins, TraI, TraJ and TraK (169, 171). The biochemical analyses of the

RP4 relaxase, TraI, and coupling protein, TraG, have determined residues which are essential for the mobilization of IncP DNA (14). These mutational studies have been instrumental in determining the initial stages of conjugation of self-transmissible plasmids.

1.3.5 IncH

IncH plasmids were initially identified in 1972 following an outbreak of chloramphenicol-resistant typhoid fever in Mexico (6). The H plasmid family is classified into the subgroups IncHI and IncHII. IncHII plasmids are compatible with IncHI plasmids and produce pili that are antigenically similar to pili of the IncHI plasmid (20). The IncHI family was subsequently subdivided into IncHI1, IncHI2 and IncHI3 following studies such as restriction digest and Southern hybridization analysis that showed significant differences within IncHI plasmids (212). The presence of an RepFIB replicon in IncHI1 plasmids differentiates this plasmid subgroup from IncHI2 plasmids as it causes one-way incompatibility with the F plasmid (178). The presence of IncHI1 plasmids in *Salmonella typhi* strains conferred chloramphenicol resistance on these pathogenic bacteria. As chloramphenicol was the drug of choice to treat *S. typhi*, the IncHI1 plasmid contributed to the emergence of typhoid fever epidemics throughout Mexico, India, Thailand and Vietnam (179). Moreover, multiple-drug resistant *S. typhi* strains harbouring IncHI1 plasmids have been isolated in Pakistan (173) and India (172). Within North America, drug resistant *S. typhi* strains have been isolated from travelers returning from South Asia (84).

A characteristic of IncHI1 and IncHI2 plasmids is that optimal conjugative transfer occurs between 26 °C and 30 °C, with a significant reduction in transmission frequency at 37 °C (189). Conjugative temperature-sensitivity within the IncHI plasmid family is mediated at the transcriptional level; transcriptional analysis of the prototypical IncHI1 plasmid R27 indicated that expression of multiple transfer genes is repressed at 37°C (5, 57, 67, 78).

The complete nucleotide sequence has been determined for the IncHI1 plasmids R27 (180 Kb) and pHCM1 (218 kb), as well as for the IncHI2 plasmid R478 (275 kb) (69, 155, 176). As expected, the regions of highest similarity between these three IncH plasmids are found within the plasmid backbone sequence (69). The R27 plasmid encodes two independent partitioning modules that ensure the faithful segregation of the IncH plasmid during vegetative replication (111). Analogous to the IncP plasmids, IncH plasmids contain two separate transfer regions (Fig. 1-1); functional and mutational analysis of the R27 plasmid Tra1 and Tra2 region has identified 20 genes that encode essential transfer proteins (108, 109, 164). The R27 plasmid encodes a coupling protein, an accessory to the coupling protein, two relaxosomal proteins, and 16 proteins that are required for the production of H-pili on the cell surface (108, 109, 164). A recent transcriptional study on R27 has revealed that each transfer region contains three operons (5).

1.4 T4SS

The Gram negative cellular envelope represents a significant barrier to macromolecular export or import. The combination of the inner and outer membrane with an intervening peptidoglycan layer necessitates the aggregation of protein complexes to circumvent this physical barrier. Gram negative bacteria have evolved multiple secretion pathways which can be classified into six groups (for review see (191)). The type IV secretion system (T4SS) forms a translocation conduit that enables DNA or protein transport into neighbouring bacterial or eukaryotic cells (for recent reviews see (34, 170)). The T4SS can be classified into three subfamilies: conjugative systems, DNA uptake and release systems, and effector translocation systems (29). The components

Figure 1-1. Circular map of the IncHI1 plasmid R27 (180 401bp) representing each ORF. The outer ORFs are transcribed in counter-clockwise direction and inner ORFs are transcribed in a clockwise direction. Adapted from (175).

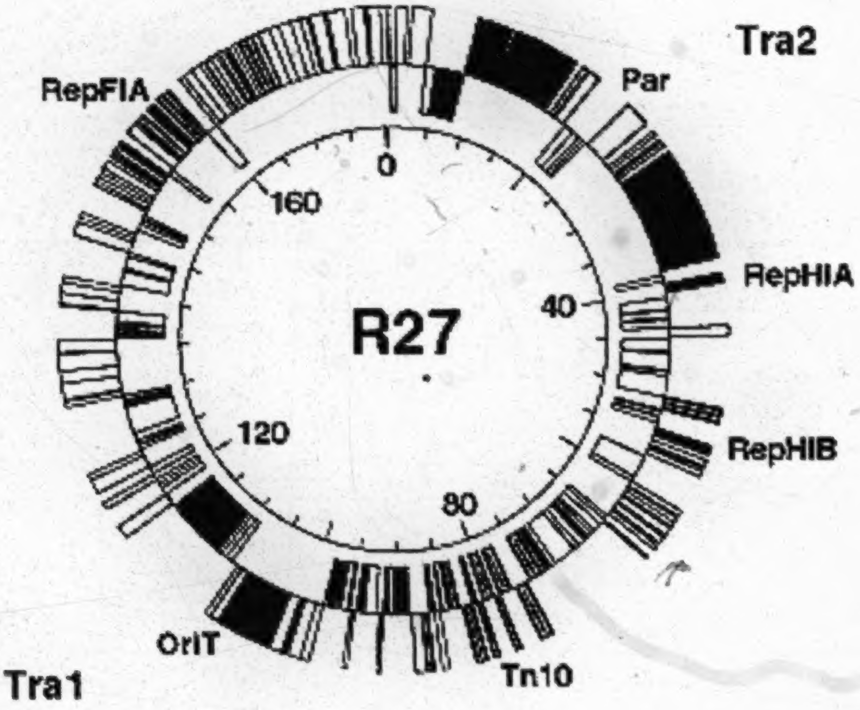
Tra2
Par
RepFIA
0
160
R27
40
RepHIA
120
RepHIB
80
OriT
Tn10
Tra1

of the conjugative system are explained in greater detail in later sections in the Introduction. The DNA uptake system relates to the aforementioned natural transformation HGT machinery of *C. jejuni* and *H. pylori*, which are the only characterized competence systems based on a T4S apparatus. A DNA release system with homology to the T4SS is the DNA secretory apparatus encoded in the gonococcal genetic island (GGI) of *N. gonorrhoeae* (45). The third subfamily of the T4SS, the system enabling the translocation of effector proteins, represents an intrinsic virulence mechanism of several bacterial pathogens (23).

1.4.1 T4SS and Pathogenesis

The Ti plasmid of *Agrobacterium tumefaciens* encodes a T4SS that mediates the transfer of T-DNA that elicitis crown gall disease in infected dicotyledonous plants (for review see (33)). The *A. tumefaciens* VirB/D4 T4SS represents the most comprehensively studied translocation apparatus with the detection of numerous VirB protein interactions enabling significant advances to be made in resolving the architecture of the T4SS. In addition to T-DNA secretion, the VirB/D4 T4SS translocates VirF, VirE2 and VirD2 into plant cells. The role of VirF in the infective process is unknown, however, the VirD2 has been found to covalently bind single-stranded T-DNA while VirE2 is a single-stranded DNA binding protein. Transport of the T-DNA-protein complex into the plant nucleus results in integration and subsequent expression of tumour genes. This inter-kingdom genetic transfer and subsequent expression of the T-DNA genome represents a significant tool in the genetic manipulation of plant genomes (200).

A T4SS encoded within *Bordetella pertussis,* the causative agent of the respiratory disease whooping cough, mediates the secretion of assembled pertussis toxin subunits (subunits S1-S5) into the exterior milieu (23). The *B. pertussis* secretion system is encoded within the Ptl operon, with the *ptl* genes sharing considerable sequence similarity to the *virB* genes of *A. tumefaciens*. Whereas, *B. pertussis* secretes the pertussis toxin into the extracellular environment, the intracellular pathogen *Legionella pneumophila* requires the chromosomally-encoded T4SS, the Dot/Icm system, for survival within phagocytic cells (198). Direct translocation of the effector protein CagA into eukaryotic cell membranes has also been demonstrated with *Helicobacter pylori* (150). This translocation event is mediated by a T4SS structure that is encoded within the 40 kb *cag* pathogenicity island (30). Homologues of T4SS proteins have also been discovered within the genomes of *Brucella spp.* and *Bartonella henselae* (146, 167). Although little is known about the specific T4SS determinants encoded by these two pathogens, initial findings suggest that these protein complexes play an intrinsic role in bacterial virulence (146, 167).

A recent phylogenetic analysis of numerous plasmid and chromosome-encoded T4SS has revealed two significant and surprising findings (58). The ancestors of all chromosomally-encoded T4SS were found to be plasmid-encoded T4SS, with little evidence of vertical inheritance of this secretion system within chromosomal genomes. For example, the *virB* operon of *Brucella* is closely-related to the broad-host range plasmids isolated from wheat and alfalfa rhizospheres (58). A second finding of the phylogenetic study was that effector translocation is a function that has evolved from plasmid conjugative systems, a suggestion that contradicts the previously postulated evolutionary relationship between DNA and protein export (32). Specifically, the T4SS of *Brucella* and *Bartonella* are cited as pathogens that have recently acquired the genetic information encoding this secretion system (58).

1.4.1 Mpf

Characterization of the IncP and IncW plasmids has focused primarily on the DNA processing proteins required for the conjugative process. Conversely, studies on the IncH have focused primarily on the proteins required for the production of exocellular pili; these proteins form the mating pair formation (Mpf) complex. As a paradigm for the conjugative plasmid, the F plasmid has had a comprehensive analysis of proteins required in each stage of the conjugative HGT event. The Mpf system of conjugative plasmids encodes a minimum of 10 proteins that form a membrane-spanning apparatus; this Mpf complex facilitates the production of sex pili on the cell surface which initiate contact with potential recipient bacteria (170). Studies on the F plasmid have indicated that contact of pili with recipient cells induces a retraction event that brings donor and recipient cells into close proximity (112). This retraction event results in the formation of "mating junctions" which are electron-dense regions that have been successfully visualized with electron microscopy (51, 166). In addition to making initial contact with recipients, sex pili have been proposed to initiate a mating signal that indicates when transfer and DNA replication should commence in donor bacteria (112). The nature of the signal and the Mpf proteins that transmit the signal to the cytoplasm of the donor cells have not been identified.

The composition of the Mpf complex in conjugative plasmids has led to the classification of T4SS into three subgroups: The P family, the F/H family and the I family (112). The primary difference between the P and F/H-type T4SS is the type of conjugative pili produced by each secretion apparatus; whereas F/H-type T4SS encode long, flexible pili the P-type T4SS encode short, rigid pili (21). The focus of this thesis will be on the F/H T4SS subgroup. The Mpf of the F plasmid is composed of proteins required for pilus tip assembly and formation (TraL, -E,-K,-B,-V,-C,-W,-F,-H). In addition to these proteins, the N-terminus of TraG is required for pilus assembly and formation

(59). The C-terminus of TraG, in combination with TraN and TraU, are necessary for mating pair stabilization (110).

Three MPF proteins have particular interest for the scope of this thesis (Table 1-1). A search of the NCBI databank has indicated homology between the C terminus of TrhK with the outer membrane pore forming secretin family (109). Secretins are stabilized in the outer membrane by small lipoproteins. Within the T3SS, the secretin InvG only adopts a oligomeric state in the presence of the lipoprotein InvH (37). TraV contains a lipoprotein motif, and an interaction has been demonstrated between TraV and TraK (85). Together these proteins represent a conduit for the translocation of macromolecules across the final barrier of Gram negative organisms. Homologues of a third MPF component, TrhB, have also been demonstrated to have a key role in conjugation. This family of bitopic, periplasmic-spanning proteins contain a N terminal TM region that is proceeded by a proline rich domain; TrhB from the F plasmid is composed of 35% proline residues in the region spanning from 135-183 aa of the protein (7). The VirB10 protein of *A. tumefaciens* has recently been identified as the ATP sensor of the Mpf complex (124). Functional ATPases within the VirB/D4 T4SS are required for an interaction among VirB10 and a VirB9-VirB7 complex located in the outer membrane (27). The VirB9-VirB7 complex has significant homology with the F plasmid TrhB-TrhV complex. The secretion of macromolecules across the cellular envelope requires ATP hydrolysis to provide energy for a T4SS-mediated HGT event. Consequently, well-conserved ATPases have been identified in each genomic source encoding a T4SS.

1.4.2 T4SS ATPases

Three ATPases have been found with the VirB/D4 T4SS of *A. tumefaciens*, VirB11, VirB4, and VirD4. A homologue of VirB11 ATPase is not encoded within the

Table 1-1. Summary of conjugative proteins from the Ti plasmid, IncH, IncW, IncP and IncF plasmid families.

R27 IncHI1 (aa[a])	F IncF1 (aa)	RP4 IncPα (aa)	R388 IncW (aa)	Ti (aa)
TrhB (452)	TraB (475)	TrbI (463)	TrwE (395)	VirB10 (377)
TrhK (410)	TraK (242)	TrbG (297)	TrwF (192)	VirB9 (293)
TrhV (316)	TraV (171)	TrbH (160)	TrwH (47)	VirB7 (55)
TraG (694)	TraD (717)	TraG (635)	TrwB (507)	VirD4 (656)
TraI (1011)	TraI (1756)	TraI (732)	TrwC (966)	VirD2 (424)

[a] Denotes the number of amino acids in each protein

F/H-type T4SS, however the *cag* pathogenicity island of *H. pylori* does contain a homologue of this protein, HP0525, and structural studies have revealed a homohexameric, double-stacked ring configuration (221). The presence of a VirB11 homologue TrbB in the P-type T4SS represents a significant difference between the P-type and F/H-type T4SS (112).

VirB4, a homologue of the TraC and TrhC protein from the F and H plasmid respectively, is the only T4SS ATPase with a structure that has not been elucidated. TraC is predicted to be a peripheral inner membrane protein, and a fusion between GFP and TrhC encoded on the IncH R27 plasmid has been a powerful tool in detecting the location of potential Mpf complexes (67). Moreover, formation of discrete foci representing a TrhC-GFP complex with R27 Mpf proteins was dependent on the presence of TrhB, TrhE and TrhL which indicates the numerous protein interactions that exist within the T4SS (68). The final group of T4SS ATPases, homologues of VirD4 from *A. tumefaciens*, are the coupling proteins that are present in every bacterial conjugative system (223).

1.5 Coupling proteins

The coupling protein plays an essential role in nucleoprotein transfer as this ATPase links the membrane-associated Mpf with the cytoplasmic-associated relaxosomal complex (for a recent review see (73)). Within the coupling protein family there is limited sequence similarity (~20-30%) with the most significant similarity present at the Walker A and B NTP-binding sequence (78). Sequence information from the IncHI2 plasmid R478 identified an H-type relaxosome/coupling group encoding relaxosomal protein (TraI), accessory protein (TraJ), and the coupling protein (TraG) (69). This H-type relaxosome/coupling group module was identified in a number of genomic sources including plasmids, integrative conjugative elements (ICE), and chromosomes (69); the majority of these sources did not encode homologues of the remaining T4S proteins. Phylogenetic analysis of coupling protein homologues encoded within this H-type module showed a weak separation between the genomic sources of the coupling protein homologues (Fig. 1-2). The phylogeny suggested logical groupings of the IncH plasmids (R27 and R478), and Integrative elements (R391 and SXT). Similarly, coupling proteins

from the F plasmid and W plasmid were grouped, as were the ATPases from the Ti plasmid and P plasmid (Fig. 1-2). The chromosomally-encoded coupling proteins were clustered together with the exception of the coupling protein from *Polaromonas JS666*, however this is consistent with the phylogenetic analysis of the TraJ modules (see Chapter 2).

1.5.1 Coupling protein structure and sequence similarities

In 2001, the structure of the cytoplasmic domain of TrwB was solved (72). From these structural data, three domains were identified within the R388 coupling protein: an all-α domain at the membrane-distal part of the protein, a nucleotide-binding motif domain, and a 70 residue N terminal domain that contains two transmembrane regions separated by a short periplasmic region (71, 72). TrwB forms a homohexamer, 90 Å in height and 110 Å in diameter. A central channel runs through the hexamer, with a diameter of ~7-8 Å at the cytoplasmic side (the all-α domain) which enlarges to ~22 Å at the membrane-associated end (72).

Functional information about the coupling protein family may be derived from the structure and sequence similarities that exist between TrwB and well-characterized ATPases. TrwB structural data showed the greatest level of similarity to the structure of the α and β subunits of F_1-ATPase. Axial movement of the F_0F_1-ATPase complex is

Figure 1-2. The coupling protein phylogeny. Distances were calculated using Dayhoff Matrix model and tree was constructed by neighbour-joining approach. Node values correspond to bootstrap values (100 replications). Coupling protein homologues encoded by mobile genetic elements and chromosomal sources were aligned using ClustalW (Gonnet matrix, gap penalty = 10, extension penalty = 0.2). The phylogenetic tree was generated using Mega3 software. The mobile genetic elements-encoding coupling protein homologes were R27 (TraG; Gen Bank accession no. NP_058332), R478 (TraG; Gen Bank accession no. NP_941281), R388 (TrwB; Gen Bank accession no. CAA44852), F (TraD; Gen Bank accession no.BVECAD), Ti (VirD4; Gen Bank accession no. NP_059816); RP4 (TraG; Gen Bank accession no.S22999); SXT (TraD; Gen Bank accession no. AAL59680);and R391 (TraD; Gen Bank accession no. AAM08004).The chromosmally-encoded Coupling protein homologes were *P.aeruginosa* (TraG; Gen Bank accession no. AAP22560); *H. influenzae* (1056.35; Gen Bank accession no. CAF29043); *Yersinia pseudotuberculosis* (api27; Gen Bank accession no. CAF28501); *N. gonorrhoeae* (TraD; Gen Bank accession no. AAW83057); and *Polaromonas JS666* (3865; Gen Bank accession no. EAM39962).

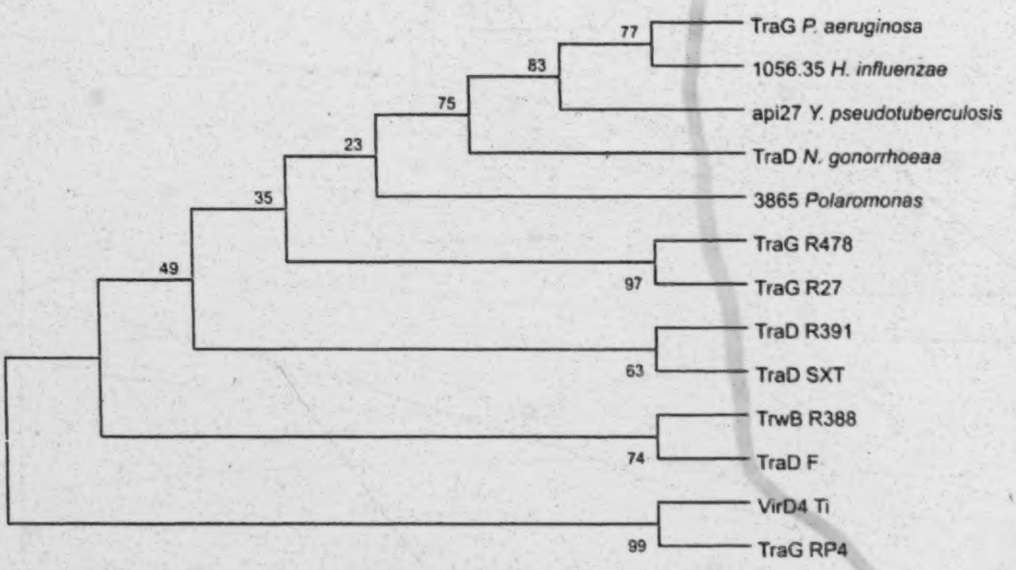
TraG *P. aeruginosa*
1056.35 *H. influenzae*
api27 *Y. pseudotuberculosis*
TraD *N. gonorrhoeaa*
3865 *Polaromonas*
TraG R478
TraG R27
TraD R391
TraD SXT
TrwB R388
TraD F
VirD4 Ti
TraG RP4
77
83
75
23
35
49
97
63
74
99

responsible for the conversion of energy in mitochondria and bacteria (1). Sequence similarity has also been observed between coupling proteins and members of the SpoIIIE/FtsK protein family (for review see (52)). The SpoIIIE protein is encoded by *Bacillus subtilis* and it plays an essential role in chromosome segregation during sporulation (217). The FtsK protein of *E. coli* coordinates chromosome segregation with cell division (208). The similarity of coupling proteins to these DNA translocases has provided evidence to support a conjugative model in which the coupling protein actively exports DNA from the donor cytoplasm.

1.5.2 Nucleotide/ATPase activity

Biochemical analyses of coupling proteins from a number of plasmid families have demonstrated that these ATPases are able to bind ATP and single-stranded and double-stranded DNA; this DNA binding ability is non-specific (169). A recent study has demonstrated that TrwB from the R388 plasmid has DNA-dependent ATPase activity (186). This ATPase activity is consistent with coupling protein mutational analyses of Walker A and B NTP binding motifs. Site-specific mutations within the NTP-binding domains of RP4 (IncP), R388 (IncW), and F (IncF) plasmids abolished conjugative transfer (14, 137, 169, 171). Similarly, the *A. tumefaciens* coupling protein VirD4 contains essential NTP binding motifs; site-specific mutations within the Walker A domain of VirD4 prevented the transfer of T-DNA to T4SS proteins thereby inhibiting conjugation (10, 103).

1.5.3 Coupling protein interactions

In order to bring the Mpf and the relaxosome into close proximity, the coupling protein must interact with each multiprotein complex. An interaction between the Mpf component, TrhB, and the coupling protein, TraG, was recently detected in the IncHI1 plasmid R27 (66). This coupling protein-Mpf interaction between these two T4SS proteins was subsequently confirmed in the IncW, IncN and IncX plasmid families (124). Interestingly, the interaction between coupling protein and Mpf has been demonstrated to be non-specific. The RP4 coupling protein TraG can interact with the Mpf proteins of both R388 and Ti plasmids, and this interaction enables the transfer of the mobilizable IncQ plasmid, RSF1010 (25, 83). Notably, the RP4 coupling protein was not able to facilitate the transfer of the Ti or R388 plasmid implying that any interactions between the relaxosomes of these plasmids and the RP4 coupling protein were non-productive (25, 83).

Coupling protein-relaxosome interactions have been documented in the IncP, IncW and IncF plasmid systems. Within the RP4 conjugative apparatus, the coupling protein TraG was shown to interact with the cognate relaxase protein TraI, and a relaxase from the mobilizable plasmid pBHR1 (169, 185). A coupling protein-relaxase interaction was also detected in the IncW system (124). Although, a similar interaction has not been detected within the IncF system, the relaxosomal protein TraM was found to interact with the coupling protein TraD (46); the C-terminus of TraD was later determined to be the domain that was required for the interaction with TraM (17).

1.6 Relaxosome/Accessory Proteins

In addition to the T4SS, conjugative plasmids encode relaxosomal proteins to process the plasmid DNA for secretion. With the exception of the relaxase, there is very little sequence similarity among relaxosomal proteins encoded by conjugative plasmids. The relaxase mediates a site- and strand-specific cleavage and joining reaction at a *nic* site which is contained within the plasmid *oriT* (origin of transfer). The result of this relaxase-mediated reaction is a covalent interaction between a conserved-tyrosine residue in the relaxase and the 5' terminal end of the single-stranded plasmid DNA; a host-encoded DNA polymerase III initiates replacement strand synthesis in a rolling-circle mechanism (102, 154). Relaxases contain three conserved motifs, and it is the single (TraG relaxase, RP4) or double (TraI relaxase,F) paired tyrosine residues located within motif I that bind the *nic* site of their respective *oriT* regions (112).

Additional relaxosomal proteins, such as TraM or TraK from the F and RP4 plasmid respectively, are required to assist in improving accessibility or stabilization of the relaxase-*oriT* complex (54, 224). Moreover, additional relaxasomal proteins may be instrumental in presenting the nucleoprotein complex to the T4SS via an interaction with the coupling protein.

1.7 Plasmid encoded barriers to HGT

Theoretically, uninhibited HGT could cause the infinite expansion of bacterial genomes which would inevitably lead to extinction of the species (105, 224). A potential explanation of why this uncontrolled genomic growth is not observed within bacteria is that prokaryotes have a pervasive bias towards genomic deletion rather than insertion (135). An alternate explanation is that there are limitations inherent in the HGT process. With transformation, these limitations include an inability to take up the DNA due to the absence of DNA uptake sequences on available DNA or a lack of sequence similarity between the host genome and foreign DNA thereby preventing integration (for review see (193)). A potential limitation to the transduction and conjugation processes is the restricted host range of bacteriophages and conjugative elements (193).

In addition to these HGT barriers, two processes are associated with conjugative elements which prevent both the redundant transmission and subsequent establishment of a mobile element into a recipient harbouring a similar plasmid or conjugative transposon. These two processes are incompatibility and entry exclusion. Incompatibility has been defined earlier in this Chapter. Entry exclusion is a second conjugative element-encoded process that represents a physical barrier to prevent redundant gene transfer.

1.7.1 Entry exclusion

Entry exclusion (Eex) is a process encoded by conjugative plasmids and integrative chromosomal elements that prevents the redundant transfer of mobile elements into recipients carrying isogenic or closely-related elements (143). Eex determinants have been described in a number of plasmids and integrative chromosomal elements, including RP4 (80, 81), F (59), R388 (121), Ti (119), SXT (130), R391 (130), and R144 (88).

Characterization of Eex determinants encoded on these mobile genetic elements has revealed two independent groups of Eex proteins. The first group of Eex proteins has been found to localize to the inner membrane. The prototypical members of this group are TrbK and TraS, encoded by the RP4 and F plasmids, respectively. These Eex determinants are not essential for conjugative transfer (59, 81), and mutational analyses have indicated that TrbK and TraS interact with a component of the Mpf in donor cells (8, 80). The involvement of a Mpf protein in the Eex phenomenon was recently confirmed with a study on the Eex proteins of the conjugative elements SXT and R391 (130). The presence of the Mpf protein TraG, a homologue of the F plasmid stabilization protein TraG, in donor cells determined the specificity of the R391 or SXT exclusion event (130).

The second group of Eex proteins is exemplified by TraT of the F plasmid (for review, see (182). TraT is a lipoprotein that localizes to the outer membrane and has been demonstrated to prevent the formation of stable mating aggregates (2). Interestingly, the presence of TraT on the cell surface has been shown to confer serum resistance to the host cell (136). Due to the location and function of TraT, this F plasmid proteins has been labeled a surface exclusion protein.

Eex activity has been observed within IncHI and IncHI2 plasmids (188). Recipients harbouring IncHI1 plasmids were able to exclude plasmids of the same IncH subgroup, but could only minimally exclude the IncH2 subgroup. The specific mediators of this phenotype in the IncH plasmids have not been identified.

1.8 Objectives

Whole genome sequencing has revealed T4SS homologues in a number of pathogenic organisms (23). From a medical perspective, a more disturbing finding is that T4SSs have an intrinsic role in the virulence of pathogens such as *Brucella spp.* (146). The coupling protein is a central member of the T4SS as it mediates an interaction with the relaxosome and Mpf components. With *in vivo* protein interaction technology, the coupling protein of the IncHI1 plasmid R27 was found to interact with the cognate Mpf protein TrhB. A primary objective of this thesis was to utilize similar interaction studies to resolve the R27 architecture that surrounds the coupling protein TraG. Functional and mutational analyses of the R27 transfer regions have identified the Mpf, relaxosome and coupling proteins which permit the mobilization of the IncH plasmid. The three putative relaxosome proteins, TraI, TraH and TraJ were screened for an interaction with TraG; an *in vivo* interaction was identified between the R27 coupling protein and TraJ. Further characterization of the TraJ-TraG has led to the reclassification of TraJ as a unique accessory protein to the IncH coupling protein.

A second objective was to characterize the functional domains of the R27 coupling protein, TraG, and determine the localization of TraG within the cellular membranes. Through mutational analysis, we identified residues within the Walker A and B NTP-binding motifs that are essential for R27 conjugation. Similarly, site specific mutagenesis was used to determine the TraG domain that interacts with the Mpf protein TrhB. A TrhC-GFP fusion has enabled the visualization of R27 Mpf complexes in the periphery of the cellular membrane. We sought to determine if the coupling protein associates with membrane in a similar distribution pattern. These localization and functional studies have provided evidence which can be used to revise the model for conjugative transfer of the IncH plasmid.

A final objective of this thesis was to determine the R27 determinants that confer an entry exclusion phenotype to IncH-harbouring cells. An R27 cosmid library representing the majority of the R27 genome was used to screen for Eex activity. The initial characterization of the R27 Eex proteins included determining the transcriptional control of the Eex genes and ascertaining their location within the bacterial cytoplasm or membrane. Finally, we sought to determine the specificity of the R27 Eex determinants by observing the Eex activity elicited when donor cells contained an R27-related or non-related plasmid. Identification and initial characterization of the R27 Eex proteins represents the first stages in discovering the mechanistic details of the Eex process.

Chapter 2

An Accessory Protein, TraJ, Associated with the Coupling Protein is Unique to the H Plasmid-Type Conjugative DNA Transfer System

Portions of this chapter have been submitted as:

Gunton, J.E., Gilmour, M.W., Lawley, T.D., and Taylor, D.E. (2005) An accessory protein, TraJ, associated with the coupling protein is unique to the H plasmid-type conjugative DNA transfer system. *Submitted to Journal of Bacteriology, October 2005*

2. An Accessory Protein, TraJ, Associated with the Coupling Protein is Unique to the H plasmid-Type Conjugative DNA Transfer System

2.1 Introduction

Bacterial conjugation is a mechanism of horizontal gene transfer. The ability of prokaryotic organisms to rapidly acquire DNA from surrounding bacteria within the environment has both evolutionary and medical implications. Conjugation is the principal route for the dissemination of antibiotic resistance determinants (131, 142, 206), and recent studies revealed that Gram-negative conjugative pili contribute to biofilm formation which can reduce the efficacy of antimicrobial treatment (41, 65). A multi-protein complex called the type IV secretion system (T4SS) enables the production of conjugative pili, which facilitate the transfer of plasmid DNA from donor to recipient bacteria (for reviews, see references (28, 29, 110). The T4SS also plays a direct role in substrate transfer.

The presence of a plasmid-encoded T4SS in *Salmonella enterica* serovar Typhi has contributed to a higher incidence of antibiotic-resistant strains and subsequently increased the complexity of typhoid fever treatment (199). The incompatibility group HI1 plasmid (IncHI1) R27 is a large (180 kb) self-transmissible plasmid that was originally isolated from an *S.* Typhi strain (176). Using insertional mutagenesis, we have determined that the proteins required for R27 transfer are located in two separate transfer regions, Tra1 and Tra2 (108, 109). Encoded within these two regions are the three multi-protein complexes that are essential for conjugative transfer: the mating pair formation (Mpf) complex, the relaxosome, and the coupling protein.

The Mpf apparatus or T4SS of bacterial plasmids is a complex of 12 or 13 proteins involved in the assembly of the conjugative pilus (59, 75). The pilus structure, following successful contact with the recipient cell, retracts into the donor cell thereby initiating a conjugative junction between the outer membranes of donor and recipient cells (51, 166). The relaxosome is a DNA-protein complex containing the relaxase protein and accessory proteins (61). In the presence of the accessory relaxosome proteins, the relaxase is able to cleave the plasmid DNA at a specific sequence called the origin of transfer (*ori*T), forming a covalent bond with the released single strand of DNA, and interacting with the coupling protein. The coupling protein, the final requirement for conjugation, is the proposed link between the Mpf and the relaxosome (66). The crystal structure of the cytoplasmic domain of TrwB, an IncW R388 coupling protein, has been analyzed (72). The hexameric ring structure of TrwB resembles the tertiary structure of a number of P-loop ATPases such as the F1 ATPase (72). TrwB has since been assigned two putative roles, to couple the Mfp and the relaxosome and also to serve as the conduit through which the nucleoprotein travels (218).

The architecture of the Mpf-coupling protein-relaxosome complex has been difficult to resolve, due in part to the inability of the transmembrane apparatus to be viewed under light or electon microscopy. Interactions between the relaxosome and coupling protein have been identified in the IncW, IncP, and IncF plasmid families (46, 124, 169). The link between the coupling protein and the Mpf has also recently been identified; the R27 coupling protein TraG interacts with the Mpf component TrhB at the cytoplasmic membrane (66). An interaction between homologues of the these two proteins has been identified in the IncW system (124). The multiple interactions occurring within the Mpf continue to be elucidated with significant advances occurring within the VirB system of *Agrobacterium tumefaciens* (for review, see reference (33).

Coupling proteins have been shown to have sequence similarity to a family of membrane-associated DNA translocases (52). FtsK, a member of the translocase family, from *Escherichia coli* is an ATPase that is essential for coordinating chromosome segregation with cell division (208). A second member of this family of proteins, SpoIIIE, is produced by *Bacillus subtilis* and mediates DNA partitioning during the process of sporulation (217). Sequence similarity was found between SpoIIIE and DNA transfer proteins (Tra) from small conjugative plasmids of Gram-positive bacteria (218). This similarity was located primarily within the region of SpoIIIE surrounding the Walker A and B boxes, which are essential for nucleoside triphosphate binding and hydrolysis (202). Biochemical studies of the coupling protein from the IncP and IncW family have revealed that this family of proteins bind ss- and ds-DNA non-specifically and also bind nucleoside triphosphates. A recent biochemical analysis of the R388 coupling protein, TrwB, has determined that this family of proteins are able to hydrolyze ATP in the presence of DNA (186). Mutations within the Walker motifs of coupling proteins from the IncH plasmid R27 and the IncP plasmid RP4 prevented conjugative transfer (171).

The R27 coupling protein is encoded within the Tra1 region of the IncHI1 plasmid and is one of the nine genes known to be essential for conjugative transfer. Three essential genes in the Tra1 region, *traI*, *traH*, and *traJ* were shown not to be involved in the production of sex pili, and therefore are not components of the Mpf (108). The TraI protein shares homology with the relaxase family of proteins, whereas TraH contains a DNA-binding motif and a N terminal coiled-coil domain (108). Although initially labeled as a relaxosome component, TraJ contains four predicted transmembrane (TM) regions comprising the majority of the 220 amino acid protein. The TM regions indicate a membrane-association which is atypical of the relaxosome family of proteins (69). As TraJ does not share characteristics with either the relaxosome or Mpf proteins, TraJ was originally classified as a relaxosome accessory protein.

TraJ homologues from a variety of genomic sources have been identified (69), and an alignment of these homologues indicated that the predicted four TM domains are well-conserved among this family of proteins. A set of three genes encoding relaxosomal protein (TraI), accessory protein (TraJ), and the coupling protein (TraG) has been identified in each of the genomic sources encoding a TraJ homologue (69). With the exception of extrachromosomal agents such as R27 and R478, the TraJ-encoding genomes did not encode any F/H-type Mpf genes. This suggests that a module of *traI-G-J* genes can be inherited independently from the T4SS components.

The objective of the present study was to identify additional R27-encoded interaction partners for TraG that are not essential for conjugative pilus formation. Here an interaction that occurs between the coupling protein and the TraJ protein is described. To determine the specificity of the TraJ-TraG interaction, coupling proteins from the RP4, R388, and F plasmids were screened for their ability to interact with R27-encoded TraJ. We extended this study to determine if the coupling proteins of these three plasmids could interact with the R27 Mpf protein, TrhB. Whereas all the coupling proteins could interact with R27-encoded TrhB, a heterologous Mpf component, the only specific interaction occurred between the cognate coupling protein, TraG, and its R27 accessory protein TraJ. In addition, TraJ homologues from different genomic sources were tested for the ability to interact with cognate and non-cognate coupling proteins. Finally, this study identifies sequence similarity between TraJ and the N terminus of the DNA translocase FtsK which allowed a revised model for conjugative transfer of the R27 plasmid to be proposed. The specific interaction with the coupling protein, genetic organization and shared homology with DNA translocases suggest that TraJ is a unique accessory protein that associates with the R27 coupling protein.

2.2 Experimental Procedures

2.2.1 Bacterial Strains and Growth Conditions

E. coli strains used in this study are listed in Table 2-1. All strains were grown in Luria Bertani (LB) broth (Difco Laboratories, Detroit, MI) at 37°C with shaking at 200 RPM unless otherwise stated. Antibiotics used in this study are listed with final concentrations of: ampicillin (100 μg/ml), kanamycin (50 μg/ml), tetracycline (10 μg/ml), rifampicin (50 μg/ml), nalidixic acid (20 μg/ml), trimethoprim (25 μg/ml).

2.2.2 DNA Manipulation and Cloning

Standard recombinant DNA methods were used as described previously (165). PCR products were amplified with terminal restriction enzymes added within the primer sequences (Table 2-2). Amplified DNA was initially cloned into pGEM-T (Promega, Madison, WI) and then digested with appropriate enzymes and subcloned into the expression vector pMS119EH/pMS119HE or the adenylate fusion vectors, pKT25 and pUT18C. Restriction enzyme endonucleases were used according to the manufacturers specifications and digested products resolved on agarose gels.

2.2.3 Protein Expression of Coupling Proteins Homologues

A His_6 tag was incorporated into the primer design for coupling protein amplification such that each protein contained a C-terminal histidine tag for detection of the recombinant proteins. Proteins were resolved on a 10% SDS-PAGE and following transfer to nitrocellulose membrane, a primary mouse anti-His_6 monoclonal antibody (Invitrogen, Carlsberg, CA) and a secondary goat anti-mouse HRP antibody were used to probe for protein expression.

Table 2-1. Bacteria and Plasmids Used in This Study

Bacterial Strain or Plasmid	Relevant Genotype, Phenotype, or Characteristic[a]	Source or Reference
E.coli		
DH5α	*supE44 lacU169* (*Φ80lacZ*ΔM15) *hsdR17 recA1 endA1gyrA96 thi-1 relA1*	Invitrogen
DY330	W3110 Δ*lacU169 gal-490* λ*cI857* Δ(*cro-bioA*)	(35)
DY330R	Temperature-resistant revertant; Rif^r	(108)
DY330N	Temperature-resistant revertant; Nal^r	(108)
BTH101	F$^-$ *cya-99 araD139 galE15 galK16 rpsL1* (*Str*^{r}) *hsdR2 mcrA1 mcrB1*	(101)
RG192	*ara leu lac*	(187)
DT1942	RG192 (Rif^r) containing pDT1942	(126)
Plasmids		
pBAD30	P$_{BAD}$ expression vector; Para; origin of replication, Cm^r	(79)
pBAD30-traG$_{FLAG}$	2.1kbp *Eco*RI/*Bam*HI-digested PCR product in pBAD30; Cm^r	This study
pMS119EH	Expression vector; P$_{tac}$-lacI^q; pMB1 origin of replication; Amp^r	(181)
pMS119EH-traG$^{H}_{His}$	2.1 kbp *Eco*RI/*Bam*HI-digested R27 (IncH) PCR product in pMS119EH; Amp^r	This study
pMS119EH-traG$^{P}_{His}$	1.9 kbp *Eco*RI/*Bam*HI-digested RP4 (IncP) PCR product in pMS119EH; Amp^r	This study
pMS119HE-traD$^{F}_{His}$	2.2 kbp *Hind*III/*Eco*RI-digested F (IncF) PCR product in pMS119HE; Amp^r	This study
pMS119EH-trwB$^{W}_{His}$	1.5 kbp *Eco*RI/*Bam*HI-digested R388 (IncW) PCR product in pMS119EH; Amp^r	This study
pKT25	p15A origin of replication; encodes CyaA$_{1-224}$;Km^r	(101)
pUT18C	ColE1 origin of replication; encodes CyaA$_{225-399}$; Amp^r	(101)
pKT25-zip	leucine zipper of GCN1 (BTH positive control); Km^r	(101)
pUT18C-zip	leucine zipper of GCN1 (BTH positive control)	(101)
pUT18C-trhC	2.7 kbp *Bam*HI/*Kpn*I- digested PCR product in pUT18C; Amp^r	This study
pUT18C-trhB	1.4kbp *Bam*HI/*Kpn*I-digested PCR product in pUT18C; Amp^r	(66)
pUT18C-traG^{R27}	2.1 kbp *Pst*I/*Bam*HI-digested R27 (IncH) PCR product in pUT18C; Amp^r	This study
pUT18C-traG^{RP4}	1.9 kbp *Pst*I/*Bam*HI-digested RP4 (IncP) PCR product in pUT18C; Amp^r	This study
pUT18C-traD^{F}	2.2 kbp *Pst*I/*Bam*HI-digested F (IncF) PCR product in pUT18C; Amp^r	This study
pUT18C-trwB^{R388}	1.5 kbp *Pst*I/*Bam*HI-digested R388 (IncW) PCR product in pUT18C; Amp^r	This study
pUT18C-traG^{R478}	2.1 kbp *Pst*I/*Bam*HI-digested R478 (IncH) PCR product in pUT18C; Amp^r	This study
pUT18C-traD^{R391}	1.8 kbp *Pst*I/*Bam*HI-digested R391 (IncJ) PCR product in pUT18C; Amp^r	This study
pUT18C-5177^{Pflo}	2.1 kbp *Pst*I/*Bam*HI-digested *Pseudomonas fluorescens* PCR product in pUT18C; Amp^r	This study
pUT18C-traG^{R27}	2.1 kbp*Pst*I/*Bam*HI-digested R27 (IncH) PCR product in pUT18C; Amp^r	(66)
pKT25-trhB	1.4 kbp *Bam*HI/*Kpn*I-digested PCR product in pKT25; Kan^r	This study
pKT25-traJ^{R27}	660 bp *Pst*I/*Bam*HI-digested R27 (IncH) PCR product in pKT25; Kan^r	This study
pKT25-traJ^{R478}	662 bp *Pst*I/*Bam*HI-digested R478 (IncH) PCR product in pKT25; Kan^r	This study
pKT25-36^{R391}	644 bp *Pst*I/*Bam*HI-digested R391 (IncJ) PCR product in pKT25; Kan^r	This study

pKT25-5176^{Pflo}	732 bp *PstI/Bam*HI-digested *Pseudomonas fluorescens* PCR product in pKT25; Kan ^{r}	This study
pDT1942	derepressed transfer mutant of R27: R27 ::TnlacZ	(126)
pDT2989	pDT1942 with mini::Tn10 inserted into traG	(108)
pOX38	F plasmid (IncF) ::mini-Tn*10*, Tc^r	(7)
pOX38::TraD 411	Kanamycin-resistance cassette insertion in TraD of pOX38 ;Kan ^{r}	(128)
pDB126	Essential transfer proteins of RP4 (IncP); Cm^r	(14)
pDB127	Derivative of pDB126 with a deletion of TraG; Cm^r	(14)
R388	IncW plasmid; Kn^r	(25)
pSU1456	72 bp insertion in *trwB* of R388; Tp^r	(25)

[a] Abbreviations: Nal^r, nalidixic acid resistance; Rif^r rifampicin resistance; Tc^r tetracycline resistance; Km^r, kanamycin resistance; Amp^r, ampicillin resistance; Str^r ,streptomycin resistance; Cm^r, chloramphenicol resistance; Tp^r trimethoprim resistance.

Table 2-2. Primers Used in This Study.

Primer Name	Sequence (5'-3')[a]	Predicted Product Size (bp)
traG-FLAG-f	TATATCTAGAATGACAAAATCAAAAAGAACCAAC	2109
traG-FLAG-r	TATAAAGCTTTTACTTGTCATCGTCGTCCTTGTAGTCATGCAATTTCCTTAGATATTTATTT	2109
traG-His-R27-f	TATATGAATTCAATGACAAAATCAAAAAGAAC	2103
traG-His-R27-r	TATATGGATCCTTAATGGTGATGGTGATGGTGCGCATGCAATTTCCTTAGATATT	2103
traG-His-RP4-f	TATAGAATTCAATGAAGAAACCCGAAACAACGCCGTG	1926
traG-His-RP4-r	TATAGGATCCTCAATGGTGATGGTGATGGTGTATCGTGATCCCCTCCCCTTC	1926
traD-His-F-f	TATAGAATTCAATGAGTTTTAACGCAAAGGATATGAC	2172
traD-His-F-r	TATAAAGCTTTCAATGGTGATGGTGATGGTGGAAATCATCTCCCGGCTCAAC	2172
trwB-His-W-f	TATAGAATTCAATGCATCCAGACGATCAAAG	1542
trwB-His-W-r	TATAGGATCCTCAATGGTGATGGTGATGGTGGATAGTCCCCTCAACAAAGGC	1542
trhC-18C-f	TATAGGATCCTAGATCAGCTAACGTCTATAATAAAG	2682
trhC-18C-r	AAGGTACCCAGGCAGCTGATTTGCTCGCAAC	2682
trhB-18C-f	TATAGGATCCAGACATTAAAAAGGCCTGGGAAAATAAAAC	1359
trhB-18C-r	TATAGGTACCGCGCGGCTTGTCAGGTTTGTAG	1359
traG-18C-R27-f	TATACTGCAGGACAAAATCAAAAAGAACCAAC	2085
traG-18C-R27-r	TATAGGATCCTCAATGCAATTTCCTTAGAT	2085
traG-18C-RP4-f	TATAGGATCCCAAGAACCGAAACAACGCCGTG	1908
traG-18C-RP4-r	TATAGGTACCCGTATCGTGATCCCCTCCCCTTC	1908
traD-18C-F-f	TATAGGATCCCAGTTTTAACGCAAAGGATATG	2154
traD-18C-F-r	TATAGGTACCCGGAAATCATCTCCCGGCTCAAC	2154
trwB-18C-W-f	TATACTGCAGGCATCCAGACGATCAAAGAAAG	1524
trwB-18C-W-r	TATAGGATCCTTAGATAGTCCCCTCAACAAAGGC	1524
trhB-25K-f	TATAGGATCCCCGACATTAAAAAGGCCTGGGAAAATAAAAC	1359
trhB-25K-r	TATAGGTACCGCGCGGCTTGTCAGGTTTGTAG	1359
traJ-R27-25K-f	TATACTGCAGGCGCTGCGGATAATTCTGCTCGTG	663
traJ-R27-25K-r	TATAGGATCCTCACATAAGTTTTTGAAAGTTAGAC	663
traJ-R478-25K-f	TATACTGCAGGCGCTGCGGATAATACAAGCAG	663
traJ-R478-25K-r	TATAGGATCCTCACATGAGTTTTTGAAAGTTAGAC	663
36-R391-25K-f	TATACTGCAGGCTTTGGCATGAGCAAGCATAAG	645
36-R391-25K-r	TATAGGATCCTCATATCTTCTTCTGCAAGTGAC	645
5176-P.flo.-25K-f	TATACTGCAGGCGCGACTTCCGCCCAGAACACG	732
5176-P.flo.-25K-r	TATAGGATCCTCAGAGATATTTCTTAAATGTACTTGC	732
traG-R478-18C-f	TATACTGCAGGTCAGATTCGAAGAGGACTAAC	2085

traG-R478-18C-r	TATAGGATCCTCAATGCAACTTCCTTAGAAATTTA	2085
traD-R391-18C-f	TATACTGCAGGAAAGAAAACGCATACGAAATGC	1821
traD-R391-18C-r	TATACTGCAGGAAAGAAAACGCATACGAAATGC	1821
5177-P.flo.-18C-f	TATATCTAGAGGCCGAGCATGCAATGGAGTCCAAG	2106
5177-P.flo.-18C-r	TATAGGTACCTCACCCCACCTGATCCAGATCGAAG	2106

[a] Underlined sequences denote restriction enzyme cleavage sites.

2.2.4 Conjugation Assay

Liquid mating: Complementation experiments with R27 were performed as described previously (108, 189). Briefly, *E. coli* strain DY330R containing either wild type R27 plasmid or an R27 plasmid containing a mini:Tn*10* insertion located within the coupling protein gene, *traG*, (pDT2989) was grown at 28°C. DY330N recipient cells were also grown at 28°C. The *traG* mutation in R27 was complemented by transforming donor cells with either pMS119EH or pMS119HE encoding coupling proteins from the F, RP4, R388 and R27 plasmid. Upon reaching an OD_{600} of 0.5-0.7, donor cells containing the pMS119EH/HE expression vector were induced for 1 hour with IPTG (isopropyl-β-D-thiogalactoside) at a final concentration of 0.4 mM. The transmission frequency into DY330N cells of pDT2989 was measured as transconjugants per donor. Donor and recipient cells were incubated for 16 hours at 28°C.

Complementation experiments with the F plasmid were performed as described above with the exception of the temperature of conjugal transfer. Instead donor and recipient cells were grown at 37°C, and mating experiments were incubated at 37°C for 16 hours.

Solid mating: Conjugative transfer of RP4 and R388 plasmids were performed as described previously (21). Briefly, donor cells (DY330R + RP4 or R388) were mixed with recipient cells (DY330N) and plated on pre-warmed LB plates for 1 hour at 37°C. Cells were harvested with LB broth and brought up to a volume of 3 mL. Complementation of coupling protein mutations in R388 and RP4 were performed as described above.

2.2.5 Bacterial Two-Hybrid (BTH)

Each conjugative transfer protein of interest was fused to the catalytic domain of adenylate cyclase from *Bordetella pertusis* via cloning into the BTH vectors, pKT25 and pUT18C. Plasmids encoding fused proteins were co-transformed into competent BTH101 cells and plated on LB plates with X-Gal (5-bromo-4-chloro-3-indolyl-β-d-galactopyranoside) at a final concentration of 100 ug ml^{-1}, and for selection the plates contained ampicillin and kanamycin. Cultures were grown at 30°C for 40-48 hours or until the colonies expressing the leucine zipper positive control became dark blue in colour due to the degradation of the chromogenic substrate X-Gal. For each interaction, two colonies were streaked on to the above media and grown at 30°C for 16 hours. These colonies were used to inoculate a 20 mL volume of LB with ampicillin and kanamycin selection and grown at 30°C for 16 hours at 250 RPM. The β-galactosidase activity of each culture was measured using the Miller assay as described previously (134). Negative values of β-galactosidase activity were represented as 0 Miller units.

2.2.6 Immunoprecipitation

Immunoprecipitation of R27 transfer proteins was performed as described previously (66). DH5α cells containing plasmids pUT18C-TraJ, pUT18C-TrhB or pUT18C-TrhC were all co-transformed with pBAD30-TraG$_{FLAG}$ for the interaction studies. Cells were induced at mid-log growth phase (OD$_{600}$ 0.5-0.7) with 0.4 mM IPTG and 0.2% arabinose for 1 hour prior to cell lysis. After the cleared lysate was separated on 10% SDS-PAGE, proteins were transferred to nitrocellulose and probed with the anti-adenylate cyclase monoclonal antibody, 3D1 (List laboratories). This monoclonal antibody is specific for the distal portion of the adenylate cyclase catalytic domain (amino acids 377-399) (117).

2.2.7 Phylogenetic analysis

The sequences of TraJ and protein homologues were aligned using ClustalW (Gonnet matrix, gap penalty=10, extension penalty=0.2) (194). A phylogenetic tree was constructed using a p-distance model from the neighbor-joining algorithm of MEGA3 (104). To test the statistical significance of the tree, 100 bootstrap samples were generated from the TraJ alignment data. The bootstrap values were similar when a complete deletion or pairwise deletion method was utilized.

A second tree was generated from a ClustalW alignment of full-length and truncated TraJ homologues from mobile genetic elements and chromosomal sources, respectively. The N terminal 30 amino acids (aa) were removed from chromosomally-encoded TraJ homologues found in *Haemophilus somnus* (ZP_00123133), *Xanthomonas axonopodis pv. citri* (NP_642577), *Pseudomonas fluorescens* (ZP_00087889), *Burkholderia fungorum* (ZP_00030777), *Pseudomonas aeruginosa* (AAN62289), *Yersinia pseudotuberculosis* (CAF28502), and *Erwinia carotovora* (YP_048677.1). For the alignment, full-length TraJ homologues were utilized from the plasmid-encoded sources R478 (CAE51739), R27 (NP_058330), R391(AAM08039), pCAR1 (NP_758667), Rts1 (NP_640164). Full length TraJ homologues were also used from the conjugative transposon SXT (AAL59721) and the *Polaromonas* sp. JS666 (ZP_00363614, where the *Polaromonas* sp. JS666 coding sequence PJS6w01001858 has been reannotated from the NCBI entry to include 29 additional codons and an alternate start codon). The ClustalW alignment of these sequences was used to generate a phylogenetic tree using the same parameters as described above.

2.2.8 Web-based computer programs

PSI-Blast (http://www.ncbi.nlm.nih.gov/BLAST/); ScanProsite (http://au.expasy.org/tools/scanprosite/); TMHMM (http://www.cbs.dtu.dk/services/TMHMM-2.0/); ClustalW (http://www.ebi.ac.uk/clustalw/);and EMBOSS pairwise local alignment (Blosum40 matrix, gap penalt =10, extension penalty=0.5; http://ebi.ac.uk/emboss/align/) were used.

2.3 Results

2.3.1 *In vivo* Detection of the R27 TraG and TraJ Interaction

We have previously used the bacterial two-hybrid (BTH) system to screen for interactions between the R27 coupling protein, TraG, and a number of R27 Mpf proteins (66). In this study, we screened for interactions between the coupling protein and transfer proteins that were not essential for the production of IncH pili (108). The R27 relaxosomal genes *traI, traH,* and the sole remaining Tra1-encoded non-MPF gene *traJ*, encoding a putative membrane-associated transfer protein, were each cloned into the pUT18C BTH vector. The R27 coupling protein gene *traG* was cloned in the appropriate reading frame of the pKT25 plasmid and the resulting gene product, $\text{TraG}_{\text{AC25}}$, was a fusion between the 78 KDa coupling protein and the C terminal 25 kDa region of the adenylate cyclase catalytic domain. Screening for pairwise interactions using the BTH system did not detect interaction between the R27 coupling protein and the R27 relaxase TraI or the relaxosome component TraH. However, co-transformation of R27 $\text{TraJ}_{\text{AC18}}$ with $\text{TraG}_{\text{AC25}}$ allowed for functional complementation of the *B. pertussis* adenylate cyclase domains. The adenylate cyclase activity was initially monitored by plating transformed BTH101 cells onto media containing X-Gal. More than 99% of the colonies containing $\text{TraJ}_{\text{AC18}}$ with $\text{TraG}_{\text{AC25}}$ were blue within 48 hours of plating. The BTH positive control (vectors containing leucine zippers) showed similar blue colonies, whereas the BTH101 cells containing empty BTH vectors were white. A standard Miller assay was used to quantify β-galactosidase activity (Figure 2-1). The *in vivo* interaction between TraJ and TraG was found to produce higher levels of β-galactosidase activity than the activity produced by the interaction of the BTH positive control (leucine zipper) (Figure 2-1) .

Figure 2-1. *In vivo* bacterial two-hybrid interactions between the R27 coupling protein, TraG, and R27 transfer proteins TraJ and TrhB. Conjugative proteins were fused with adenylate cyclase domains and co-produced in BTH101. The BTH controls are BTH101 cells containing pUT18C and pKT25 (negative control), and pUT18C-leucine zipper with pKT25-leucine zipper (positive control). Liquid cultures of transformed BTH101 cells were analyzed for β-galactosidase activity using a Miller assay (134). A representative experiment is shown.

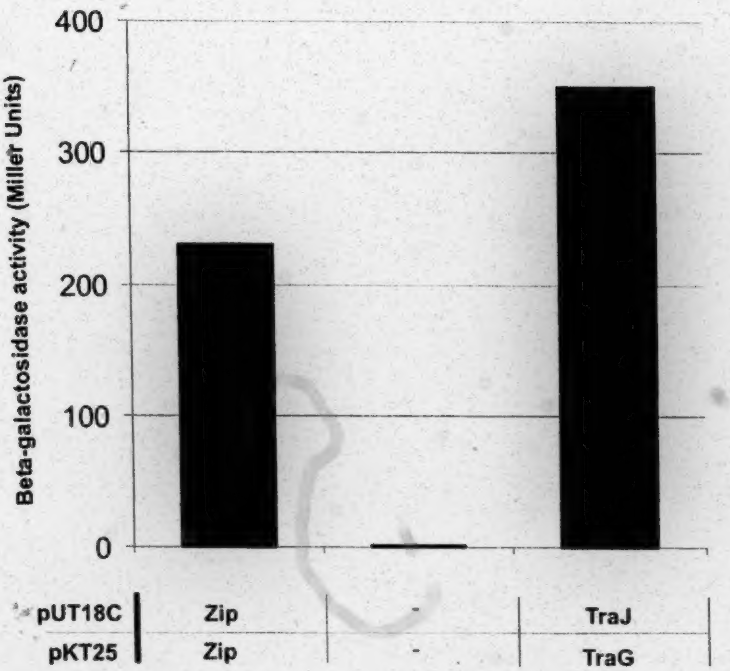

Beta-galactosidase activity (Miller Units)
400
300
200
100
0
pUT18C
pKT25
Zip
Zip
-
-
TraJ
TraG

The R27 coupling protein TraG and R27-encoded TraJ, both contain multiple, well-conserved predicted TM domains (69, 73). To ensure that this interaction was not a non-specific interaction of membrane-associated proteins caused by over-expression of R27 transfer proteins, the R27 *virB4* homologue *trhC* was cloned into the BTH vector pUT18C. The VirB4-family of proteins are well-characterized, inner-membrane associated ATPases (for review, see reference (100). When $\text{TraG}_{\text{AC25}}$ was co-transformed with $\text{TrhC}_{\text{AC18}}$ into BTH101 and plated on media containing X-Gal, >99% of the colonies were white after 48 hours of incubation. The inability of TrhC to interact with TraG implies that the productive TraG-TraJ interaction is not simply due to predicted co-localization of transfer proteins at the cytoplasmic membrane.

2.3.2 Immunoprecipitation of a TraG and TraJ complex

To confirm the interaction between the R27 coupling protein and accessory protein, TraJ, we purified R27 tagged-protein complexes using an immunoprecipitation technique. The C terminus of TraG was fused with a FLAG tag, an octopeptide of Asp-Tyr-Lys-Asp-Asp-Asp-Asp-Lys. In the presence of sepharose beads labeled with anti-FLAG antibody, the $\text{TraJ}_{\text{AC18}}$ construct was precipitated by $\text{TraG}_{\text{FLAG}}$ (Figure 2-2A). The monoclonal antibody 3D1, which recognizes an epitope in the 18 kDa adenylate cyclase fragment of *B. pertussis*, detected precipitated $\text{TraJ}_{\text{AC18}}$ in the presence of $\text{TraG}_{\text{FLAG}}$(117). The labeled-sepharose beads were unable to precipitate $\text{TraJ}_{\text{AC18}}$ when $\text{TraG}_{\text{FLAG}}$ was omitted from the immunoprecipitation experiment (Figure 2-2A). This ensured that the R27 accessory protein, TraJ, was not bound non-specifically by a component of the immunoprecipitation reaction. The precipitation of a TraG-TraJ complex confirmed the BTH data in which the R27 coupling protein interacted with the non-Mpf protein, TraJ. To ensure that the TraG and TraJ interaction is not due to over-expression, the VirB4 homologue from R27, $\text{TrhC}_{\text{AC18}}$, was included in an

Figure 2-2. Co-immunoprecipitation of an IncH R27 TraJ-TraG complex .

A) The cellular lysates of DH5 α cells expressing $\mathrm{TraJ}_{\mathrm{AC18}}$ and $\mathrm{TraG}_{\mathrm{FLAG}}$ were mixed with M2 anti-FLAG affinity gel beads, washed, and resolved with 10% SDS-PAGE. After transfer to nitrocellulose, the samples were probed with the anti-adenylate cyclase monoclonal antibody 3D1. As a control for non-specific precipitation of $\mathrm{TraJ}_{\mathrm{AC18}}$, a cellular lysate containing only $\mathrm{TraJ}_{\mathrm{AC18}}$ protein was mixed with M2 anti-FLAG affinity gel beads and resolved as described above.

B) $\mathrm{TrhC}_{\mathrm{AC25}}$ and $\mathrm{TraG}_{\mathrm{FLAG}}$ were co-expressed in DH5α and the cellular lysate (**CL**) was resolved by 10% SDS-PAGE, transferred to a nitrocellulose membrane and probed with monoclonal antibody 3D1. The cell lysate was then incubated with M2 anti-FLAG affinity gel beads and resolved, as above, to obtain an immunoprecipitate sample (**IP**).

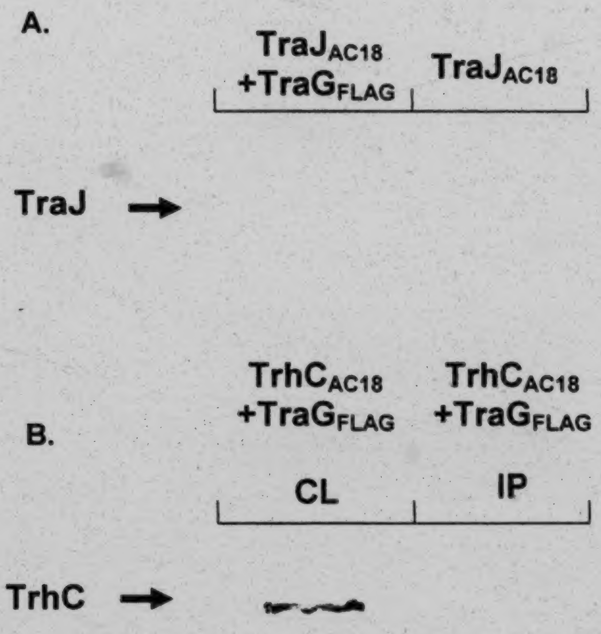
A.
$TraJ_{AC18}$ $+TraG_{FLAG}$
$TraJ_{AC18}$
TraJ →
B.
$TrhC_{AC18}$ $+TraG_{FLAG}$
$TrhC_{AC18}$ $+TraG_{FLAG}$
CL
IP
TrhC →

immunoprecipitation experiment with $\text{TraG}_{\text{FLAG}}$. The BTH study had indicated that these two R27 predicted membrane-associated proteins did not interact (see above). Although the $\text{TrhC}_{\text{AC18}}$ was soluble and detectable in the conditions prior to immunoprecipitation (Figure 2-2B, cleared lysate), $\text{TraG}_{\text{FLAG}}$ was unable to precipitate $\text{TrhC}_{\text{AC18}}$ (Figure 2-2B, immunoprecipitation). Furthermore, the inability of the R27 coupling protein to interact with $\text{TrhC}_{\text{AC18}}$ confirms that the interaction of $\text{TraJ}_{\text{AC18}}$ and $\text{TraG}_{\text{FLAG}}$ is not due to non-specific interaction between the 18KDa adenylate cyclase domain and $\text{TraG}_{\text{FLAG}}$.

2.3.3 Coupling Proteins Determine the Specificity of Interactions with T4SS and Relaxosome/Accessory Components.

Recent studies on the coupling proteins and VirB10 homologues from the IncW R388 plasmid, IncN plasmid pKM101, and IncX plasmid R6K, demonstrated that each coupling protein was able to interact with cognate and heterologous VirB10 proteins (124). To expand upon this study, the coupling proteins from the conjugative plasmids R27 (IncH), RP4 (IncP), F (IncF), and R388 (IncW), were cloned into the pUT18C vector from the BTH system. When each coupling protein was co-transformed into BTH101 cells in the presence of R27 Mpf component $\text{TrhB}_{\text{AC25}}$, the *in vivo* interaction data showed that successful interactions were obtained between each coupling protein and the R27 VirB10-homologue, TrhB (Figure 2-3A). The strength of the interactions between the coupling proteins and TrhB were similar in activity to the levels produced by a leucine zipper interaction which represented the BTH positive control. The interaction between TraG^{RP4} and TrhB showed β-galactosidase activities that consistently were greater than the levels produced by the interaction between non-cognate TraD^{F} and TrwB^{W} with TrhB. However, the high levels of β-galactosidase activity produced by the interaction of each non-cognate coupling protein with TrhB was remarkable given the lower levels of overall homology shared between members of the coupling protein

Figure 2-3. Bacterial-two hybrid interaction data demonstrating the diversity and specificity of protein interactions associated with R27 relaxosome protein, TraJ, the R27 Mpf protein, TrhB, and the coupling proteins from IncH (R27), IncF (F plasmid), IncP (RP4) and IncW (R388) plasmids. The BTH plasmid, pKT25, was used to construct IncH R27-adenylate cyclase fusion proteins, $\mathrm{TraJ}_{\mathrm{AC25}}^{\mathrm{H}}$ and $\mathrm{TrhB}_{\mathrm{AC25}}^{\mathrm{H}}$. The coupling protein homologs were cloned into pUT18C, resulting in the expression of $\mathrm{TraG}_{\mathrm{AC18}}^{\mathrm{H}}$, $\mathrm{TraD}_{\mathrm{AC18}}^{\mathrm{F}}$, $\mathrm{TraG}_{\mathrm{AC18}}^{\mathrm{P}}$ and $\mathrm{TrwB}_{\mathrm{AC18}}^{\mathrm{W}}$. Protein interaction was determined by assaying for the β-galactosidase activity produced by co-expression of A) $\mathrm{TraJ}_{\mathrm{AC25}}^{\mathrm{H}}$ or B) $\mathrm{TrhB}_{\mathrm{AC25}}^{\mathrm{H}}$ with $\mathrm{TraG}_{\mathrm{AC18}}^{\mathrm{H}}$, $\mathrm{TraD}_{\mathrm{AC18}}^{\mathrm{F}}$, $\mathrm{TraG}_{\mathrm{AC18}}^{\mathrm{P}}$ and $\mathrm{TrwB}_{\mathrm{AC18}}^{\mathrm{W}}$. The BTH controls are BTH101 cells containing pUT18C and pKT25 (negative control), and pUT18C-leucine zipper with pKT25-leucine zipper (positive control). A representative experiment is shown.

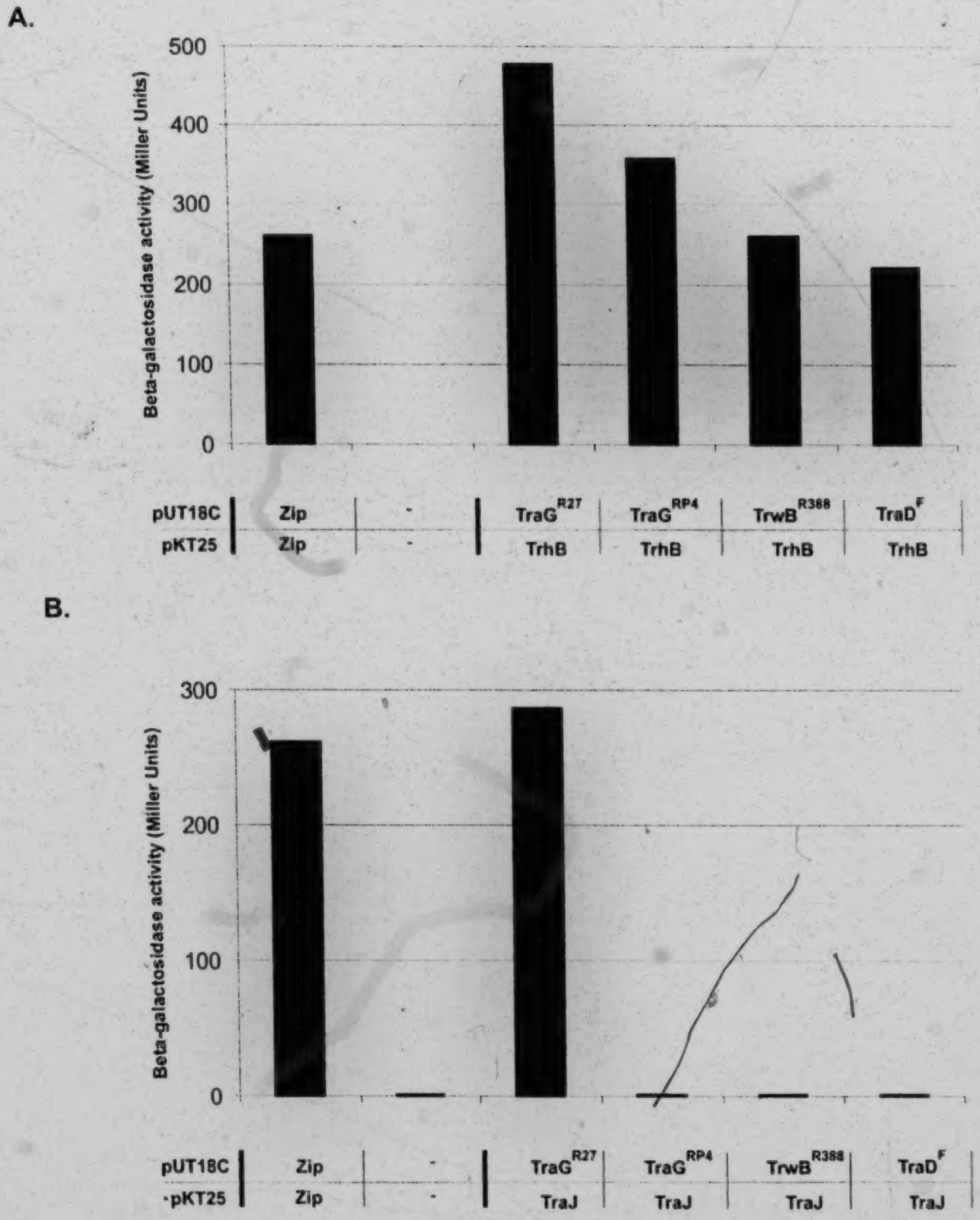
A.
Beta-galactosidase activity (Miller Units)
500
400
300
200
100
0
pUT18C
pKT25
Zip
Zip
-
-
TraG^R27
TrhB
TraG^RP4
TrhB
TrwB^R388
TrhB
TraD^F
TrhB
B.
Beta-galactosidase activity (Miller Units)
300
200
100
0
pUT18C
pKT25
Zip
Zip
-
-
TraG^R27
TraJ
TraG^RP4
TraJ
TrwB^R388
TraJ
TraD^F
TraJ

family. The coupling proteins from the RP4, R388 and F plasmids had similar levels of sequence similarity with TraG^{R27}: TraG^{RP4} 19.6% identity over alignment length of 749, TraD^{F} 19.5% identity over alignment length of 845, and TrwB^{R388} 20.1% identity over alignment length of 750.

As the interface between coupling protein and Mpf is proposed to occur at the cytoplasmic membrane, an interaction was sought between the putative membrane-associated accessory protein TraJ and the non-cognate coupling proteins TraG^{RP4}, TraD^{F}, and TrwB^{R388}. These BTH studies should indicate if the lack of specificity in the coupling protein-Mpf interaction extended to the interaction between the coupling protein and TraJ. Notably, the only *in vivo* interaction that was detected using the BTH technology was a strong interaction between the R27 coupling protein and the R27 TraJ protein (Figure 2-3B). The coupling proteins from the RP4, R388, and F plasmids were unable to interact with the TraJ protein, as the β-galactosidase measurements for these interactions gave only background β-galactosidase levels.

Using insertional mutagenesis studies on the transfer region 1 (Tra1) of R27, TraJ was determined to be essential for conjugation (108). As the three non-cognate coupling proteins, TraG^{RP4}, TraD^{F}, and TrwB^{R388} could not interact with TraJ in a BTH screen, it appears likely that these three non-cognate coupling proteins would not be functionally interchangeable with the R27 coupling protein TraG^{R27}. Conversely, these heterologous coupling proteins may be able to interact with the R27 relaxosome components TraH or TraI, or to bind the single-stranded R27 DNA directly. As these coupling proteins can interact with the R27 Mpf structure, a successful interaction with the relaxosome may be sufficient to enable complementation of R27 containing a *traG* mutation. DY330R cells containing R27 harbouring a mini-Tn*10* insertion in *traG* were transformed with the expression vector pMS119EH/HE expressing C-terminal His tagged TraG^{R27}, TraG^{RP4}, TraD^{F}, and TrwB^{R388}. Immunoblot analysis confirmed expression of each coupling protein (Figure 2-4). The coupling protein from R27, TraG^{R27}, was the only protein that restored conjugative transfer of the R27 *traG* mutant (Table 2-3). RP4, R388, and F plasmids harboring coupling protein mutations, were successfully complemented by the pMS119EH/HE vectors expressing their cognate coupling proteins (Table 2-3). The complementation levels did not reach wild type transfer frequency in each case, which may be due to interference in protein interactions caused by the C terminal histidine tag (169).

These results suggest that the TraJ accessory protein is specific for the H-type coupling protein and although non-cognate coupling proteins are able to interact with the H-type T4SS, the heterologous coupling proteins could not complement R27 harbouring a mutation in the coupling protein. The diversity of coupling protein interaction with the T4SS and the specificity of the coupling protein accessory protein and relaxosome interaction has been schematically represented in Figure 2-5.

2.3.4 Functional Co-Inheritance of TraJ and TraG Homologues.

Recent sequence and bioinformatic analyses of the IncHI2 plasmid R478 revealed that an H-type relaxosome/coupling group consisting of *traI*, *traG*, and *traJ* homologues is present in a number of genomic sources (69). This H-type group has been located in genomes that do not encode any well-conserved H-type Mpf components, indicating that *traI-traG-traJ* comprise a module that was inherited independently from T4SS genes. Phylogenetic analysis of TraJ homologues encoded within this co-inherited module has revealed three families of TraJ proteins (Figure 2-6). Notably, there is a clear separation on the phylogenetic tree between the TraJ homologues encoded on chromosomes (Family 1) and the homologues encoded on plasmids and the conjugative transposon SXT (Family 2 and 3). The single exception to this is the TraJ homologue,

Figure 2-4. Expression profile of coupling proteins from the R27, RP4, R388 and F plasmids from the IncH, IncP, IncW and IncF families, respectively. DY330R cells harbouring the R27 plasmid containing a transposon insertion in the *traG* gene, pDT2989, were co-transformed with pMS119EH encoding the coupling proteins from the aforementioned plasmid families. The cellular lysates of the IPTG induced, co-transformed cells were resolved by 10% SDS-PAGE and transferred to a nitrocellulose membrane. The C-terminal His-tagged TraG^{R27} (78 kDa), TrwB^{R388} (56 kDa), TraD^{F} (82 kDa), TraG^{RP4} (70 kDa) proteins were detected by monoclonal anti-His antibody.

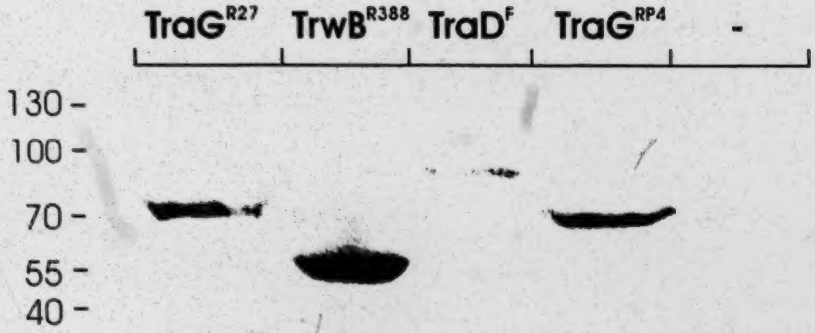
TraG^{R27}
TrwB^{R388}
TraD^{F}
TraG^{RP4}
-
130 -
100 -
70 -
55 -
40 -

Table 2-3. Conjugation results from complementation experiments of coupling protein mutations with cognate and non-cognate coupling proteins.

Expression Vector Containing Coupling Proteins [b]	Transfer Frequency[a] Complementation of R27 *traG* Mutation [c]	Complementation of Cognate Coupling Protein Mutations [d]
$traG^{R27}$	2.3×10^{-2} (5%)	NA
$traG^{RP4}$	$<1\times10^{-7}$	1.7×10^{-2} (6%)
$traD^{F}$	$<1\times10^{-7}$	2.2×10^{-2} (3%)
$trwB^{R388}$	$<1\times10^{-7}$	2.0×10^{-1} (30%)

[a] Transfer frequency expressed as transconjugants per donor. The experiment was repeated in two independent experiments. NA, not applicable.

[b] Expression vector, pMS119EH, was transformed into cells containing respective donor plasmids, which were then induced for 1 hour at a IPTG concentration of 0.4 mM.

[c] Mutations were introduced into *traG* using CAT cassette insertional mutagenesis, deletions or site-specific mutagenesis as described in Materials and Methods. The average transfer frequency of R27 is 4.4×10^{-1}, and a *traG* mutation showed no detectable levels of conjugation ($<1\times10^{-7}$).

[d] The average transfer frequency of RP4 is 2.8×10^{-1}, F is 7.4×10^{-1}, and R388 is 6.6×10^{-1}, and mutations of the coupling protein genes from each respective plasmid resulted in no detectable levels of conjugation ($<1\times10^{-7}$).

Figure 2-5. Summary of protein interactions between VirB10-homolog TrhB (red), coupling proteins (blue), relaxosome proteins (green), and the coupling protein accessory protein (purple). Lower-case letters indicate incompatibility group. Solid and dotted arrows indicate interactions identified in this study and previously described interactions(46, 124, 171), respectively.

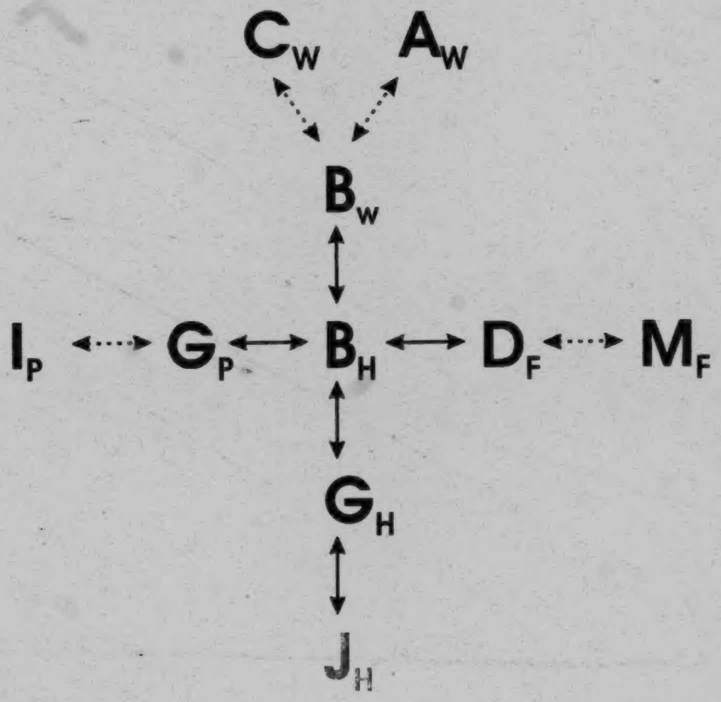
C_W
A_W
B_W
I_P
G_P
B_H
D_F
M_F
G_H
J_H

Figure 2-6. The TraJ protein phylogeny. The bootstrap support values of the phylogenetic tree are from the p-distance neighbor-joining method. Boxed sequences denote the genes used in BTH studies. Accession Nos. R478 (CAE51739), R27 (NP_058330), SXT (AAL59721), R391 (AAM08039), pCAR1 (NP_758667), Rts1 (NP_640164), *Polaromonas* sp. JS666 (ZP_00363614, *note: the *Polaromonas* sp. JS666 coding sequence PJS6w01001858 has been reannotated from the NCBI entry to include 29 more codons and an alternate start codon), *Haemophilus somnus* (ZP_00123133), *Xanthomonas axonopodis pv. citri* (NP_642577), *Pseudomonas fluorescens* (ZP_00087889), *Burkholderia fungorum* (ZP_00030777), *Pseudomonas aeruginosa* (AAN62289), *Yersinia pseudotuberculosis* (CAF28502), and *Erwinia carotovora* (YP_048677.1).

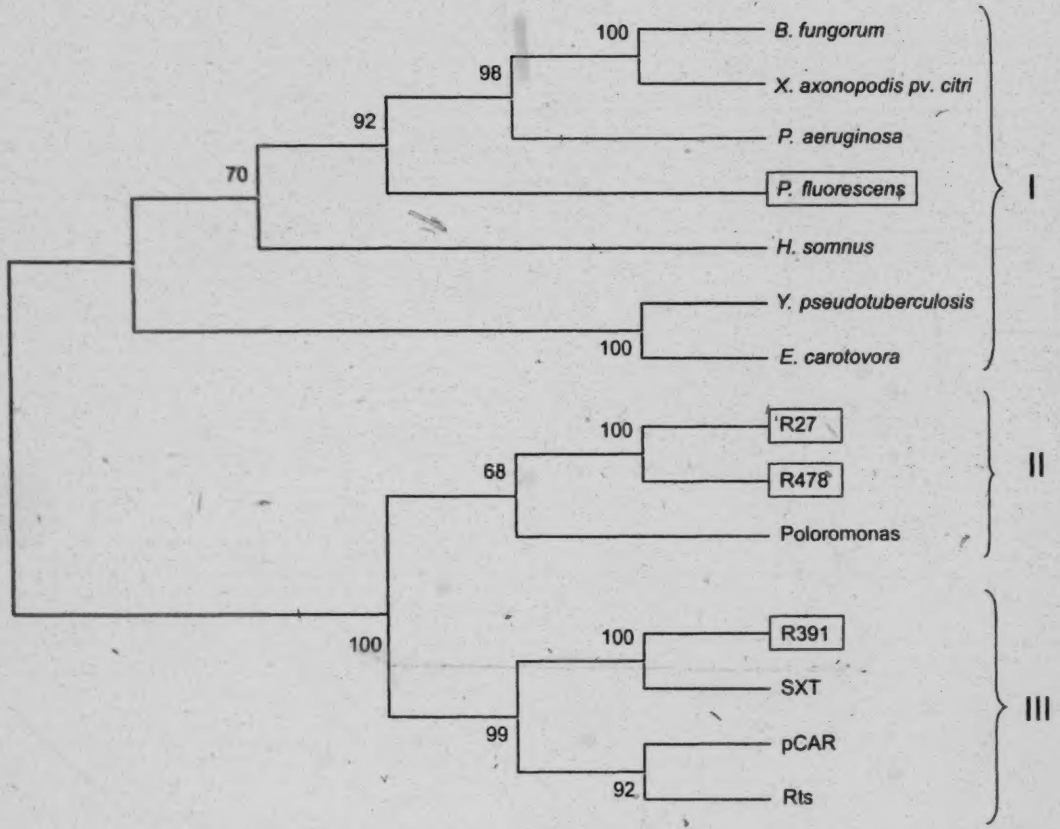
100
B. fungorum
98
X. axonopodis pv. citri
92
P. aeruginosa
70
P. fluorescens
H. somnus
Y. pseudotuberculosis
100
E. carotovora
I
100
R27
68
R478
Poloromonas
II
100
R391
100
SXT
99
pCAR
92
Rts
III

PJS6w01001858, encoded from *Polaromonas* sp. JS666. The *Polaromonas* TraJ-homologue is grouped within Family 2, with the IncH plasmids, R27, and R478. The NCBI database reference for *Polaromonas* (NZ_AAFQ01000004) simply describes the molecular type as genomic DNA. Furthermore, all of the TraJ-homologues encoded from a chromosomal source have an additional approximately 30 aa at the N terminus of the protein. The only chromosomal-encoded TraJ homologue that does not contain this N terminal addition is from *Polaromonas* sp. JS666. A phylogenetic tree was generated in which the N-terminal 30 aa domain was removed from each chromosomal-encoded TraJ homologue, and there was no difference observed in the protein grouping.

To ascertain if an interaction between the coupling protein and accessory protein was a common feature within this module of *traI-G-J* genes, we selected representative TraJ homologues from each of the three Families. Four TraJ homologues encoded on R27 (Family 2), R478 (Family 2), R391 (Family 3), and the *Pseudomonas fluorescens* chromosomal DNA (Family 1) were cloned into the BTH vector pKT25. The coupling protein homologues encoded on each genomic source were subsequently cloned into the BTH vector, pUT18C. The *in vivo* interaction data clearly demonstrate that the cognate TraJ-TraG interaction from each distinct genomic source is conserved (Figure 2-7). The diversity of this TraJ-TraG interaction was characterized by using the BTH technology to determine if non-cognate TraJ homologues would interact with each coupling protein homologue. As expected, the highly related IncH plasmids, R27 and R478 (Family 2), encoded TraJ homologues which were interchangeable in interactions with their coupling proteins (Figure 2-7). The R391 plasmid-encoded TraJ (Family 3) and TraG homologues were not able to interact with the respective proteins from the three other genomic sources. Intriguingly, the coupling protein homologue from the *P. fluorescens* genome showed a strong interaction with TraJ from R27 (Family 2). In contrast, there was no evidence of

Figure 2-7. Bacterial two-hybrid data demonstrating the conservation of the interaction between TraJ and TraG homologs. The *traJ* homologous genes from R27, R478, R391 and *Pseudomonas fluorescens* (Pfl) were cloned into the BTH plasmids pKT25. The *traG* homologous genes from the same genomic sources were cloned into pUT18C and co-transformed into BTH101 in a pairwise combination with each pKT25-TraJ construct. The BTH controls are BTH101 cells containing pUT18C and pKT25 (negative control), and pUT18C-leucine zipper with pKT25-leucine zipper (positive control). Liquid cultures of BTH101 containing the BTH vectors were analyzed for β-galactosidase activity using a Miller assay (134). A representative experiment is shown.

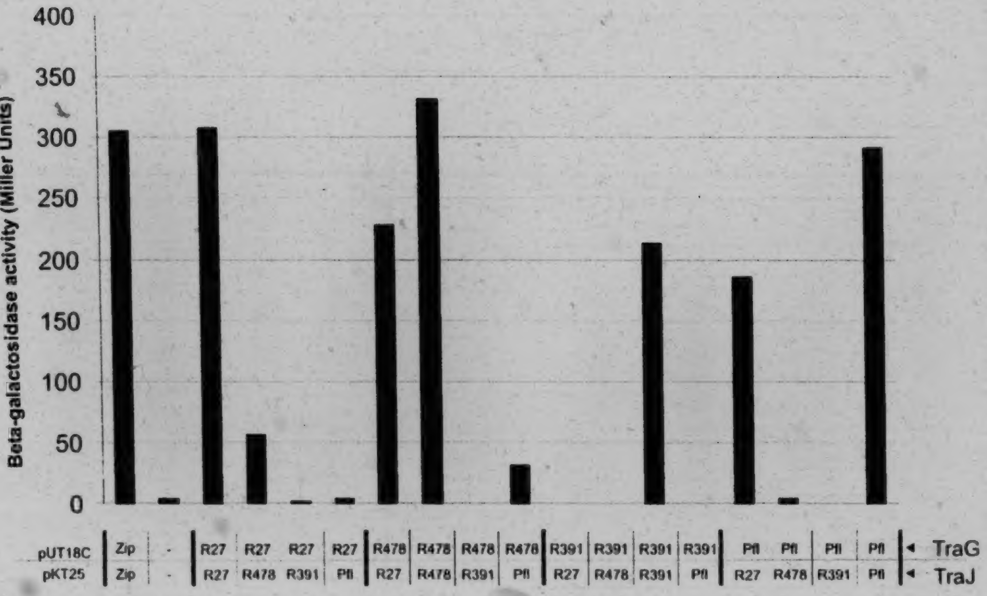
Beta-galactosidase activity (Miller Units)
400
350
300
250
200
150
100
50
0
pUT18C
pKT25
Zip
Zip
-
-
R27
R27
R27
R478
R27
R391
R27
Pfl
R478
R27
R478
R478
R478
R391
R478
Pfl
R391
R27
R391
R478
R391
R391
R391
Pfl
Pfl
R27
Pfl
R478
Pfl
R391
Pfl
Pfl
TraG
TraJ

an interaction with the opposite configuration, in which TraG from R27 was tested with the *P. fluorescens* TraJ homologue (Family 1).

2.4 Discussion

The Type IV secretion system (T4SS) can be classified into three subfamilies: the effector translocation system, the DNA uptake and release system, and the conjugative system (29). The conjugative system is often encoded on self-transmissible plasmids residing in Gram-negative and Gram-positive bacteria. Determining the architecture of plasmid-encoded T4SS has been the focus of recent studies on incompatibility group F, W, P, and H plasmids. A bacterial-two hybrid (BTH) screen using the T4SS proteins of the IncHI1 plasmid R27 revealed an interaction between the coupling protein, TraG, and mating pair formation (Mpf) complex protein, TrhB (66). Here, we extend the investigation to resolve the conjugative architecture surrounding the R27 coupling protein. BTH *in vivo* technology was used to detect interactions between the R27 coupling protein and three essential transfer proteins, TraJ, TraH, and TraI, which are not involved in conjugative pili formation. An *in vivo* interaction was detected between TraG and TraJ, and subsequently confirmed using an immunoprecipitation technique. The characterization of the Tra1 region of R27 determined that TraJ is essential for IncH plasmid transfer but as TraJ is not required for pili formation, it was initially identified as a relaxosome protein (108). Subsequent analysis of TraJ has revealed four predicted TM domains that are well-conserved among the numerous TraJ homologues, indicating a membrane-association that is dissimilar to the cytoplasmic-associated relaxosome proteins. Furthermore, the discovery that TraJ is able to interact with the membrane-associated R27 coupling protein has led to the re-classification of TraJ as a coupling protein-accessory protein.

The requirement of an accessory protein by a coupling protein has to our knowledge not been reported previously. A corresponding accessory protein, containing multiple TM domains is not present in the well-characterized conjugative plasmids F, RP4, or R388. The Mpf of the IncH and IncF plasmids are related and have recently been grouped as F-type (110); the presence of an accessory protein encoded by the IncH plasmid R27 represents a distinct separation between these two systems. Furthermore, our BTH screen revealed that the coupling proteins encoded by the F, RP4, and R388 plasmids were not able to interact with the R27 accessory protein, TraJ, indicating that coupling protein-accessory protein interaction is highly specific.

A direct interaction between the relaxase, a relaxosome component found in all self-transmissible plasmids, and the coupling protein has been demonstrated with RP4 and R388 plasmids from the incompatibility group P and W plasmid families, respectively (124, 169). Conversely, the coupling protein from the F plasmid, TraD, has only been found to interact with relaxosomal component TraM (46). An interaction between TraD and the F plasmid relaxase, TraI, has not been detected although attempts have been made to find this interaction (L.S. Frost, personal communication). A potential deficiency of the BTH system is the steric interference that may be caused by the fusion of the *Bordetella pertussis* adenylate cyclase domains to the proteins under study. Therefore, additional interaction techniques are required to confirm the lack of an interaction between R27-encoded TraG and TraI, prior to concluding that the R27 plasmid is more F-like than P-like with respect to the coupling protein-relaxosome interaction.

Complementation of conjugative plasmids containing coupling protein mutations by non-cognate coupling proteins has indicated that the Mpf-coupling protein interaction is non-specific (25, 83, 124). TraG, encoded on the IncP RP4 plasmid, has been found to functionally interact with the T4SS of the Ti plasmid in the mobilization of the IncQ plasmid RSF1010 (83). Furthermore, the RP4 coupling protein can interact with the

IncW R388 Mpf proteins to facilitate the mobilization of RSF1010 (25). In both studies, however, TraG was unable to mobilize the Ti plasmid or R388 plasmid, implying that the coupling protein was unable to interact with non-cognate relaxosomal proteins. In a recent study, the coupling proteins from the IncW, IncN, and IncX families were discovered to interact with cognate and heterologous Mpf proteins (124). Notably, the specificity within the conjugative system was determined to exist between the coupling protein and the relaxosome; the coupling protein from the IncN plasmid, pKM101, could not interact with the R388 relaxosome component TrwA (124).

We have expanded these studies to include the RP4, R388, F, and H plasmids. TrhB is an R27 Mpf protein and a well-conserved VirB10 homologue. We determined through BTH analysis that this Mpf protein could interact with the coupling proteins from the RP4, R388, F, and H plasmids. The strength of the interactions between non-cognate coupling proteins and TrhB, as determined by a Miller assay showed similar levels but the interaction between TrhB and TraG^{RP4} consistently yielded Miller units in excess of the BTH positive control. The strength of the interaction may not be surprising given the ability of the RP4 coupling protein to interact with the Mpf proteins of the Ti and R388 plasmids. The interaction between TraG^{RP4} with such a diverse array of Mpf systems may represent an additional tool that facilitates the transmission and maintenance of the IncP plasmid in a broad host range of bacteria (153).

A module consisting of three genes, *traI-traG-traJ*, has been found to be present in a number of genomic sources, including a conjugative transposon, plasmids, and chromosomes (Fig. 2-8A) (69). A phylogenetic analysis of TraJ homologues revealed a clear separation of those accessory proteins encoded on the conjugative transposon (SXT) and plasmids (R27, R478, R391, pCAR1, Rts1), and proteins encoded on the chromosomes (*Polaromonas* sp. JS666, *Haemophilus somnus, Xanthomonas axonopodis pv. citri, Pseudomonas fluorescens, Burkholderia fungorum, Pseudomonas*

Figure 2-8. A) Genetic organization of the *traJ* and *traG* homologous sequences from five plasmids (R27, R478, R391, pCAR1, Rts1), one conjugative transposon (SXT), and eight chromosomes (*Polaromonas* sp. JS666, *Haemophilus somnus, Xanthomonas axonopodis pv. citri, Pseudomonas fluorescens, Burkholderia fungorum, Pseudomonas aeruginosa, Yersinia pseudotuberculosis* and *Erwinia carotovora*). The *traJ* and *traG* homologous sequences are shown as green and blue arrows, respectively. The source of the genes is shown on the left with the gene prefix in parentheses (example: the R27 gene 'G' corresponds to '*traG*') .

B) Schematic representation of the homology shared by R27-encoded TraG and TraJ proteins with an FtsK DNA translocase, *Schewanella oneidensis* MR-1 (NP_717901). Arrows indicate the region of FtsK to which the R27 transfer proteins share the greatest level homology. The level of this homology is represented as a percent identity with the alignment length represented in parentheses, as determine by EMBOSS pairwise local alignment. TM regions are indicated by hatched regions as predicted by TMHMM. The yellow boxes indicate Walker A boxes as determined by ScanProsite; the white boxes indicate putative Walker B boxes predicted by similarity to the Walker B motif (R/K-X(7-8)-h(4)-D) (201).

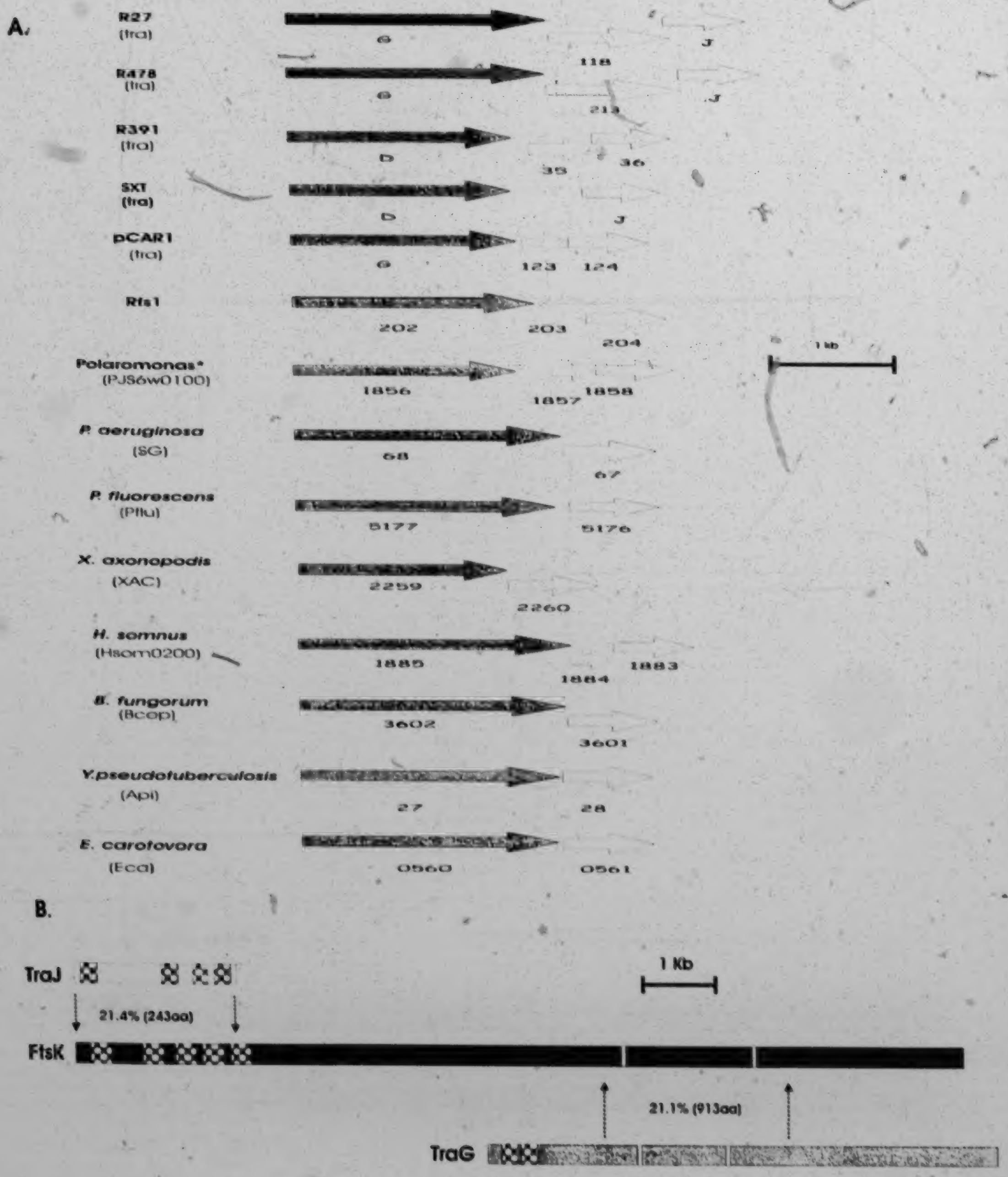
A.
R27
(tra)
G
J
R478
(tra)
G
118
213
J
R391
(tra)
D
35
36
SXT
(tra)
D
J
pCAR1
(tra)
G
123
124
Rfs1
202
203
204
Polaromonas*
(PJS6w0100)
1856
1857
1858
1 kb
P. aeruginosa
(SG)
68
67
P. fluorescens
(Pflu)
5177
5176
X. axonopodis
(XAC)
2259
2260
H. somnus
(Hsom0200)
1885
1884
1883
B. fungorum
(Bcep)
3602
3601
Y.pseudotuberculosis
(Api)
27
28
E. carotovora
(Eca)
0560
0561
B.
TraJ
21.4% (243aa)
FtsK
1 Kb
21.1% (913aa)
TraG

aeruginosa, *Yersinia pseudotuberculosis*, and *Erwinia carotovora*). The major exception to this phylogenetic separation is the TraJ homologue encoded on *Polaromonas*. All of the chromosomally-encoded TraJ homologues, except the TraJ encoded on *Polaromonas*, were grouped into Family 1 of the phylogenetic tree. The TraJ homologue from *Polaromonas* was grouped in Family 2 with the IncH plasmids R27 and R478. In addition, with the exception of *Polaromonas* all of the TraJ homologues encoded on chromosomes were larger than the homologues encoded on the plasmids or conjugative transposon. Sequence alignments revealed an N terminal 30 amino acid region that was present on the TraJ homologues from the chromosome genomic sources.

Another significant difference between *Polaromonas* and six of the seven chromosomes under study was the presence of an open reading frame (ORF) between the *traG* and *traJ* homologues (Fig. 2-8A). *H. somnus* also contained an ORF between the two homologueous genes. Together, there is evidence to suggest that the *traI-traG-traJ* module present in the *Polaromonas* species phylogenetic analysis indicates that the genomic source of this module may be a plasmid, although this was not indicated in the initial draft assembly of the *Polaromonas* genome.

Notably, we observed that a genomic source containing an R27 *traJ* homologue always contained a *traG* homologue in close proximity (<1.5 kb).This co-inheritance yielded proteins that retained the ability to interact; BTH analysis revealed a strong interaction between the cognate homologues of TraG and TraJ encoded in R27, R478, R391, and *Pseudomonas fluorescens*. These genomic sources represented the three families of TraJ homologues, as determined by phylogenetic analysis. Once again, the accessory protein-coupling protein interaction was found to be specific as only the TraJ and TraG homologues encoded on the IncH plasmids R27 and R478 (Family 1) were able to be exchanged and retain the ability to interact. The homologueous proteins from R391 (Family 2) did not demonstrate any interaction with non-cognate coupling or accessory proteins. The coupling protein homologue from *P. fluorescens* (Family 1) was able to interact with TraJ from R27, however this interaction was not reproducible in the opposite orientation (TraG from R27 and TraJ homologue from *P. fluorescens*). The finding that a reproducible, non-cognate interaction between TraG and TraJ homologues was limited to genomes within the same family confirms the specificity of the coupling protein-accessory protein interaction.

An analysis of genomes containing the module of *traI-G-J* genes revealed that there was extensive variability in the distance between the *traI* and *traG* genes, ranging from overlapping sequences on the pCAR1 plasmid genome, to a separation of 68.8 kbp on the *Xantham axonopodis pv. citri* chromosomal genome (69). Conversely, the IncH plasmid R27 had the maximum distance separating the *traG* and *traJ* genes, and this was at a distance of only 1095 bp. The genetic proximity and orientation of *traG* and *traJ* genes are shown in Figure 2-8A. Notably, *traG* is upstream of the *traJ* gene in each of the genomic sources.

During the search of the NCBI databanks for homologues of TraJ from IncH R27, we identified that TraJ shares sequence similarity with the FtsK/SpoIIIE family of proteins. IncHI1 R27 TraJ has limited sequence similarity to the N terminus of SpoIIIE (NP_345365) from *Streptococcus pneumoniae* (27% identity over 110 aa, and 20.1% identity over an alignment length of 249 aa). The N termini of these DNA translocases contain between four or five TM domains; this membrane-associated region has been demonstrated to be involved in targeting SpoIIIE and FtsK to the site of cell division (16, 174, 203). Notably, the TraJ protein also contains four well-conserved TM domains, and the accessory protein is essential for the conjugative transfer of R27 (69, 108).

The sequence and structural similarity of coupling proteins to FtsK/SpoIIIE-type proteins has been well-documented (52). The sequence similarity is strongest in the Walker motifs located in the C terminal regions of these ATPases. An alignment of

R27-encoded TraJ and TraG to FtsK (NP_717901) of *Shewanella oneidensis* illustrates the domains to which the conjugative transfer proteins share sequence similarity (TraJ: 21.4% identity over an alignment length of 243 aa; TraG: 21.1% identity over an alignment length of 913 aa) (Figure 2-8B).

Co-inheritence of *traG* and *traJ* sequences has been observed in numerous chromosomal, plasmid and other mobile genetic elements (17) and this gene 'pair' encodes for conjugative transfer proteins that function together as indicated by the interaction data presented in this study. We propose the domains comprising TraG and TraJ together resemble the domain architecture of the FtsK/SpoIIIE DNA translocase proteins. The arrangement of features in these translocases includes five N-terminal TM domains followed by Walker A and B NTP-binding motifs. Similarly, the TraJ peptide is comprised almost entirely of four conserved TM domains and TraG contains two N-terminal TM domains as well as the remainder of the DNA translocase domains, including the Walker A/B motifs. It is thereby possible that members of the FtsK/SpoIIIE family embody the Rosetta Stone protein sequence (129) for the now separately-encoded TraG and TraJ and this observation enables the prediction of the functional roles of these proteins during plasmid transfer. The coupling-accessory protein complex encoded by R27 may form a stable DNA translocase that mediates the transfer of DNA into the secretory conduit of the Mpf. As TraJ homologues are not found in other well-characterized incompatibility groups such as IncF or IncP, coupling proteins can seemingly accomplish both membrane localization and DNA translocation in the absence of the TraJ-like accessory protein; each member of the coupling protein family has two TM domains that are sufficient for localization to the cytoplasmic membrane, and the structural and functional similarities between TraG and DNA translocases has been established (218). Furthermore, the majority of conjugative DNA transfer systems do not encode a TraJ homologue, however, in genetic elements producing both TraG and TraJ, the accessory protein may provide additional functions other than membrane localization and stabilization. Among R27-encoded TraJ and the numerous TraJ homologues, two positively-charged residues (typically containing Lys and Arg) between the second and third TM domains have been observed (17), and it may be possible that this accessory protein is involved in translocation of the single-stranded DNA intermediate through the cytoplasmic membrane.

Chapter 3

Subcellular Localization and Functional Domains of the Coupling Protein, TraG, from R27

Portions of this chapter have been published as:

Gunton, J. E., Gilmour, M.W., Alonso, G. and Taylor, D.E. (2005) Subcellular localization and functional domains of the coupling protein, TraG, from Incompatibility H1 plasmid. *Microbiology*, 151(11): 3549-3561

RT-PCR analysis was performed by Dr. G. Alonso.

3. Subcellular localization and functional domains of the coupling protein, TraG, from Incompatibility H1 plasmid R27

3.1 Introduction

Horizontal gene transfer enables the rapid dissemination of genetic material between prokaryotic organisms. The primary mechanism of this genetic exchange is conjugation (29) and the proteins that are essential for conjugative transfer are encoded on plasmids or conjugative transposons. The successful transfer of plasmid DNA from donor to recipient cell is due to the assembly of protein complexes within the cytoplasm, periplasm, cytoplasmic-membrane, and outer-membrane of the donor cells. The cytoplasmic relaxosome is a nucleo-protein complex composed of plasmid DNA and plasmid-encoded proteins, and is responsible for DNA processing prior to transfer of plasmid DNA to the membrane-associated type IV secretion system (T4SS) (106, 152). The T4SS, also referred to as the mating pair formation complex (Mpf), is comprised of 12-15 membrane-associated proteins which span the inner and outer membrane of the donor cell (75, 110). A multimeric protein, the coupling protein, is responsible for bridging the relaxosome and Mpf complexes thereby facilitating the conjugative transfer of plasmid DNA (66, 122, 124).

Coupling proteins are polytopic inner membrane proteins containing two transmembrane regions near the amino (N) terminus. The N and carboxy (C) terminal regions of the proteins are located within the cytoplasm and a periplasmic region separates the two transmembrane domains (39, 72, 103, 116, 151, 169). The three dimensional structure of the cytoplasmic domain of TrwB, a coupling protein encoded on the incompatibility (Inc) group W plasmid R388, revealed a hexameric, spherical particle with a central channel that ranges in diameter from 7-8 Å at the cytoplasmic side to 22 Å at the membrane end (72). Biochemical analysis of coupling proteins from R388, RP4 (IncPα) and F (IncFI) plasmids have revealed that this family of proteins are able to bind in a non-specific fashion to DNA (94, 137, 169). In addition, coupling proteins have conserved motifs such as the Walker-type nucleoside triphosphate (NTP) binding domains. Recent analysis on TrwB has revealed that this coupling protein is a DNA-dependent ATPase (186). Mutational analyses of the Walker motifs of TraG, the coupling protein from RP4, indicated that the Lys and Asp residues, at positions 187 and 449 of RP4, were essential for conjugation of the IncP plasmid (14).

The most recent advance in the study of coupling proteins has been the identification of the Mpf component to which the coupling protein binds. The coupling proteins TraG and TrwB from the R27 and R388 plasmids were both independently determined to interact with the VirB10-like proteins, TrhB and TrwE, respectively (66, 124). In the Ti plasmid of *Agrobacterium tumefaciens*, VirB10 is a well-conserved T4S component and it has been recently proposed to be the ATP energy sensor of the T4SS (28).

The cellular location of the coupling protein has only been demonstrated in *A. tumefaciens*. VirD4 was found to associate with the poles of *A. tumefaciens*, and this polar localization was determined to occur in the absence of other essential conjugation proteins (103). Subsequent localization experiments with *A. tumefaciens* revealed that a T4S protein, VirB6, co-localized with VirD4 at the poles of the cell (96, 99). In contrast, a GFP fusion to the T4S protein, TrhC, from R27 revealed that this VirB4 homologue was found at random positions around the periphery of the cell (67). The fluorescent foci formed when TrhC was labeled with GFP resulted in membrane-associated protein complexes that required a number of R27 T4S proteins (68).

Our goal was to characterize the coupling protein TraG from the IncHI1 resistance plasmid R27, originally isolated from *Salmonella enterica* serovar Typhi (108, 176). The IncHI plasmids are unique in that conjugative transfer is optimal at 30°C while at 37°C transfer is significantly reduced (189). Reverse transcriptase-polymerase chain reaction demonstrated that *traG* expression is reduced at 37 °C, as compared with 30°C. Site-specific mutagenesis within *traG* demonstrated that well-conserved residues in the NTP-binding Walker regions are essential for R27 conjugation. In addition, bacterial two-hybrid and immunoprecipitation interaction data determined that substitutions in the four periplasmic-spanning residues of TraG prevented an interaction with the VirB10 homologue, TrhB. Notably, these periplasmic substitutions did not completely abolish conjugative transfer of the R27 plasmid. Finally, immunofluorescence microscopy demonstrate TraG formed fluorescent foci at random positions in the membrane of *Escherichia coli*. This localization is in contrast to the VirD4 polar localization in *A. tumefaciens*, The position and number of foci formed by TraG are similar to the distribution of TrhC within the cell.

3.2 Experimental Procedures

3.2.1 Bacterial strains, growth conditions and plasmids.

Escherichia coli strains used in this study are listed in Table 3-1. All strains were grown in Luria Bertani (LB) broth (Difco Laboratories, Detroit, Mich.) at 37 °C with shaking at 200 RPM unless otherwise stated. Antibiotics used in this study are listed with final concentrations: ampicillin (100 µg ml^{-1}), kanamycin (50 µg ml^{-1}), tetracycline (10 µg ml^{-1}), rifampicin (50 µg ml^{-1}), nalidixic acid (20 µg ml^{-1}), and trimethoprim (25 µg ml^{-1}).

Table 3-1. Bacteria and plasmids used in this study.

Bacterial strain or plasmid	Relevant genotype, phenotype, or characteristic[†]	Source or reference
E. coli		
DH5α	*supE44 lacU169 (Φ80lacZΔM15) hsdR17 recA1 endA1gyrA96 thi-1 relA1*	Invitrogen
XL1-Blue	*recA1 endA1gyrA96 thi-1hsdR17 supE44 relA1* lac [F' *proAB lacI*^{q}ZΔ*M15* Tn*10*]	Stratagene
DY330	W3110 *ΔlacU169 gal-490* λcI857 Δ(*cro-bioA*)	(35)
DY330R	Temperature-resistant revertant; Rif^r	(108)
DY330N	Temperature-resistant revertant; Nal^r	(108)
BTH101	F $^-$*cya-99 araD139 galE15 galK16 rpsL1* (Str^r) *hsdR2 mcrA1 mcrB1*	(101)
RG192	*ara leu lac*	(187)
DT1942	RG192 (Rif^r) with pDT1942	(126)
Plasmids		
pMS119EH	Expression vector; P$_{tac}$-lacI^q; pMB1 origin of replication; Amp^r	(181)
pJEG217	*traG,* 2.1 kb *Eco*RI/*Bam*HI-digested R27 (IncH) PCR product in pMS119EH; Amp^r	This study
pJEG217-G210D	pJEG217 with G210D substitution; Amp^r	This study
pJEG217- K211R	pJEG217 with K211R substitution; Amp^r	This study
pJEG217-ΔGK	pJEG217 with ΔGK (residues 210-211 aa) deletion; Amp^r	This study
pJEG217-D510S	pJEG217 with D510S substitution; Amp^r	This study
pJEG217-E511K	pJEG217 with E511K substitution; Amp^r	This study
pJEG217-ΔDE	pJEG217 with ΔDE (residues 510-511 aa) deletion; Amp^r	This study
pMWG385	pJEG217 with residues FRSD substituted for SSSS at positions 40-43 aa; Amp^r	This study
pKT25	p15A origin of replication; encodes CyaA$_{1-224}$;Km^r	(101)
pUT18C	ColE1 origin of replication; encodes CyaA$_{225-399}$; Amp^r	(101)
pKT25-zip	leucine zipper of GCN1 (BTH positive control); Km^r	(101)
pUT18C-zip	leucine zipper of GCN1 (BTH positive control)	(101)
pUT18C-trhB	1.4 kb *Pst*I/*Bam*HI-digested R27 (IncH) PCR product in pUT18C; Amp^r	(66)
pKT25-traG	2.1 kb *Bam*HI/*Kpn*I-digested PCR product in pKT25; Kan^r	(66)
pKT25-traG:S4	2.1 kb *Bam*HI/*Kpn*I-digested PCR product in pKT25 with residues FRSD substituted for SSSS at positions 40-43 aa ; Kan^r	This study
pMS119EH-trhB$_{FLAG}$	1.4 kb *Eco*RI/*Bam*HI-digested PCR product in pMS119EH; Amp^r	(66)
pDT1942	derepressed transfer mutant of R27: R27 ::TnlacZ	(126)
pDT3152	pDT1942 with a trimethoprim resistance dihydrofolate reductase gene (*dhfrIIc*) inserted into *traG*; Tp^r	This study

[†] Abbreviations: Nal^r, nalidixic acid resistance, Rif^r, rifampicin resistance, Tc^r, tetracycline resistance, Km^r, kanamycin resistance, Amp^r, ampicillin resistance, Str^r, streptomycin resistance, Cm^r, chloramphenicol resistance.

3.2.2 RNA extraction.

A flask containing 100 ml of LB was inoculated from an overnight culture of *E. coli* harboring either wild type R27 or de-repressed R27 (drR27) grown at either 30 °C or 37 °C (126). The 100 ml culture was grown at the same temperature as the overnight culture and the cells were harvested when the culture reached an OD_{600} of 0.3. Total bacterial RNA was purified using the RNeasy Midi Kit (Qiagen), in accordance with the manufacturer's directions. To ensure that the RNA was devoid of contaminating DNA, the preparation was treated with Turbo DNase (Ambion). The RNA was precipitated with ethanol and dissolved in diethyl pyrocarbonate-treated water. RNA levels were quantified using an Ultraspec 4000 spectrophotometer (Pharmacia).

3.2.3 Reverse transcriptase-Polymerase chain reaction (RT-PCR)

For RT-PCR amplification of *traG* transcripts, 2 µg of total RNA was used as template. RNA was retrotranscribed into cDNA utilizing the SuperScriptII RT (Invitrogen) with the random hexamers included in the kit. A 1/10 dilution of each retrotranscription was subjected to PCR using the primer pairs specific for the two adjacent genes (Table 3-2). A negative control containing no template and a negative control with total RNA that had not been retrotranscribed were included in each PCR reaction. A positive control of R27 template DNA was prepared for each primer pair and PCR reactions generated products of predicted sizes. The *E. coli pfkA* housekeeping gene, which encodes phosphofructokinase, was included as a positive control for the bacterial transcripts. Amplified products were resolved on a 1 % agarose gel stained with ethidium bromide. RT-PCR amplifications were performed at least twice with total RNA preparations obtained from a minimum of three independent extractions. Similar results were obtained in all experiments.

Table 3-2. Primers used for RT-PCR analysis of the transcriptional profile and mutational analyses of the *traG* gene of R27

Primer ID	Primer Name	Sequence (5'-3')[†]	Predicted Product Size (bp)
1-8	*traI-traG-f*	AATAGGGGTGTGCCGTTTTAC	523
	traI-traG-r	TGCCACCATGCTCCACCAA	
1-9	*traG118-2-f*	TCCTGCCATTCGGTAAACTTCA	405
	traG118-2-r	CGCATAATAACTTCTCTGGGTCAA	
Control	*pfkA-f*	GTGGCGGTACGTTCCTCGGTTCT	762
	pfkA-r	TTTTTCGCGCAGTCCAGCCAGTC	
TraG:Tp^{r}	*traG-Gil163-f*	GGGCAATAACGCCATCTTTGCTGTTGACCGGCGGGCACCCTTCGCTGCTGCCCAAGGTTG	237
	traG-Gil164-r	ACGACCCTGTGCGAGTAAGTTTATCATTGAATTGTTTATGGTGCACTCAACCGTGACTTC	
TraG:G210D	*traG-Gun46-f*	CGTCGGTACCGMTAAAACGGTAC	2085
	traG-Gun47-r	GTACCGTTTTAKCGGTACCGACG	
TraG:K211R	*traG-Gun44-f*	CGGTACCGGTABAACGGTACTTC	2085
	traG-Gun45-r	GAAGTACCGTTVTACCGGTACCG	
TraG:ΔGK	*traG-Gun54-f*	CCTCATTACCGGAAACGTCGGTACCGTACTTCAGCGCTTACTGAGCATC	2085
	traG-Gun55-r	GATGCTCAGTAAGCGCTGAAGTACGGTACCGACGTTTCCGGTAATGAGG	
TraG:D510S	*traG-Gun48-f*	GTATTTTCGTCAVCGAAGCACAC	2085
	traG-Gun49-r	GTGTGCTTCGBAGACGAAAATAC	
TraG:E511K	*traG-Gun50-f*	GTATTTTCGTCGACMAAGCACACTC	2085
	traG-Gun51-r	GAGTGTGCTTKGTCGACGAAAATAC	
TraG:ΔDE	*traG-Gun52-f*	GAATCAGTATTTTCGTCGCACACTCTGCCATAAAC	2085
	traG-Gun53-r	GTTTATGGCAGAGTGTGCGACGAAAATACTGATTC	
TraG:S4	*traG-Gil169-f*	CGTCATAATGCTGGTTATGGGCTCTAGTTCATCTGGGGTGAATATTGCCCC	2085
	traG-Gil170-r	GGGGCAATATTCACCCCAGATGAACTAGAGCCCATAACCAGCATTATGACG	

[†] Modified nucleotides (B,K,M,V) were incorporated into primer sequences to generate pJEG217 substitutions. These modifications correspond to mixtures of nucleotides, where B=T+C+G, K=T+G, M=A+C, V=A+C+G. Sequencing reactions confirmed the single nucleotide which was used for the substitution reaction.

3.2.4 Site-directed mutagenesis of Walker A and B motifs of TraG.

Site-specific mutagenesis of the R27 coupling protein was performed as described previously (68). Briefly, the template for the site-directed mutagenesis experiments was pJEG217 (pMS119EH-TraG$_{His6}$). Complementary pairs of oligonucleotides were designed to mutate the Walker A region and Walker B region of the *traG* gene (Table 3-2). Similarly, primer pairs were used to mutate the periplasmic region (5' ATGGGCTTTCGTTCAGATGGGGTG) of *traG*, where the underlined region indicates the nucleotides that were substituted (Table 3-2). *Pfu Turbo* polymerase (Stratagene) was used in a thermocycling reaction with the Walker A or Walker B complementary primers. The parental DNA template of wild type *traG* gene was digested with *Dpn*I (Invitrogen). Newly synthesized DNA containing mutations within the Walker A or B motifs was transformed into XL1-Blue *E. coli* ultracompetent cells (Stratagene) for re-circularization and propagation. The pJEG217 constructs containing Walker A or B mutations were sequenced within the appropriate motifs, and restriction digestion was used to confirm the size of the *traG* constructs. Immunoblot analysis was used to ensure that the mutations within the TraG $_{His6}$ constructs did not affect the stability or expression of the coupling protein. A monoclonal anti-His antibody (Invitrogen) was used to probe the nitrocellulose membrane after transfer from resolving the whole cell lysate by10 % SDS-PAGE. For detection purposes, a secondary rabbit anti-mouse antibody conjugated to horseradish peroxidase (HRP) was used.

3.2.5 Insertional mutagenesis of traG on drR27

A gene disruption in *traG* was created using the *E. coli* recombination system, as described previously (108, 222). A trimethoprim resistant dihydrofolate reductase cassette, *dhfrIIc*, was inserted into *traG* of R27. A linear DNA construct was created using PCR primers that amplified *dhfrIIc* and also contained ~ 40 base pairs (bp) terminal arms homologueous to *traG* at positions 528-563 and 1545-1585 (Table 3-2).

Presumptive *traG* mutants were screened using PCR to detect a 237 bp size increase in *traG*.

3.2.6 Conjugation

Complementation experiments with R27 were performed as described previously (108, 189). Briefly, DY330R cells containing drR27 plasmid or an R27 plasmid containing a mutation within the coupling protein gene, *traG*, were grown at 28°C. DY330N recipient cells were also grown at 28 °C. pDT3152, an R27 plasmid containing a *traG* mutation, was complemented by transforming donor cells with pJEG217 or variants. Upon reaching an OD_{600} of 0.5-0.7, donor cells containing the complementation constructs were induced for 1 hour with isopropyl-β-D-thiogalactoside (IPTG) at a final concentration of 0.4 mM. Donor and recipient cells were incubated for 16 hours at 28°C. Transconjugants and donors were then plated on selective media after serial dilutions. The transmission frequency was expressed as transconjugants per donor.

3.2.7 Immunofluorescence (IMF) microscopy.

E. coli cells containing pJEG217 were processed for immunofluorescence microscopy according to Kumar *et al.* (103). Briefly, *E. coli* cells were grown at 30°C, unless stated otherwise, to an OD_{600} of 0.5-0.7, then treated for 1 hour with IPTG at a final concentration of 0.4 mM. After washing with phosphate buffered saline (PBS), cells were fixed with 4% paraformaldehyde for 1 hour on ice. The cells were washed three times with PBS and resuspended in 300 μl of 25 mM Tris-HCl, 1.8 % glucose, and 10 mM EDTA pH 8.0. The resuspension was mixed for 10 minutes on ice with lysozyme at a final concentration of 2 mg ml^{-1}. 50 μl of the treated cells were spotted onto wells of poly-L-lysine coated slides and allowed to adhere for 15 minutes at room temperature. Excess liquid was aspirated from the slides, and the dry slides were washed 10 times with PBS before the addition of 2 % bovine serum albumin (BSA) blocking solution. Slides were incubated with BSA at 37°C for 30 minutes, prior to the addition of mouse anti-His antibodies (Invitrogen). Slides were incubated at 4°C overnight. After washing 10 times with PBS, the slides were incubated with goat anti-mouse antibody conjugated to Alexa Fluor 488 for 1 hour at room temperature. After further washing with PBS, the slides were mounted with an antifade mounting media (*p*-phenyldiamine in 40% glycerol). Images were collected with a Leica DMI 6000 B microscope equipped with a Hamamatsu Orca ER camera. Image analysis was performed using OpenLab 4.0.2 software.

3.2.8 Bacterial Two-Hybrid System

The conjugative proteins were fused to the catalytic domain of adenylate cyclase from *Bordetella pertussis* via cloning into the BTH vectors, pKT25 and pUT18C (101). Plasmids encoding fused proteins were co-transformed into competent BTH101 cells and plated on LB plates with ampicillin, kanamycin and X-Gal (5-bromo-4-chloro-3-indolyl-β-d-galactopyranoside) at final concentrations of 100 ug ml^{-1}. Cultures were grown at 30°C for 40-48 hours or until the colonies expressing the leucine zipper-positive control became dark blue in color due to the degradation of the chromogenic substrate X-Gal. For each interaction, two colonies were streaked on to the above media and grown at 30°C for 16 hours. These colonies were used to inoculate a 20 ml volume of LB with ampicillin and kanamycin selection and grown at 30°C for 16 hours at 250 RPM. The β-galactosidase activity of each culture was measured using the Miller assay as described previously (134).

3.2.9 Immunoprecipitation

Immunoprecipitation was performed as described previously with minor modifications (66). Briefly, DH5α cells containing pKT25-TraG or pKT25-TraG:S4 were co-transformed with pMS119EH-TrhB$_{FLAG}$. Cells were induced at mid-log growth phase (OD$_{600}$ 0.5-0.7) with 0.4 mM IPTG for one hour before lysis. Harvested cells were resuspended in 1 mL of lysis buffer (PBS pH 7.4, 150 mM NaCl, 1% NP-40, 7.15%

sucrose, lysozyme 0.2 mg/ml, 1X anti-protease cocktail (Complete; Boerhinger Mannheim)) freeze-thawed three times and sonicated for three minutes (30 second pulses, 10 second breaks, Fisher 300 sonicator). The cell lysates were mixed with 40 µl of ANTI-FLAG M2-agarose affinity gel (Sigma). The affinity gel was pre-blocked with 5% (wt/vol) BSA for 16 hours. The cellular lysates and affinity gel were rotated at 4 °C for 16 hours. The gel was then washed three times with 1 ml of lysis buffer. Proteins were eluted from the gel by boiling in LSB buffer + DTT and resolved on a 10% SDS-PAGE gel, transferred to nitrocellulose and blocked with 10% (w/v) milk, 0.1% Tween 20 in PBS. A primary antibody of anti-adenylate cyclase (rabbit serum #L24023, specific for the catalytic domain (D. Ladant)) was applied to the nitrocellulose, washed, and a secondary antibody (anti-rabbit HRP, Sigma) was applied for one hour.

3.2.10 Web-based computer programs

PSI-Blast (http://www.ncbi.nlm.nih.gov/BLAST/); ClustalW (Gonnet matrix, gap penalty = 10, extension penalty = 0.2; http://www.ebi.ac.uk/clustalw/) and TMHMM (http://www.cbs.dtu.dk/services/TMHMM-2.0/) were used.

3.3 Results

3.3.1 Temperature-dependent transcription of *traG*

TraG is encoded in the Tra1 region of R27 which contains genes coding for five Mpf proteins, two relaxosome proteins, a coupling protein accessory protein, and the coupling protein (108). The origin of transfer (*oriT*) is also located in the Tra1 region of R27 and the *oriT* separates Tra1 into divergently transcribed genes. A single operon in Tra1, the H operon, encodes the following genes: *traH*, ORF121, *traI*, *traG*, ORF118, *traJ*, ORF116 and ORF115 (Alonso, G. and Taylor, D.E., submitted for publication). To determine the effect of temperature on the expression of the H operon, reverse-transcriptase PCR (RT-PCR) was performed. Total RNA was extracted from cells harboring R27 and drR27 at both 30°C and 37°C. For RT-PCR, primers were selected that would amplify *traG* and the adjacent genes in the H operon, *traI* and ORF118 (Table 3-2, Fig. 3-1a). For each reaction, DNA template controls were included to confirm the accuracy of the primer sets, 1-8 and 1-9. When reverse transcriptase was excluded from the RT-PCR, there was no evidence of H operon transcript amplification with the 1-8 primer set. The total RNA preparation did not contain DNA that was detected with the 1-8 primer set; trace amounts of DNA contamination, however, within the 1-9 primers may be responsible for the faint band present in *traG* - 118 lane b.The *E. coli* housekeeping protein phosphofructokinase (*pfk*) was selected as an internal control for the RT-PCR temperature analysis. Primers specific for the *pfkA* gene were included in the RT-PCR analysis (Fig. 3-1a).

The amplification of RNA from both *traI-traG* and *traG*-ORF118 was markedly different when an RNA template was extracted from cells grown at 30°C or 37°C (Fig. 3-1b). The RT-PCR is only a semi-quantitative technique, however the difference in the transcript levels indicates that the effect of temperature on conjugation results from regulation at the transcriptional level. The 1-8 and 1-9 primer sets indicate that there is transcriptional activity of the H operon at both 30°C and 37°C. The transcript levels of *pfkA*, the RT-PCR control, were similar when the template was RNA extracted from cells grown at 30°C or 37°C (Fig. 3-1b).

3.3.2 Generation of NTP-binding motif mutations in *traG*

We have previously cloned *traG* into the expression vector pMS119EH, with a His_6 tag on the 3' end of the gene, to form the construct pJEG217 (Table 3-1). The His-tagged coupling protein contains a Walker A motif (GxxGxGKS/T) and a Walker B motif (hhhhDE; where h is a hydrophobic residue) commencing at amino acid positions 205 and 506, respectively (Fig. 3-2a, b)(168). The Walker motifs are

Figure 3-1. (a) RT-PCR analysis of the co-transcription of R27 *traG* gene with the adjacent genes, *traI* and ORF 118. For each primer set, three lanes are shown a) RT-PCR using an RNA template isolated from cell harboring R27 grown at 30°C, b) Negative control of the same RNA template with no reverse transcriptase, and c) Positive control of a DNA template from cells containing R27. The pfK corresponds to phosphofructose kinase which is an internal control. (b) Characterization of the transcriptional profile of R27 *traG* gene using RT-PCR with RNA from cells harboring a) WT R27 grown at 30°C, b) WT R27 grown at 37°C, c) derepressed R27 grown at 30°C, and d) derepressed R27 grown at 37°C. The pfk control represents RT-PCR of RNA extracted in the above conditions, demonstrating the presence of equivalent levels of RNA in each sample.

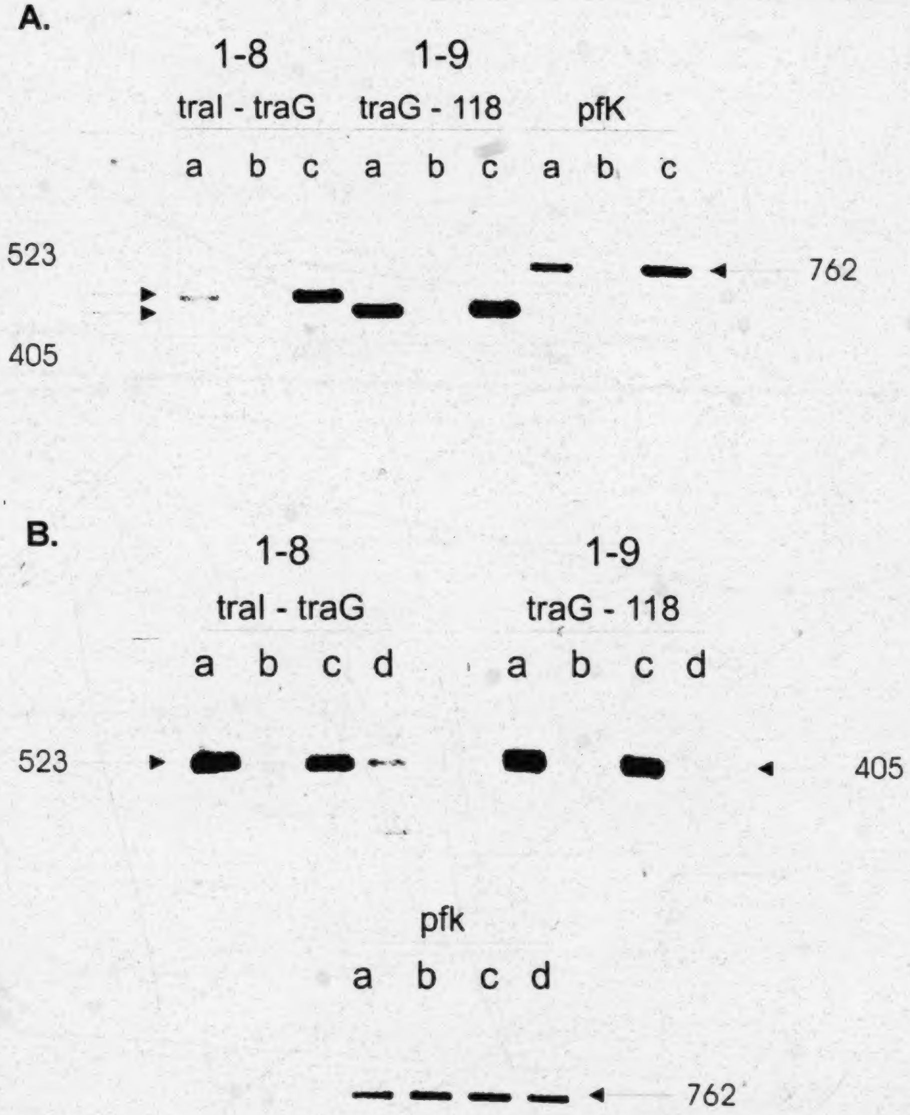
A.
1-8
1-9
traI - traG
traG - 118
pfK
a b c a b c a b c
523
405
762
B.
1-8
1-9
traI - traG
traG - 118
a b c d a b c d
523
405
pfk
a b c d
762

involved with NTP-binding and hydrolysis, and these motifs represent the region with the highest level of sequence similarity among coupling proteins (Fig. 3-2a, b)(168). Site-specific mutagenesis was performed on the Walker A and Walker B motifs of pJEG217, and the resultant plasmid constructs were transformed into DY330R cells harboring pDT3152 (drR27 with a *traG* mutation). The residues that were substituted for the well-conserved Gly and Lys residues (GK) of Walker A and the Asp and Glu residues (DE) of Walker B, were selected using a matrix designed for creating "safe substitutions" that minimized protein instability (Fig. 3-2c) (19). Within the Walker A region, the small, non polar Gly was substituted with the negatively charged, polar Asp (G210D). The positively charged, polar Lys was replaced with the large, positively charged Arg residue (K211R). A complete deletion of the Walker A subregion Gly-Lys (ΔGK) was also created in pJEG217. Within the Walker B region, the Asp residue with an acidic side chain was substituted with the small, non polar Ser (D510S). The negatively charged, polar Glu residue was replaced with positively charged, polar Lys (E511K). Finally, the Walker B subregion (ΔDE) was deleted from pJEG217.

3.3.3 Mutations in the NTP-binding motifs of TraG inhibit plasmid transfer

To determine the effect of the Walker A or B mutations on the functionality of the R27 coupling protein, a *traG* mutation was created in the drR27 plasmid. The drR27 construct was named pDT3152 (Table 3-1). Insertion of a trimethoprim resistance cassette into the 5' region of *traG* abolished the conjugative ability of drR27 (Table 3-3). In the characterization of the Tra1 region of R27, a mini::Tn*10* cassette had been randomly inserted into 3' end of *traG* creating the drR27 construct pDT2956 (108). A recent study on the Walker A and B motifs of TrhC from R27, however, revealed that a mini:Tn*10* insertion in the 3' end of *trhC* downstream of the Walker A motif, may have allowed the production of a TrhC peptide containing a wild-type Walker A region

Figure 3-2. (a) Alignment of Walker A and (b) Walker B boxes from coupling proteins from R27 (TraG; Gen Bank accession no. NP_058332), R388 (TrwB; Gen Bank accession no. CAA44852), F (TraD; Gen Bank accession no.BVECAD) and RP4 (TraG; Gen Bank accession no.S22999). The numbers indicate the amino acids preceding the Walker A and B boxes. Motifs were aligned using ClustalW and shaded in GeneDoc using the conservation mode at level two. Asterisks indicate the conserved residues selected for substitution mutagenesis. (c) Schematic representation of the TraG protein from R27, where the cross-hatched boxes indicate transmembrane regions and the Walker A and Walker B regions have been expanded. Arrows point to the amino acids that were selected for the site-specific mutagenesis studies.

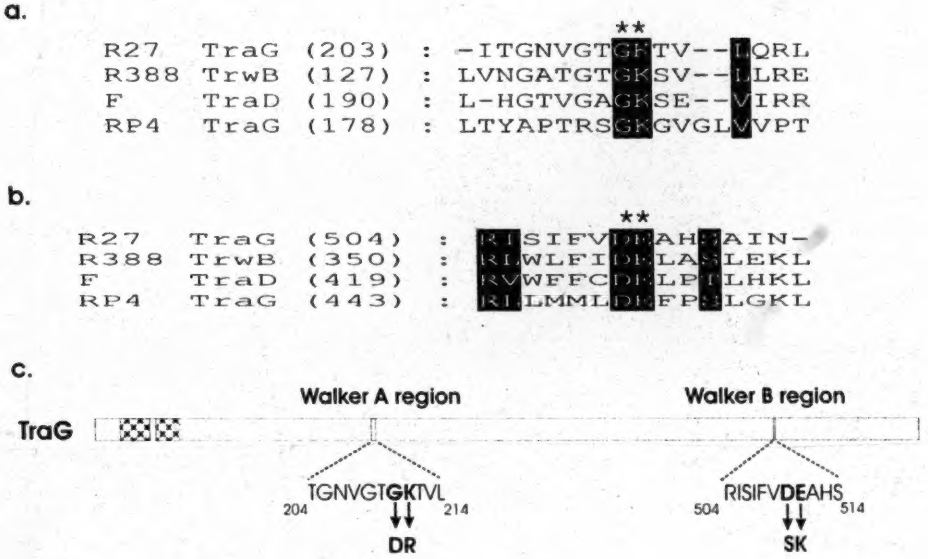
a.
**
R27 TraG (203) : -ITGNVGTGKTV--LQRL
R388 TrwB (127) : LVNGATGTGKSV--LLRE
F TraD (190) : L-HGTVGAGKSE--VIRR
RP4 TraG (178) : LTYAPTRSGKGVGLVVPT
b.
**
R27 TraG (504) : RISIFVDEAHSAIN-
R388 TrwB (350) : RIWLFIDELASLEKL
F TraD (419) : RVWFFCDELPTLHKL
RP4 TraG (443) : RILMMLDEFPSLGKL
c.
Walker A region
Walker B region
TraG
TGNVGTGKTVL
204
214
DR
RISIFVDEAHS
504
514
SK

Table 3-3. Complementation of pDT3152 with pJEG217 or Walker A or B mutant derivatives of pJEG217.

Walker Mutation[†]	pJEG217 mutations[‡]	Transmission frequency[§]
None	Wild Type	$1.3\text{X}10^{-4}$
	Vector alone	$<1\ \text{X}10^{-7}$
A	G210D	$<1\ \text{X}10^{-7}$
	K211R	$<1\ \text{X}10^{-7}$
	Deletion of GK	$<1\ \text{X}10^{-7}$
B	D510S	$<1\ \text{X}10^{-7}$
	E511K	$<1\ \text{X}10^{-7}$

[†] The Mutations correspond to the conserved residues of the Walker A (GK) and Walker B (DE) motifs of TraG.

[‡] The pMS119EH vectors expressing wild type or mutated TraG protein were transformed into DY330R cells containing an R27 *traG* mutant (pDT3152). Transformants were assayed for the ability to transfer to DY330N recipient cells.

[§] Transmission frequency expressed as transconjugants per donor. Values represent the average frequency of two independent experiments.

(68). To eliminate the possibility of production of partial peptides of TraG containing Walker motifs from pDT2956, we created the *traG* mutant pDT3152, which contains a trimethoprim resistant dihydrofolate reductase cassette situated ~ 60 bp upstream of the Walker A encoding region. The functionality of the TraG constructs containing Walker A or B mutations was determined using a standard conjugative transfer complementation experiment. DY330R cells containing pDT3152 were transformed with pJEG217 and its mutant derivatives, and the conjugative ability of the R27 *traG* mutant was determined. The plasmid pJEG217 containing wild-type (WT) Walker A and B motifs was able to complement pDT3152, albeit at a frequency of 1.3 $X10^{-4}$ transconjugants/donor. This frequency was decreased by three logs compared to drR27 transfer (~ 10^{-1} transconjugants/donor). The lower level of complementation could be due to polar effects of the insertional mutagenesis in *traG* on the H operon (108). There was no complementation of pDT3152 with the six TraG Walker A or B mutants within the detection limits of the conjugation assay, <1 $X10^{-7}$ transconjugants per donor (Table 3-3). These data suggest that the NTP binding motifs are essential for the conjugative transfer of R27. These findings are consistent with results obtained in Walker A and B mutagenic studies on the coupling protein, TraG, from RP4 (14), and Walker A mutations in the *A. tumefaciens* coupling protein VirD4 (103) .

3.3.4. Production and stability of TraG$_{His6}$ containing mutations within the Walker A and B regions.

The inability of pJEG217 containing Walker A or B mutations to complement pDT3152 could be a result of a mutation causing instability in the mutant coupling protein. To ensure that the substitutions and deletions within the Walker A or B motifs of the R27 coupling protein did not affect protein expression or stability, the steady state levels of WT and mutant proteins were compared by semiquantitative immunoblot analyses. When equivalent amounts of protein were loaded in SDS-PAG and transferred to a nitrocellulose membrane, an anti-His antibody revealed similar levels of protein expression for four pJEG217 mutants, G210D, ΔGK, D510S, and E511K (Fig. 3-3). Degradation products were detected in the cell extract of cells harboring pJEG217, however, three mutants ΔGK, D510S, and E511K appeared to contain significantly higher levels of degradation products. Although the expression levels of these three pJEG217 variants were similar to WT pJEG217, the mutations may have slightly altered the stability of the coupling protein. There was a partial reduction in the amount of coupling protein detected in the cell extract of DY330R containing pDT3152 and pJEG217 with a K211R mutation (Fig. 3-3). Notably, the deletion of the Asp and Glu residues (ΔDE) of the Walker B region of TraG in pJEG217, created an unstable protein as there was no detectable levels of protein in the immunoblot (Fig. 3-3).

3.3.5. The TraG periplasmic residues are essential for an interaction with TrhB

Using the bacterial two-hydrid (BTH) technique we have recently demonstrated that the coupling protein, TraG, of R27 interacts with its cognate Mpf component TrhB (66). N and C terminal truncations of TrhB revealed that the first 220 amino acids were sufficient to interact with TraG. To identify the domain of TraG that enables this coupling protein-Mpf interaction, we employed the BTH technique. As the majority of TrhB (418 of 452 aa; 93 %) is predicted to be within the periplasm of the cell, we investigated the role of TraG's periplasmic-associated residues in the TraG-TrhB interaction. Computational analysis of TraG by TMHMM (http://www.cbs.dtu.dk/services/TMHMM-2.0/) predicted that only four residues, two of which are charged, Phe-Arg$^+$-Ser-Asp$^-$, separate the two transmembrane domains of the R27 coupling protein. Through site-specific mutagenesis we replaced the Phe, Arg and Asp residues with the small, polar Ser residue, thereby creating a TraG protein with a periplasmic spanning domain of Ser-Ser-Ser-Ser (Fig. 3-4). This triple Ser mutation was

Figure 3-3. Production and stability of pJEG217 (TraG$_{HIS6}$) and pJEG217 constructs containing mutations within the Walker A or Walker B regions, expressed from DY330R harbouring pDT3152 (drR27 with a *traG* mutation). A mouse anti-His antibody was used in the immunoblot to detect the TraG coupling proteins after induction with IPTG. The lanes indicate amino acid substitutions and deletions of the WT sequence from Walker A (GK) and Walker B (DE) boxes. Approximately equal amounts of total protein were loaded from each cell lysate, as the amount of sample used was equalized based on optical density measurements of sample cultures prior to processing the lysate. Coomassie staining of SDS-PAG used to resolve WT and substituted coupling proteins, confirmed equal protein amounts were loaded in each lane.

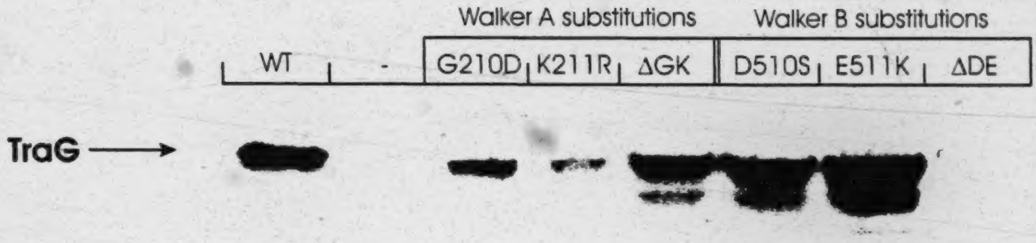
Walker A substitutions
Walker B substitutions
WT
-
G210D
K211R
ΔGK
D510S
E511K
ΔDE
TraG

Figure 3-4. The N terminus of the coupling proteins from R27 (TraG; GenBank accession no. NP_058332), R388 (TrwB; GenBank accession no. CAA44852), F (TraD; GenBank accession no.BVECAD) and RP4 (TraG; GenBank accession no.S22999). The predicted topology of the coupling proteins is indicated by solid lines (cytoplasmic) and dotted lines (periplasmic). Residues that are predicted to be in the periplasm are in bold. The transmembrane regions are shown as cylinders and were predicted using the TMHMM program. Asterisks indicate the residues of TraG that were substituted.

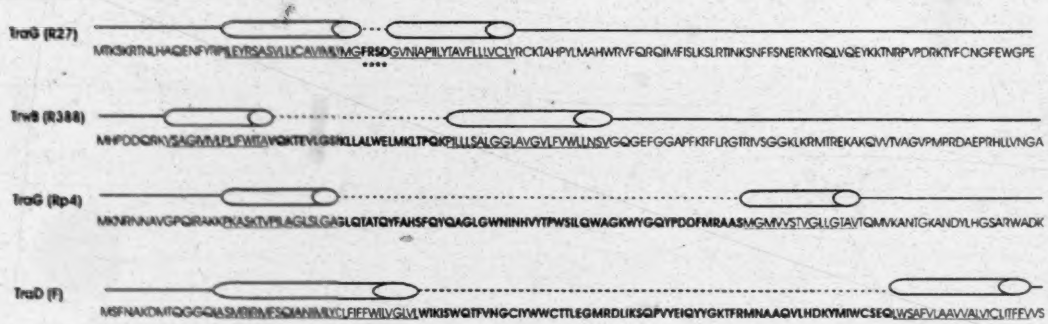
TraG (R27)
MTKSKRTNLHAQENFYRPILEYRSASVLLICAVIMLIMGFRSDGVNIAPIILYTAVFLLLVCLYRCKTAHPYLMAHWRVFQRQIMFISLKSLRTINKSNFFSNERKYRQLVQEYKKTNRPVPDRKTYFCNGFEWGPE
****
TrwB (R388)
MHPDDQRKVSAGMVLPLIFWITAVQKTEVLGSKLLALWELMKLTPQKPILLLSALGGLAVGVLFVWLLNSVGQGEFGGAPFKRFLRGTRIVSGGKLKRMTREKAKQWTVAGVPMPRDAEPRHLLVNGA
TraG (Rp4)
MKNRNNAVGPQIRAKKPKASKTVPILAGLSLGAGLQTATQYFAHSFQYQAGLGWNINHVYTPWSILQWAGKWYGQYPDDFMRAASMGMVVSTVGLLGTAVTQMVKANTGKANDYLHGSARWADK
TraD (F)
MSFNAKDMTQGGQIASMRIRMFSQIANIMLYCLFIFFWILVGLVLWIKISWQTFVNGCIYWWCTTLEGMRDLIKSQPVYEIQYYGKTFRMNAAQVLHDKYMIWCSEQLWSAFVLAAVVALVICLITFFVVS

made in *traG* cloned in the BTH vector, pKT25, thus creating the construct pKT25-*traG*:S4.

Co-transformation of the BTH vectors pUT18C-*trhB* and pKT25-*traG* in BTH101 resulted in functional complementation of the 18KDa and 25KDa domains of the *Bordetella pertussis* adenylate cyclase protein. Adenylate cyclase activity resulted in the conversion of ATP to cAMP which activates the expression of catabolite genes such as *lacZ* encoding β-galactosidase (101). Within 48 hours, >99 % BTH101 cells containing pUT18C-*trhB* and pKT25-*traG* were blue, when spread on LB plates containing the chromogenic substrate X-gal (5-bromo-4-chloro-3-indolyl-β-d-galactopyranoside). BTH101 cells containing pUT18C-*trhB* and pKT25-*traG*:S4 were >90 % white, with a small number of cells showing faint blue centres. The β-galactosidase activity of the faint blue colonies were assayed using the Miller assay (134). The BTH positive control (leucine zipper) and negative control (empty vectors) as well as BTH101 cells containing vectors encoding WT TraG and TrhB were also included in the Miller assay. Whereas the TraG-TrhB interaction showed levels similar to the BTH positive control, the TraG:S4-TrhB interaction did not exceed the negative control levels of the BTH empty vectors (Fig. 3-5). These data suggest that the periplasmic-spanning residues, FRSD, of the coupling protein TraG are involved in the interaction with the Mpf protein, TrhB.

To confirm that the TraG:S4 mutation did not interfere with the stability or expression of the coupling protein, we assayed the pKT25-*traG*:S4 for the ability to interact with pUT18C-*traJ*. The TraJ protein is an essential protein for R27 transfer and it has recently been characterized and was found to be an accessory protein to the coupling protein of the R27 plasmid ((108), Gunton, J. and Taylor, D.E. Submitted for publication)). Using the BTH system, we documented an interaction between TraG and TraJ from R27. This interaction enabled us to determine the stability and functionality of

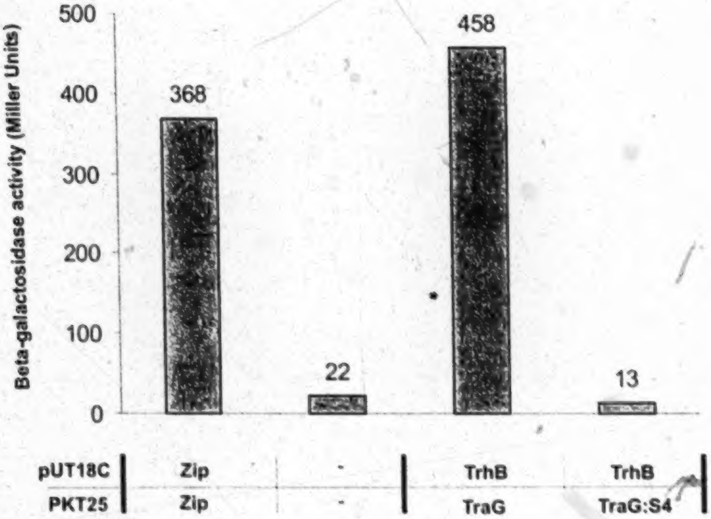
Beta-galactosidase activity (Miller Units)
500
400
300
200
100
0
368
22
458
13
pUT18C
PKT25
Zip
Zip
-
-
TrhB
TraG
TrhB
TraG:S4

the TraG:S4 construct. The BTH data indicated that both the WT TraG and TraG:S4 were able to interact with TraJ; BTH101 cells co-transformed with pUT18C-*traJ* and pKT25-*traG*:S4, or pUT18C-*traJ* and pKT25-*traG* were >99 % blue. These data suggest that the domain through which TraG interacts with TraJ is not shared with the periplasmic domain required for the interaction with TrhB.

To verify the *in vivo* BTH data in which substitutions in the periplasmic domain of TraG abrogated an interaction with TrhB, we attempted to precipitate a complex of epitope-tagged TrhB and TraG:S4. Whereas TrhB containing a C terminal FLAG epitope (Asp-Tyr-Lys-Asp-Asp- Asp-Asp-Lys) precipitated $\mathrm{TraG_{AC}}$, the anti-adenylate cyclase antibody did not detect $\mathrm{TraG{:}S4_{AC}}$ precipitated by $\mathrm{TrhB_{FLAG}}$ (Fig. 3-6). This biochemical analysis confirms that the periplasmic residues of the R27 coupling protein are essential for a successful interaction with the Mpf protein TrhB.

To determine if the substitution of Phe-Arg-Ser-Asp to Ser-Ser-Ser-Ser within the periplasmic region of TraG was functional for conjugative transfer, a complementation experiment was conducted. The four Ser periplasmic substitution was made in pJEG217, thus creating the vector pMWG385 which encoded $\mathrm{TraG{:}S4_{His6}}$. DY330R cells harboring drR27 containing a *traG* mutation (pDT3152) were transformed with pMWG385. Immunoblot analysis of pMWG385 in pDT3152 with the anti-His antibody showed TraG:S4 expression levels similar to the expression of WT TraG from pJEG217 in pDT3152 (data not shown). Interestingly, the TraG:S4 construct was able to complement an R27 *traG* mutant, albeit at lower levels than a WT TraG supplied *in trans* (Table 3-4).

3.3.6 The R27 coupling protein forms membrane-associated fluorescent foci

A GFP fusion to the R27 Mpf protein TrhC revealed that in the presence of R27 conjugative proteins, fluorescent foci randomly localized at the periphery of the cell (67, 68). These TrhC-dependent foci are

Figure 3-6. Co-immunoprecipitation of TraG and not a TraG:S4 construct by the R27 Mpf protein, TrhB. Cellular lysates of DH5α cells expressing TraG_{AC} and $\text{TrhB}_{\text{FLAG}}$, and $\text{TraG:S4}_{\text{AC}}$ and $\text{TrhB}_{\text{FLAG}}$ were mixed with M2 anti-FLAG affinity gel beads, washed, and resolved with 10% SDS-PAGE. After transfer to nitrocellulose, proteins precipitated by the TrhB protein were probed with an anti-adenylate cyclase polyclonal antibody. The immunoprecipitate (**IP**) and cleared lysate (**CL**) of cells expressing TraG_{AC} and $\text{TrhB}_{\text{FLAG}}$, or $\text{TraG:S4}_{\text{AC}}$ and $\text{TrhB}_{\text{FLAG}}$ are shown, with arrows indicating the wild type and periplasmic-substituted R27 coupling protein.

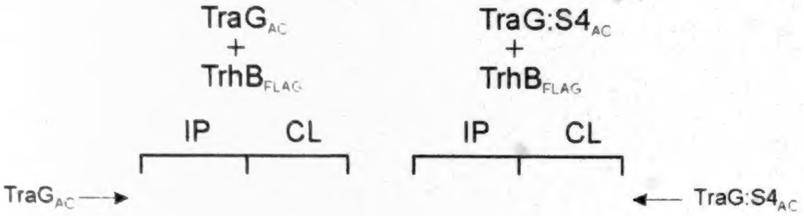
TraG$_{AC}$ + TrhB$_{FLAG}$
IP
CL
TraG:S4$_{AC}$ + TrhB$_{FLAG}$
IP
CL
TraG$_{AC}$
TraG:S4$_{AC}$

Table 3-4. Complementation of pDT3152 with pJEG217 and a TraG:S4 construct, pMWG385 for conjugation.

R27 plasmid	TraG pMS119EH [†]	Transmission frequency[‡]
pDT1942	n/a	5.8X 10^{-1}
pDT3152	Vector alone	<1X10^{-7}
pDT3152	Wild type	1.8 X10^{-3}
pDT3152	TraG:S4	3.5 X10^{-4}

[†] The pMS119EH vectors expressing wild type or mutated TraG protein were transformed into DY330R cells containing an R27 *traG* mutant (pDT3152). Transformants were assayed for the ability to transfer to DY330N recipient cells.

[‡] Transmission frequency expressed as transconjugants per donor. Values represent the average frequency of two independent experiments.

proposed to represent aggregates of R27 proteins at discrete positions within the cell membrane. Further characterization of these foci indicated that foci formation was temperature dependent; at 37°C TrhC-GFP containing cells were confluent green in color whereas at 30°C, in the presence of additional R27 proteins, discrete foci were visible (67).

To determine if TraG localized to the same position as these Mpf complexes, we utilized immunofluorescence (IMF) microscopy to probe for the location of TraG $_{His6}$ proteins. Interestingly, the IMF studies revealed that DY330R cells harboring pJEG217 had fluorescent foci at the cell membrane, resembling the foci formed by TrhC-GFP. Furthermore, unlike TrhC, these discrete foci were present both at 30°C and 37°C, and were found in both the presence and absence of any other drR27 proteins (Fig. 3-7). When TrhC-GFP was expressed from the expression vector, pMS119EH, foci could not be formed at 30 °C or 37 °C in the absence of drR27 proteins (67).

To determine the cellular position of the TraG foci, each cell was divided into six equal domains, with the first and sixth domain representing the polar positions of the cell. The second and fifth domain represented the quarter cell position and the third and fourth domain were combined to represent the mid-cell region. The polar, quarter and mid-cell positions each formed one-third of the entire cell length. In each condition tested, at 30°C and 37°C, and in the presence and absence of any other drR27 proteins, foci were found in the poles, quarter and mid cell positions (Table 3-5). The distribution of the foci was slightly more in the polar position (ranging from 34-36 % of foci at this position), and quarter-cell position (range of 35-38%) as compared to the mid-cell position (range of 27-29%). The average number of foci per cell in DY330R cells containing only pJEG217 was 5.9 and 5.3 at 30°C and 37°C, respectively. In the presence of pDT3152 and pJEG217, DY330R cells contained 5.6 foci at both 30°C and 37°C (Table 3-5).

Figure 3-7. Subcellular localization of $\text{TraG}_{\text{His6}}$ from R27. The location of TraG was determined by immunofluorescence microscopy. The fluorescent foci were observed in DH5α harboring (a) pJEG217 at 30°C and (b) pJEG217 at 37°C. *E. coli* containing pDT3152, a *traG* mutant, showed similar foci when transformed with pJEG217 and grown at (c) 30°C and (d) 37°C. Arrows indicate foci on the periphery of the cell.

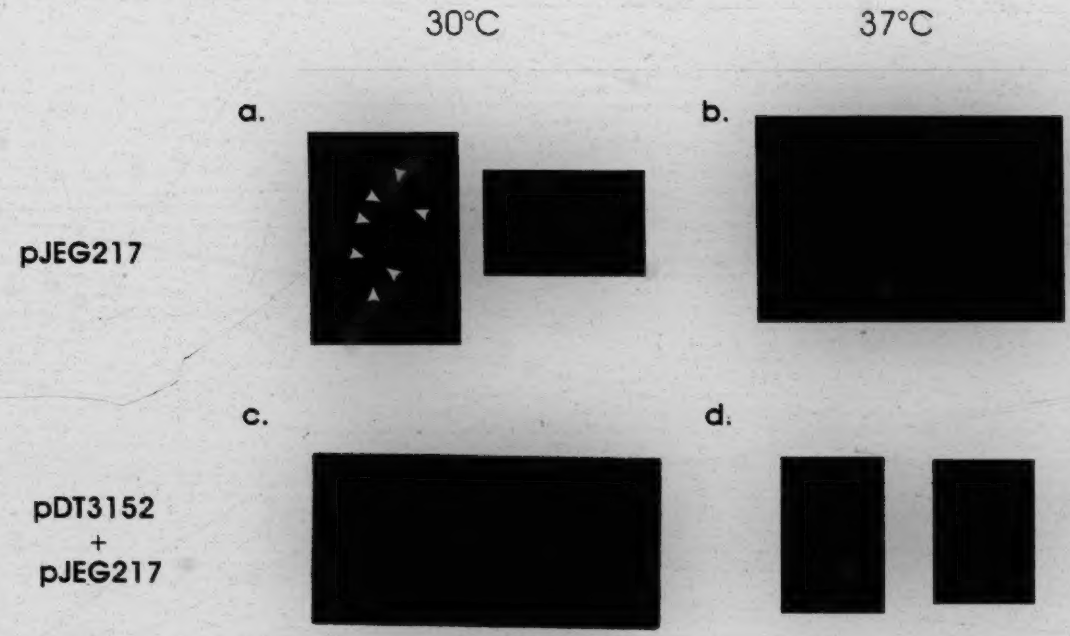
30°C
37°C
a.
b.
pJEG217
c.
d.
pDT3152
+
pJEG217

Table 3-5. Immunofluorescence data representing the effect of temperature and additional R27 proteins on the subcellular localization of pJEG217, $\text{TraG}_{\text{His6}}$.

		Percentage of foci at the cell position:			
Temperature (°C)	Plasmids (no. of cells)[†]	Polar	Quarter-cell	Mid-cell	Foci/cell (no. of foci)
30	pJEG217 alone (101)	34	38	28	5.9 (589)[‡,§]
	pJEG217 + pDT3152 (104)	36	35	29	5.6 (578)[§]
37	pJEG217 alone (106)	34	37	29	5.3 (561)[‡,*]
	pJEG217 + pDT3152 (98)	35	38	27	5.6 (548)[*]

[†] The plasmids correspond to the vectors present within the DY330R cells and the no. of cells indicates total cells counted for that condition.

[‡] In the comparison of foci/cell of pJEG217 alone at 30°C versus pJEG217 alone at 37°C, the *P*-value is 0.001. A two sample, two-tailed T test was performed to determine *P*-value. A *P*-value of <0.05 indicates that a value is statistically significant.

[§] With the comparison of the foci/cell of pJEG217 alone versus pJEG217 and pDT3152 at 30°C the *P*-value is 0.028.

[*] With pJEG217 alone versus pJEG217 and pDT3152 at 37°C the *P*-value is 0.078

3.4 Discussion

Bacterial conjugation is a primary mechanism for horizontal gene transfer. The role of the coupling protein in conjugation had been originally proposed as merely a required connection between the membrane-associated Mpf proteins and the cytosolic relaxosome complex (26). The resolution of the hexameric, pore-forming structure of the coupling protein TrwB, in conjunction with the presence of well-conserved NTP-binding motifs in the coupling protein family suggests that coupling proteins may play a more complex role in conjugation (72). The recently proposed "shoot and pump" model suggests that the coupling protein secretes the relaxase into the conduit created by the T4SS and subsequently threads the DNA portion of the substrate through a channel that is formed by the hexameric coupling protein (122). Furthermore, the *A. tumefaciens* coupling protein, VirD4, has been found to require functional NTP binding motifs for bridging the inner and outer subassemblies of VirB/D4 T4SS (28). Clearly, the coupling protein plays a vital role in the transfer of plasmid DNA from donor to recipient cells.

In our characterization of the transfer regions of the IncHI plasmid R27 we determined that the coupling protein, TraG, is essential for conjugative transfer (108). In this study, we further characterized the coupling protein encoded on the R27 plasmid. A unique feature of the IncH1 plasmids is that conjugative transfer of this family of plasmids is significantly reduced at 37°C (189). Electron microscopic analysis of cells harboring R27 plasmid grown at 37°C revealed an absence of H-pili on the cell surface (127). As pili are required to bring the donor and recipient cells into close proximity, the lack of pili explains the inhibition of transfer at 37°C. Transcriptional analysis of the Mpf gene, *trhC*, indicated that transcription was inhibited at 37°C, thus explaining the lack of H-pili observed during the electron microscopy studies (67). The transcription analysis of *traG*, and the adjacent *traI* and ORF118 genes, at both 30 °C and 37 °C revealed a decrease in the transcript levels at 37°C, as compared to the RNA levels present at 30°C.

Whereas *traG* is encoded in the Tra1 region, *trhC* is encoded within the Tra2 region of R27. The decreased transcript levels of an operon in Tra1 encoding non-Mpf proteins, would indicate a global temperature regulator is controlling R27 conjugation genes in the Tra1 and Tra2 region. A recent analysis of the effect of temperature on R27 transcription has revealed that H-NS and HhaA proteins have an inhibitory effect on the transcription of a number of Tra1 and Tra2 genes at 33°C (57). A comprehensive analysis of the temperature regulation of each R27 transfer gene has been recently completed (Alonso, G. and Taylor, D.E., submitted for publication).

The C terminus of the coupling family, including the Walker-type NTP-binding domains, share weak similarity to the DNA translocases FtsK and SpoIIIE from *E. coli* and *Bacillus anthracis*, respectively (52). The SpoIIIE protein has DNA-dependent ATP hydrolysis activity that is used to pump DNA during sporulation (16). The R388 coupling protein also has DNA-dependent ATP hydrolysis activity, and the Walker motifs of R388, RP4 and F plasmid have been demonstrated to be involved in conjugation (137, 169, 186). Mutational analyses of the Walker A and B motifs of the RP4 coupling protein, TraG, revealed that only two mutations completely abolished RP4 transfer: K187T in Walker A, and D449N in Walker B (14). NTP-binding studies further determined that the K187T mutation rendered the coupling protein unable to bind ATP (171). Mutational analysis of the *A. tumefaciens* coupling protein, VirD4, demonstrated the importance of the Walker A motif (103). VirD4 mutants containing the substitutions, G151S and K152T, were defective in the transfer of both DNA and VirE2 to plant cells. Furthermore, using a transfer DNA immunoprecipitation (TrIP) technique, the VirD4 K152T mutant was found to prevent substrate transfer to the *A .tumefaciens* T4SS proteins VirB6 and VirB8 (10). We have expanded the mutational studies of the Walker A and Walker B motifs of the coupling protein family. Substitution of the Gly and Lys residues of the Walker A motif and Asp and Glu residues of the Walker B motifs abolished the capacity of the R27 coupling protein to restore conjugative ability in a complementation assay. A deletion of the Walker A Gly and Lys residues, at positions 210 and 211, had the same effect on the transmission of the R27 plasmid. These results are not unexpected as alignment of coupling protein homologues indicated that the Gly-Lys and Asp-Glu residues of the Walker A and B motifs, respectively, are found in the majority of coupling proteins (Fig. 3-2). Notably, the R388 coupling protein TrwB has been identified as a DNA-dependent ATPase (186). The discovery that a coupling protein is able to hydrolyze ATP substantiates the finding that key, well-conserved residues in the Walker A and B regions are necessary for conjugative transfer.

The recent discovery that coupling proteins are able to interact with the VirB10 family of proteins suggests a mechanism by which plasmid DNA moves from the cytoplasm to the membrane-associated T4SS (66, 124). A more detailed contact pathway has been proposed by tracking the movement of plasmid DNA in *A. tumefaciens* using the TrIP technique; the T-DNA transfer intermediate interacts with the coupling protein VirD4 initially, and subsequently contacts VirB11, VirB4, VirB6,VirB8, VirB2, and VirB9 (28). Using non-polar *virB* mutations, the pathway of the T-DNA substrate has been expanded to propose that VirB10 interacts with the T-DNA after the substrate's interaction with VirB6 and VirB8 (28). The R27 Mpf protein TrhB, a VirB10 homologue, is likely bitopic with the majority of the protein extending into the periplasm. TrhB has only 11 residues preceding the single transmembrane domain, as predicted by computational analysis with TMHMM. A 220 aa N terminal peptide of TrhB (452 aa) retained the ability to interact with the R27 coupling protein TrhB (66). Interestingly, a shorter N terminal peptide of TrhB, 133 aa in length, was not able to bind TraG but was able to interact with full-length TrhB. TrhB contains a proline rich (17.9%) region between amino acids 135-173; such a proline rich region is a common feature of VirB10 homologues (66). We had postulated that the proline-rich region of TrhB may be involved in the interaction with the coupling protein, TraG (66). Within the R27 coupling protein, there are only four residues, Phe-Arg-Ser-Asp, that are predicted to be associated with the periplasm. The bacterial two hybrid interaction (BTH) screen revealed that a substitution of these residues with four Ser residues was sufficient to abolish a TrhB-TraG interaction. The essential role of periplasmic-associated residues in the interaction with TrhB was verified using a co-immunoprecipitation experiment in which an epitope-tagged TrhB was capable of precipitating only WT TraG and not a TraG:S4 construct. Surprisingly, when this coupling protein containing the periplasmic substitutions, TraG:S4, was supplied *in trans* in a complementation assay with an R27 *traG* mutant, the TraG:S4 construct was able to restore conjugative ability. The complementation level, however, was almost one log lower than the transfer levels of an R27 *traG* mutant complemented with WT TraG. The ability of the TraG:S4 construct to complement a *traG* mutation could be explained by the coupling protein interacting with multiple points in the T4SS apparatus, and not solely with TrhB. The BTH and co-immunoprecipitation techniques identify only binary interactions, which is considerably different than the interactions that may occur with the coupling protein and a full complement of R27 T4S proteins.

The Phe-Arg-Ser-Asp residues of TraG do not represent a common motif within the periplasmic regions of the coupling proteins from the RP4, R388 and F plasmids (Fig. 3-4). Furthermore, there is significant variability in the number of residues separating the hallmark transmembrane regions of the coupling protein; TraD had the largest number of periplasmic-associated residues with 62 aa and TraG of R27 had the smallest number with only 4 aa separating the transmembrane regions. One common feature of the coupling protein family is the interchangeability of the coupling proteins between non-cognate T4SS (25, 83). This has been further demonstrated using BTH technology in which the R388 VirB10 homologue, TrwE, was found to interact with non-cognate coupling proteins from the IncN plasmid pKM101 and IncX plasmid R6K (124). The R27

VirB10 homologue, TrhB, has also been found to interact with non-cognate coupling proteins encoded on the F, RP4, and R388 plasmids (Gunton, J. and Taylor, D.E. submitted for publication). The BTH and immunoprecipitation data obtained with the R27 TraG:S4 construct suggest that the periplasmic region is essential for the interaction with TrhB. A shared feature of the VirB10 homologues is the proline-rich region in the amino terminus. This structural feature may be interacting in a non-specific fashion, with the periplasmic residues of the coupling protein thus allowing for the observed interchangeability of coupling proteins between heterologous T4SS.

Immunofluorescence (IMF) microscopy was used to determine that R27 $\text{TraG}_{\text{His6}}$ protein forms multiple fluorescent foci within the periphery of the cell. Similar foci were observed when GFP was fused to the C terminus of the R27 Mpf protein, TrhC (Gilmour *et al.*, 2001). Notably, DY330R cells containing $\text{TraG}_{\text{His6}}$ or TrhC-GFP formed the same number of foci in the cellular membrane; there was an average of five to six foci in cells containing the R27 coupling protein or TrhC. With both TraG and TrhC, foci were found throughout the cell periphery with a moderate bias towards the quarter and polar positions of the cell (67). The position of R27 protein-dependent foci in the cell is strikingly different than the position of the R27 plasmid DNA; GFP-labeled R27 plasmid DNA localized to discrete positions at the mid and quarter cell position (67, 111). Electron microscopy revealed that the H-pilus, product of the R27 T4SS, can assemble and extend from random positions on the cell membrane and is not limited to this mid or quarter cell position (67).

As R27 conjugation is influenced by temperature, TraG-dependent foci formation was investigated in cells grown at 37°C. Although foci were found at both 30°C and 37°C there was a statistically significant decrease in the number of foci formed when cells expressing TraG alone were grown at 37°C instead of at 30°C, a temperature that is permissive for R27 conjugative transfer (*P*-value=0.001). Furthermore, there was a significant change in the number of foci at 30°C, when cells expressing TraG also harbored the R27 plasmid (*P*-value=0.028). These data suggest that in the absence of essential R27 proteins, the number of TraG-associated foci per cell is slightly higher at 30°C, as compared to the foci number formed at 37°C; temperature may be involved in more than simply transcriptional control of the R27 genome. Additionally, in the presence of R27 proteins, the number of TraG foci decreases when compared to cells expressing TraG alone. As expected, this decrease is not significantly different in the presence and absence of pDT3152 at 37°C, as at this elevated temperature, transcription of the majority of R27 genes is significantly reduced (67); Alonso, G. and Taylor, D.E., submitted for publication).

The ability of a coupling protein to localize to discrete positions within the cell, in the absence of other T4S proteins, is not a unique phenomenon. The *A. tumefaciens* coupling protein, VirD4, localized to the poles of the cell, independent of other Vir proteins or a T4S apparatus (103). The *A. tumefaciens* T4S protein VirB6 also localizes to the poles, however like TrhC from the R27 plasmid, this localization is dependent on the presence of a subset of conjugative proteins, VirB7-VirB11 (99). This dependence of VirB6 positioning on Ti plasmid-encoded VirB proteins, however, has not been demonstrated in a recent study, suggesting that additional work is required to resolve the architecture and temporal assembly of the Vir T4SS (96).

The TraG periplasmic-spanning residues and well-conserved residues in the Walker-type ATP-binding domains have been shown to be involved in the functionality of the R27 coupling protein. Moreover, the independent cellular localization of foci formed by the coupling protein is similar in position and number to potential T4S complexes encoded by the R27 plasmid. These data support a model of conjugation in which the coupling protein localizes to the periphery of the cell and associates with the T4S protein

TrhB with periplasmic-spanning residues, thus enabling plasmid DNA to traverse the donor cell envelope.

Chapter 4

Entry exclusion in the IncHI1 plasmid R27 is mediated by TrhZ and EexH

Portions of this chapter have been submitted to *Journal of Bacteriology* as:

Gunton, J. E., Ussher, J. E. R, Wetsch, N.M., Alonso, G., and Taylor, D.E. (2005). Entry exclusion in the IncHI1 plasmid R27 is mediated by TrhZ and EexH.

RT-PCR analysis was performed by Dr. G. Alonso.

4. Entry exclusion in the IncHI1 plasmid R27 is mediated by TrhZ and EexH

4.1 Introduction

Horizontal DNA transfer enables the rapid dissemination of genetic information with evolutionary and medical implications. Bacterial conjugation is a mechanism of horizontal gene transfer requiring cell-cell contact (214). An early study of extrachromosomal inheritance in bacteria revealed that the conjugation frequency of F+ strains decreased significantly when the recipient was an F+ strain when compared to the conjugal mating frequencies when F- strain were the mating recipients (115). This conjugative inefficiency is due to two processes, entry exclusion and plasmid incompatibility (143). Plasmid incompatibility is defined as the inability of two co-resident plasmids to be stably inherited in the absence of selective pressures (144), in contrast entry exclusion inhibits the initial entry of DNA from donor cells harbouring isogenic or closely related plasmids (143).

En[illegible] exclusion (Eex) activity has been described in conjugative elements from a diverse array of incompatibility families including IncP (80, 81), IncW (121), IncF (2, 4), IncN (157), IncI (87, 88) and recently, IncJ (130). Notably, each conjugative element proficient in Eex activity can be grouped into two Eex classes: those plasmids that encode one Eex polypeptide and those plasmids that encode two independent polypeptides which confer Eex to recipient cells when mated with donors harbouring related plasmids. RP4 is a well-studied member of the first Eex class of plasmids, as the IncPα plasmid encodes the lipoprotein TrbK, which is the only necessary determinant responsible for the Eex phenotype in this broad-host range plasmid (81). Cellular localization studies of cells harbouring the RP4 plasmid revealed that TrbK is predominantly associated with the inner membrane of the cell envelope; the mechanism by which TrbK elicits an Eex phenotype in recipient cells has been proposed to be due to an interaction with the mating apparatus in donor cells containing a RP4-related plasmid (80).

The most intensively studied member of the second Eex class of plasmids in which two exclusion polypeptides elicit an Eex phenotype is the F plasmid. Similar to the TrbK protein of RP4, the F plasmid Eex protein TraS has been localized to the inner membrane of F plasmid-containing cells (3); Moreover, there is evidence to suggest that a similar interaction occurs between TraS and TraG, the stabilization protein of the F plasmid mating apparatus (59). The F plasmid also encodes the lipoprotein TraT, a second independent exclusion protein, which localizes to the outer membrane of the cell and prevents stable mating pair formation (156, 182).

Previous studies on the IncHI plasmid family has identified an Eex activity mediated by the IncHI1 plasmid pRG1251, however the specific protein(s) encoding for this event were not identified (188). Conjugative plasmids of the IncHI1 family were originally isolated in *Salmonella enterica* serovar Typhi, the causative agent of typhoid fever. These mobile genetic elements were found to encode multiple drug resistance determinants, thereby increasing the difficulty in treating the bacteria-induced fever (55, 155). A unique feature of the IncHI plasmids is the temperature-sensitive feature of their transfer; optimal conjugation of IncHI plasmids occurs at 30°C, with reduced conjugation rates at 37°C (189). Recent transcriptional studies of genes essential for the transfer of the prototypical IncHI1 plasmid R27, indicate that the temperature-control is mediated at a transcriptional level (67).

The objective of this work was to identify the R27 determinants that mediate Eex activity in the IncH plasmid family. A screen of a cosmid library containing the majority of the R27 plasmid sequence revealed that the Z operon, located in the Tra2 region of R27, was able to confer an R27 Eex phenotype to recipient cells. Subsequent subcloning of the Z operon identified the R27 exclusion proteins as TrhZ and EexH (previously named

Orf016). RT-PCR analyses of the Z operon indicated that transcription of the R27 exclusion proteins is repressed at 37°C, a temperature which was non-permissive for R27 conjugation. The specificity of the exclusion action elicited by TrhZ and EexH on R27-related and non-related plasmids was determined using an exclusion assay. Bacterial fractionation studies revealed the cellular location of the R27 exclusion proteins TrhZ and EexH within the inner and outer membrane, respectively. A possible mechanism for Eex in R27 is discussed.

4.2 Experimental Procedures

4.2.1 Bacterial strains, growth conditions, and plasmids

Escherichia coli strains and plasmids used in this study are listed in Table 1. *E. coli* strains were grown at 30 °C (DY330R) or 37 °C (RG-11) in Luria Bertani (LB) broth (Difco Laboratories, Detroit, Mich.) with shaking or on LB agar plates. Antibiotics used in this study are listed with final concentrations: ampicillin (100 µg ml^{-1}), kanamycin, (50 µg ml^{-1}), streptomycin (100 µg ml^{-1}), rifampicin (20 µg ml^{-1}), chloramphenicol (16 µg ml^{-1}), tetracycline (10 µg ml^{-1}), trimethoprim (12.5 µg ml^{-1}), potassium tellurite (15 µg ml^{-1}).

4.2.2 Reverse transcriptase PCR (RT-PCR)

RT-PCR of the Z operon was performed as described previously using the primers listed in Table 4-2 (78).

4.2.3 Entry Exclusion (EEX) Studies

All EEX matings (with the exception of those involving DY330R containing IncPα conjugative plasmid RP4 as a donor strain) were initiated from overnight cultures that

Table 4-1. Bacterial Strains and Plasmids used in this study

Bacterial strain or plasmid	Relevant genotype, phenotype, or characteristic[†]	Source or reference
E. coli		
DH5α	*supE44 lacU169* (Φ80*lacZΔM15*) *hsdR17 recA1 endA1gyrA96 thi-1 relA1*	Invitrogen
XL1-Blue	*recA1 endA1gyrA96 thi-1hsdR17 supE44 relA1* lac [F' *proAB lacI*^{q}Z*ΔM15* Tn*10*]	Stratagene
DY330	W3110 Δ*lacU169 gal-490* λcI857 Δ(*cro-bioA*)	(35)
DY330R	Temperature-resistant revertant; Rif^{r}	(Lawley et al., 2002)
RG11	K-12 derivative; Str^{r}	This study
J53-1	*pro met;* Nal^{r}	(Bachman, 1972)
Plasmids		
R27	Inc HI1; Tc^{r}	(Taylor & Levine, 1980)
pDT1942	Derepressed R27; R27::Tn*lacZ*	(Waters et al., 1992)
pAS252-2-3	Inc HI2; Cm^{r}	This study
pHH1508a	Inc HI1; Te^{r} Tp^{r} Str^{r}	(Bradley et al., 1982)
pRG1251	Inc HI1; Cm^{r}	(188)
RP4	Inc P; Km^{r}	(Haase et al., 1995)
R478	Inc HI2; Cm^{r}	(Gilmour et al., 2004)
F	Inc F; Km^{r}	(Frost et al.,1994)
pMS119EH/HE	Expression vector;P$_{tac}$–lacI^{q}; pMB1 origin of replication; Amp^{r}	(Strack et al., 1992)
TrhO-EH	948bp PCR product with *Eco*RI and *Bam*HI cut sites in pMS119EH; Amp^{r}	This study
EexH-HE	840bp PCR product with *Hind* III and *Bam*HI cut sites in pMS119HE; Amp^{r}	This study
017-EH	522bp PCR product with *Eco*RI and *Bam*HI cut sites in pMS119EH; Amp^{r}	This study
TrhZ-EH	837bp PCR product with *Eco*RI and *Bam*HI cut sites in pMS119EH; Amp^{r}	This study
TrhO-TrhZ-EH	3147bp PCR product with *Eco*RI and *Bam*HI cut sites in pMS119EH; Amp^{r}	This study
EexH$_{His}$-HE	858bp PCR product with *Hind* III and *Bam*HI cut sites in pMS119HE; Amp^{r}	This study
TrhZ$_{His}$-EH	855bp PCR product with *Eco*RI and *Bam*HI cut sites in pMS119EH; Amp^{r}	This study
pJEG144	pDT1942 with *cat* in TrhO	This study
pJEG142	pDT1942 with *cat* in EexH	This Study
pJEG139	pDT1942 with *cat* in *orf017*	This study
pJEG141	pDT1942 with *cat* in TrhZ	This study

[†] Abbreviations: Nal^{r}, nalidixic acid resistance, Rif^{r}, rifampicin resistance, Tc^{r}, tetracycline resistance, Km^{r}, kanamycin resistance, Amp^{r}, ampicillin resistance, Str^{r}, streptomycin resistance, Cm^{r}, chloramphenicol resistance, Tp^{r} trimethoprim resistance.

Table 4-2. Primers used in this study to clone the genes of the Eex operon and for transcriptional analysis of the Eex operon.

Primer ID	Primer Name	Sequence(5'-3') †	Predicted Product Size (bp)
TrhO-EH	TrhO-GUN13	F: TGAATTCAATGGCATCCGAGCACGTCCAG	948
	TrhO-GUN14	R: TGGATCCTTATAATGTGGCCTCTATATTATTATC	
EexH-HE	EexH-GUN15	F: TAAGCTTATGCTTAAATTAGAACTG	840
	EexH-GUN16	R: TGGATCCTTAATCATTTTCAGTCCTCATAGTCG	
orf 017-EH	orf 017-GUN17	F: TGAATTCAATGATTAGAGTTTCAGC	522
	orf 017-GUN18	R: TGGATCCTTATGATTGCTCCTTTTGCAAAAATTC	
TrhZ -EH	TrhZ -GUN19	F: TGAATTCAATGAAATATATATTGACCG	837
	TrhZ -GUN20	R: TGGATCCTTATTGAACAGGGTGATGGGC	
EexH_{His}-HE	EexH_{His}-GUN188	R:TATAGGATCCTCAATGGTGATGGTGATGGTGATCATTTTCAGTCCTC ATAGTCG	858
TrhZ_{His}-EH	TrhZ_{His} -JRU13	R:TATAGGATCCTCAATGGTGATGGTGATGGTGTTGAACAGGGTGATGGGC	
2-19 (RT-PCR)	orf 017	F: AGGCACTGATGTCTGGTTACTC	695
	TrhZ	R CAACCGCTGCTGCATTACTGTC	
2-20 (RT-PCR)	orf 016	F: ACGGAATGTGGCTTGTTGATGG	930
	orf 017-orf 016	R: TGACGAATAGGTGCAACGACTCC	
2-21 (RT-PCR)	orf 016-TrhO	F: TTGCCCATCCGATTACACAGAC	662
	orf 016-TrhO	R: CGACCATCAACAAGCCACATTC	
Control (RT-PCR)	PfkA	F: GTGGCGGTACGTTCCTCGGTTCT	762
	PfkA	R: TTTTTCGCGCAGTCCAGCCAGTC	

† Restriction endonuclease sites are underlined.were sub-cultured (1/20 dilution) and donor and recipient strains grown until the mid-log growth phase (A_{550} = 0.4-0.6). All recipient strains were induced with 0.4 mM isopropyl-β-D-thiogalactoside (IPTG) for one hour.

were sub-cultured (1/20 dilution) and donor and recipient strains grown until the mid-log growth phase (A_{550} = 0.4-0.6).After IPTG induction, 0.1 mL of donor cells were mixed in 1.5 mL eppendorf tubes with 0.4 mL of recipient cells and 0.5 mL of LB media. The eppendorf tubes were inverted multiple times and then left to incubate for 16 hours at 30 °C. Following incubation serial dilutions were set up for each mating (undiluted to 10^{-6} dilution) in phosphate buffer saline (PBS) solution and plated on LB agar plates with the appropriate antibiotic selection. Eex indices (EI) were determined by dividing the transfer frequency of donor plasmids into plasmid-free recipients by the transfer frequency of the donor cells into recipients containing the plasmid of interest.

For the EEX studies involving DY330R containing IncPα conjugative plasmid RP4 as the donor, overnight cultures were sub-cultured (1/20 dilution) and grown at 37 °C until strains reached mid-log growth phase (A_{550} = 0.48). From here, all recipient strains were induced with 0.4 mM IPTG. After IPTG induction, 0.5 mL of donor and recipient cells each were added and spread across an LB agar plate without antibiotic selection. Plates were incubated for 3 hours at 37 °C to allow for bacterial conjugation. After 3 hours incubation, 1mL of PBS solution was spread on individual agar plates. After spreading the PBS solution, plates were tilted and remaining solution was collected into a 1.5mL eppendorf tube. The cells were harvested two more times and the collected cells, the undiluted sample, were adjusted to a volume of 3 mL. Serial dilutions were set up for each mating (undiluted to 10^{-6} dilution) and plated on LB agar plates with the appropriate antibiotic selection and incubated at 37 °C for 16 hours before enumeration. EI levels were determined as described above.

4.2.4 DNA Manipulations and Mutagenesis

IncHI1 plasmid R27 DNA was isolated and purified with a Qiagen (Mississauga, Ont.) Large-Construct Kit. Expression and cloning vectors were isolated and purified using either the Qiagen Midi-prep kit (Qiagen Inc.) or the Qiagen Spin Mini-prep kit

(Qiagen Inc.). Standard recombinant DNA methods were carried out as described by Sambrook et al. (165). Restriction endonucleases were used according to the manufacturer's instructions, and digested DNA was analyzed by agarose gel electrophoresis.

Procedures for generation of drR27 mutants *trhZ, trhO, orf017, eexH, and orf004* are described in further detail in (109).

4.2.5 Bacterial Fractionation

The bacterial cell fractionation procedure was based on a previous study by Gauthier *et.al.* (63). Briefly, DH5α cells harbouring either TrhZ$_{His}$ EH or EexH$_{His}$ HE were grown overnight in LB media at 37°C with shaking at 200 RPM. The culture was subcultured 1/20 in 20 ml of LB media and grown for 3 hours in the conditions described above; upon reaching mid-log growth conditions (OD$_{600}$ 0.5-0.6) the cultures were induced with 0.42 mM IPTG for 1 hour. Cells were harvested, washed in phosphate-buffered saline and re-suspended in 1 ml of sonication buffer (10 mM Tris [pH 7.0]) with 1X complete protease inhibitor cocktail (Boehringer-Mannheim, Mannheim, Germany). Lysozyme was added to a final concentration of 10 μg/ml, and cells were incubated at 4°C for 30 minutes. The periplasmic fraction was collected after centrifugation of the lysozyme-treated cells (at 8,000 X *g* for 10 minutes). The pellet was resuspended in 1 ml of sonication buffer and sonicated for 3 minutes (30 second pulses,10 second breaks, Fisher Sonicator 300). Unlysed cells were collected by centrifugation at 16,000 X *g* for 2 minutes, and the supernatant containing the cytoplasmic and membrane fractions was centrifuged at 100,000 X *g* for 1 hour (Optima Max-E Ultracentrifuge, TLA 120.2 rotor, 350,000 X g). The supernatant representing the cytoplasmic fraction was collected and the membrane pellet was washed with sonication buffer. The pellet was resuspended in 0.5 ml of sonication buffer with 0.5% *N*-laurylsarcosine, which selectively solubilizes the inner membrane, and the resuspension was rotated at room temperature for 30 minutes before centrifugation (100,000 X *g* for 1 hour). The supernatant representing the cytoplasmic fraction was collected and the pellet was washed with sonication buffer with 0.5% *N*-laurylsarcosine. The pellet was resuspended in 0.5 ml of sonication buffer with 0.5% *N*-laurylsarcosine and 0.1% sodium dodecyl sulfate (SDS). This resuspension represented the outer membrane fraction. The antibodies that were used to ensure appropriate separation of fractions were anti-DnaK (Stressgen,Victoria, BC), anti-SecY (Minotech, Crete, Greece), and anti-OmpA (158).

4.2.6 Electron Microscopy

Transmission electon microscopy (TEM) was performed as described previously by (127). Briefly, transconjugant colonies were applied to freshly prepared Formvar-coated copper grids by briefly touching the grids to isolated colonies. The samples were stained with the addition of of 1% phosphotungstic acid staining solution pH 7.0, with excess stain blotted away with filter paper. Grids were examined with a Philips model 410 transmission electron microscope.

4.2.7 Web-based computer programs

PSI-Blast (http://www.ncbi.nlm.nih.gov/BLAST/); ClustalW (Gonnet matrix, gap penalty = 10, extension penalty = 0.2; http://www.ebi.ac.uk/clustalw/); TMPred (http://www.ch.embnet.org/software/TMPRED_form.html); ScanProsite (http://ca.expasy.org/tools/scanprosite/); EMBOSS pairwise local alignment (Blosum40 matrix, gap penalty = 10, extension penalty = 0.5; http://ebi.ac.uk/emboss/align/); and SignalP (http://www.cbs.dtu.dk/services/SignalP/) were used.

4.3 Results

4.3.1 EexH and TrhZ mediate entry exclusion activity of the R27 plasmid.

A plasmid-encoded Eex phenomenon has been observed within the incompatibility H plasmid family (188). To identify the specific mediators of the exclusion event encoded by the IncHI1 plasmid R27, a cosmid library of the large conjugative plasmid (140) was screened for IncH exclusion activity (Table 4-3). The exclusion activity is reported as an exclusion index (EI) which is defined as the frequency of transfer of R27 to a plasmid-free recipient divided by the frequency of transfer of R27 to a recipient of interest; therefore a high EI indicates inhibition of R27 conjugative transfer. In the screen of the R27 cosmid bank for Eex activity, the highest EI level (EI = 201) was recorded when donor cells harbouring R27 were mated with recipient cells containing the cosmid pJEG801 (Table 4-3). The pJEG801 cosmid encodes the R27 coordinates 4.1-41.8 kb. This region of R27 contains the transfer region 2 (Tra2) that is located from coordinates 2.1-38.0 kb (109). Notably, lower EI levels of 28 and 16 were recorded when R27 was mated into recipients cells containing the cosmids pJEG800 and pJEG803, respectively; these two cosmids also encode regions of the R27 Tra2 sequence (Table 4-3).

The single cosmid encoding regions of R27 Tra1, pDT1693, demonstrated background levels of EI (EI=0.8). A region of Tra1 extending from orf115 to *trhX* was unable to be screened for R27 Eex activity. The presence of the origin of transfer (*oriT*) within Tra1 resulted in an inability to clone a region of the R27 Tra1 sequence (109, 140). To identify the individual genes encoding the R27 Eex phenotype the cosmid clone encoding the smallest region of the Tra2 region which demonstrated exclusion activity was further characterized. The clone pJEG800 contains the R27 sequence corresponding to the coordinates 4.1-28.0 Kb; the R27 genes located in this region extend from orf4 to orf23. Within this region, four contiguous genes comprise the Z operon; *trhO*,orf016, orf017 and *trhZ* are flanked by the double partitioning determinants of R27 (111). Notably, the Z operon is present in all three R27 cosmid clones (pDT800,

Table 4-3. R27 Cosmid library screen for entry exclusion activity.

Cosmid clone[†]	Coordinates[‡]	Restriction enzyme[§]	Tra Region encoded[*]	Transfer Frequency[¶]	EEX index[#]
No insert	-	-	-	$1.9X10^{-4}$	1
pJEG800	4.1-28.0	*Xba*I	Tra2	$6.8X10^{-6}$	28
pJEG801	4.1-41.8	*Xba*I	Tra2	$0.9X10^{-6}$	210
pJEG802	41.8-51.3	*Xba*I	-	$3.2X10^{-4}$	0.6
pDT1693	111.4-155.6	*Sal*I	Tra1	$2.5X10^{-4}$	0.8
pDT1602	144.1-173.6	*Sal*I	-	$3.9X10^{-4}$	0.5
pJEG803	164.4-28.0	*Xba*I	Tra2	$1.2X10^{-5}$	16

[†] Cosmids were constructed using pHC79 and pUCD5 and electroporated into RG192-2 cells.

[‡] The R27 map coordinates of the sequence contained within the cosmid library. The coordinates are from the R27 GenBank sequence (NC_002305).

[§] Restriction endonuclease used to generate the R27 fragments.

[*] The presence of sequence encoding partial Tra1 regions (98.1-117.3) or Tra2 regions (2.1-38.0) within the cosmid clones are indicated.

[¶] Transfer frequency is listed as transconjugants per donor. The transfer frequency represents the average frequency from at least two independent experiments.

[#] EEX index is calculated by dividing the transfer frequency of cells harbouring an empty cosmid with the transfer frequency of cosmid clones containing R27 fragments.

pDT801 and pDT803) that showed Eex activity. To ascertain the potential role this operon may play in IncH Eex, the region encoding *trhO-trhZ* was cloned into the IPTG-inducible expression vector pMS119HE (Figure 4-1). When *trhO-trhZ* was expressed in recipient cells and mated with donors harbouring the R27 plasmid, EI levels of 3001 were observed. Sub-cloning of the individual genes and screening for R27 Eex activity resulted in the identification of TrhZ and orf016 as R27 exclusion proteins (Figure 4-1). Due to the discovery of an Eex function mediated by orf016, I changed the nomenclature of this R27 gene to *eexH* (entry exclusion IncH).

Interestingly, there was a significant difference in the R27 EI levels mediated by *eexH* and *trhZ*. Whereas the entire region of *trhO-trhZ* and *trhZ* were able to exclude the R27 plasmid at an EI of ~ 3000, the *eexH* gene and the *trhO*-orf017 region conferred a higher R27 EI of >10,000 (Figure 4-1). These data indicate the IncH plasmid R27 encodes two functional Eex proteins which inhibit the redundant conjugative transfer of this genetic element.

4.3.2 Temperature-dependent transcription of Z operon

A hallmark feature of the IncHI plasmids is optimal conjugative transfer at 25-30°C with reduced transfer ability at 37°C (189). To determine the effect of temperature on the transcription of the R27 exclusion genes *trhZ* and *eexH*, RT-PCR analysis of the Z operon was performed. Total RNA was extracted from cells harbouring wild-type (WT) R27 or drR27 at 30°C and 37°C. Primers were designed to amplify adjacent genes in the Z operon transcript (Table 4-2, Figure 4-2a). For each reaction, control DNA was used to ensure accurate amplification by the primers 2-19, 2-20, and 2-21 (Figure 4-2b). In the absence of reverse transcriptase there was no evidence of contamination by the primers, however when the polymerase was present there was amplification of the Z operon transcript (Figure 4-2b).

Figure 4-1. Open reading frame map of the Tra2 region of R27, with an enlarged map of the operon encoding the entry exclusion proteins TrhZ and EexH of R27. Gray orfs indicate genes required for the conjugative transfer of R27 and the black orfs indicate genes that are not essential for transfer. White orfs indicate the partitioning genes of the R27 that encode stability determinants. The black bent arrow represents a proposed promoter region upstream of the TrhO-TrhZ operon.

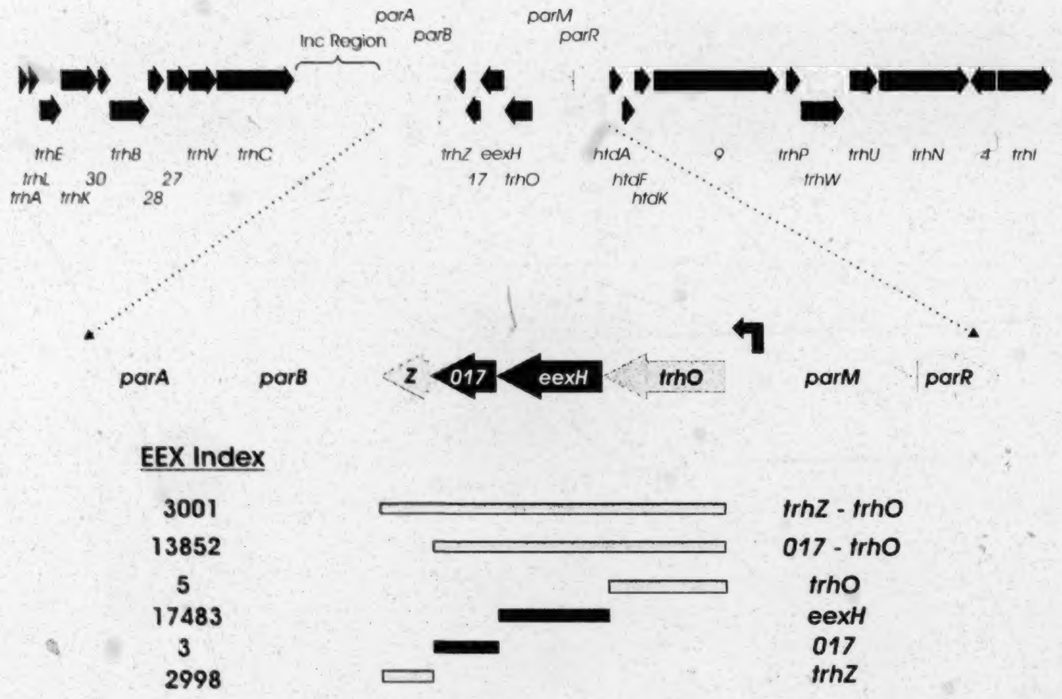
parA
parB
parM
parR
Inc Region
trhE
trhB
trhV
trhC
trhL
30
27
trhA
trhK
28
trhZ
eexH
17
trhO
htdA
htdF
htdK
9
trhP
trhU
trhN
4
trhI
trhW
parA
parB
Z
017
eexH
trhO
parM
parR
EEX Index
3001
trhZ - trhO
13852
017 - trhO
5
trhO
17483
eexH
3
017
2998
trhZ

Figure 4-2. (A) Operon map of the *trhO-016-eexH-trhZ* R27 genes where arrows indicate the region amplified by the RT-PCR primers 2-19, 2-20 and 2-21. (B) Confirmation of the *trhO-trhZ* operon structure by RT-PCR analysis of the co-transcription of R27 genes *trhO-016-eexH-trhZ*. For each primer set, three lanes are shown a) RT-PCR using an RNA template isolated from cell harboring R27 grown at 30°C, b) negative control of the same RNA template with no reverse transcriptase, and c) positive control of a DNA template from cells containing R27. (C) Characterization of the transcriptional profile of R27 *trhO-trhZ* operon using RT-PCR with RNA from cells harboring a) WT R27 grown at 30°C, b) WT R27 grown at 37°C, c) derepressed R27 grown at 30°C, and d) derepressed R27 grown at 37°C. The pfK corresponds to phosphofructose kinase which is an internal control.

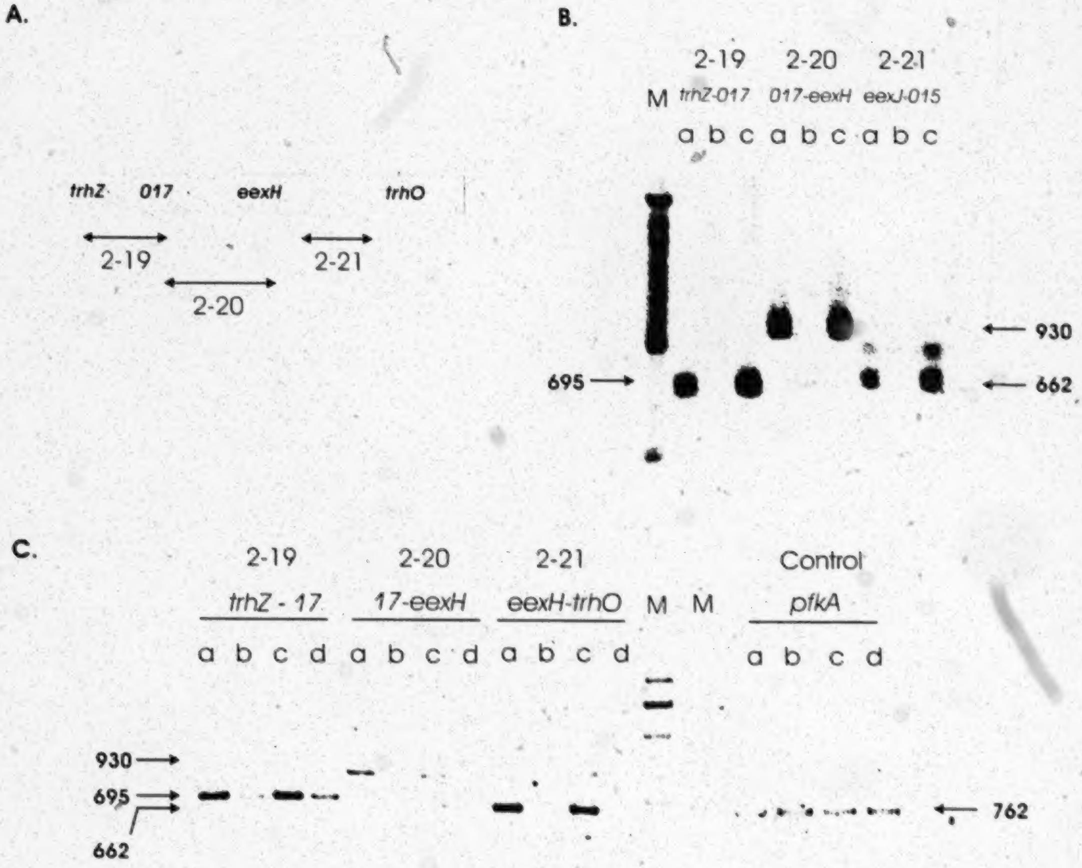
A.
trhZ
017
eexH
trhO
2-19
2-21
2-20
B.
2-19
2-20
2-21
M
trhZ-017
017-eexH
eexJ-015
a b c a b c a b c
695
930
662
C.
2-19
2-20
2-21
Control
trhZ - 17
17-eexH
eexH-trhO
M
M
pfkA
a b c d a b c d a b c d
a b c d
930
695
662
762

When the primers 2-19, 2-20, and 2-21 were added to RNA extracted at 30°C and 37°C from cells harbouring drR27 or WT R27, lower amplification of the Z operon transcript was observed at 37 °C than at 30°C (Figure 4-2c). RT-PCR is only a semi-quantitative technique but there was a significant difference in the Z operon transcript levels at 30°C and 37°C, with the former being greater than the latter. The 2-20 primer set amplifying orf017-*eexH* showed the greatest difference in amplification levels, with no detectable product present when the RNA template was extracted from cells grown at 37°C harbouring WT R27 or drR27 (Figure 4-2c). As a control to ensure that the levels of RNA template used for the RT-PCR reactions were equivalent, the *E.coli* housekeeping gene *pfkA*, encoding phosphofructokinase, was amplified (Figure 4-2c). There was no difference in the level of *pfkA* amplification of RNA extracted from cells grown at 30°C and 37°C harbouring WT R27 or drR27.

4.3.3 Effect of R27 entry exclusion proteins on the transfer of related and non-related conjugative plasmids

The specificity of the Eex activity mediated by TrhZ and EexH was determined by mating recipient cells expressing the R27 Eex proteins with donor cells harbouring R27-related and non-related plasmids. The IncHI1 R27 had been found to elicit an EI of 3001 when mixed with recipient cells expressing the Eex protein TrhZ (Figure 4-1). Similarly, when donor cells contained the closely-related IncHI1 plasmid pRG1251, the TrhZ-encoding recipients were able to exclude the donors to an EI of 1781 (Table 4-4). When the donor cells harboured the IncHI2 plasmids pAS252-2-3 and R478, the EI levels decreased to 640 and 526, respectively. The EI levels decreased further to 207 when donor cells containing the IncHII plasmid pHH1508a were mixed with recipient cells expressing TrhZ. Non-related IncP RP4 plasmid and IncF F plasmid were only slightly inhibited in conjugation with recipient cells encoding TrhZ, as the EI levels were 10 and 19 respectively (Table 4-4).

When EexH was included in the Eex assay, the trend observed with TrhZ of decreasing EI levels corresponding to increasing donor plasmid diversity was not present. Whereas donor cells containing the R27 IncHI1 plasmid elicited EI levels of 17483 when mixed with recipient cells expressing EexH, the EI levels were markedly lower at 461 when the donor cells harboured closely-related IncHI1 plasmid pRG1251. The EexH mediated EI levels associated with the IncHI2 plasmids pAS252-2-3 and R478 were decreased further at 209 and 95. Surprisingly, the most distantly related IncH mobile element in this study, the IncHII plasmid pHH1508a, obtained the second highest EI of 1353, when mixed with EexH containing cells. The two plasmids not related to the IncH family, the RP4 and the F plasmid, were both conjugally inhibited by EexH to varying levels; the F plasmid registered an EI of 353 and RP4 elicited an EI of only 39 (Table 4-4).

4.3.4 Localization of TrhZ and EexH in the bacterial cell

In order to determine the cellular location of the R27 Eex proteins TrhZ and EexH, a bacterial fractionation experiment was performed. The bacterial cells were fractionated into cytoplasmic, inner membrane, periplasmic, and outer membrane fractions by lysozymal treatment, sonication, ultracentrifugation and selective solubility with the detergent sarkosyl. The fractionation method used in this study exploits the differential lipid composition of the inner and outer membranes to separate the bacterial cell envelope; solubilization of the inner membrane with sarkosyl has been shown to be an effective means of separating the membranes of *E. coli* (56, 63, 141).

Characterization of plasmid-encoded Eex proteins has revealed that this family of proteins commonly contains signal sequences and hydrophobic domains implying

Table 4-4. Specificity of the Entry Exclusion process mediated by TrhZ and EexH.

Donor strain containing:[†]		Exclusion Indices[‡] when recipients[§] harbour:		
Plasmid	Incompatibility Group	pMS119EH	TrhZ-pMS119EH	EexH-pMS119HE
drR27	IncHI1	5	3001	17483
pRG1251	IncHI1	8	1781	461
pAS252-2-3	IncHI2	4	640	209
R478	IncHI2	2	526	95
pHH1508a	IncHII	1	207	1353
F pro lac:: Tn5	IncF	1	19	353
RP4	IncP	1	10	39

[†] *E.coli* DY330R serve as the donor strain

[‡] EEX index is calculated by dividing the transfer frequency of cells harbouring an empty cosmid with the transfer frequency of cosmid clones containing R27 fragments.

[§] *E.coli* RG11 serve as the recipient strain

Table 4-5. Summary of entry and surface exclusion genes from Gram-negative plasmids

Plasmid (Inc group)	Gene	Protein Size (aa)	Transfer phenotype of exclusion mutant[†]	Motifs[‡] (aa)	Hydrophobicity region[§](aa)	Signal sequence[¶] (aa cut site)	Reference
R27 (HI)	*trhZ*	130	+	None	3-19	Yes (18-19)	This study
R27 (HI)	*eexH*	279	+	None	4-23	Yes (23-24)	This study
F factor (FI)	*traT*	244	+	Lipoprotein (12-22)	7-29, 139-156	Yes (26-27)	(59)
F factor (FI)	*traS*	173[*]	+	None	34-53, 63-79, 108-131	No	(59)
RP4 (Pα)	*trbK*	69	+	Lipoprotein (13-23)	6-22	Yes (22-23)	(80)
Ti	*trbK*	75	+	None	5-24	Yes (20-21)	(119)
R391 (J)	*eexR*	143	+	None	12-28, 41-59, 74-100	Yes (27-28)	(130)
SXT	*eexS*	143	+	None	12-30, 41-59, 83-103	Yes (27-28)	(130)
pKM101 (N)	*eex*	75	N/A	Lipoprotein (5-15)	4-24	Yes (14-15)	(157)
R388(W)	*eex*	76	N/A	Lipoprotein (7-17)	None	Yes (18-19)	(121)
R144(I)	*excA*	220	N/A	None	24-45, 59-76	No	(87)
R144 (I)	*excB*	147	N/A	None	None	No	(87)
ColE1	*mbeD*	77	N/A	None	None	No	(220)

[†] Ability of mutant to transfer via conjugation to recipient cells. Detectable matings marked as "+". N/A corresponds to not available in the literature.

[‡] Conserved domain database (http://www.ncbi.nlm.nih.gov) and ScanProsite (http://ca.expasy.org/tools/scanprosite/).

[§] TMPred (http://www.ch.embnet.org/software/TMPRED_form.html)

[¶] SignalP (http://www.cbs.dtu.dk/services/SignalP/)

[*] The *traS* sequence has been extended to encode an additional 72 bp or 24 aa (Accession number P09129)

membrane-association (Table 4-5). The bacterial fractionation data of R27-encoded Eex proteins determined that $EexH_{His}$ predominantly localized to the outer membrane of the cell (Figure 4-3A). Small amounts of $EexH_{His}$ were detected in the inner membrane fraction with no detectable protein in the cytoplasmic or periplasmic fractions. Conversely, $TrhZ_{His}$ was found primarily in the inner membrane fraction with trace amounts of protein in the outer membrane fraction (Figure 4-3B).

The cytoplasmic and periplasmic fractions had no detectable levels of $TrhZ_{His}$. These data suggest that the R27 Eex proteins function in different regions of the bacterial cell envelope. As a control for the appropriate fractionation of the bacterial cell components, the isolated fractions were probed with anti-DnaK, anti-SecY and anti-OmpA antibodies (Fig. 4-3C). DnaK is a cytoplasmic heat shock protein (Hsp) that is involved in λ DNA replication (120). The Hsp protein was detected in the cytoplasmic fraction with trace amounts in the soluble periplasmic fraction (Fig. 4-3C). The SecY protein is a member of the inner membrane-associated Sec system that translocates proteins out of the cytosol (for review see reference (139); SecY was found predominantly in the inner membrane fraction, with trace amounts of protein in the periplasmic fraction (Fig. 4-3C). The OmpA protein is a porin-like integral membrane protein found in the outer membrane of many Gram-negative organisms(44). The 35 KDa OmpA was detected in the inner and outer membrane fractions, with a small amount detected in the cytoplasmic fraction. A 62 KDa band, OmpA*, detected by the rabbit anti-OmpA serum, was present only in the outer membrane fraction. The OmpA localization result was identical to the distribution of this outer membrane protein in fractionation experiment of a recent study on Eex in IncJ integrative elements (130).

Figure 4-3. TrhZ and EexH localize to the inner and outer membrane, respectively. Bacteria were fractionated into cytoplasm (C), inner membrane (IM), periplasm (P), and outer membrane (OM) fractions with an equal percentage of each fraction volume loaded on SDS-PAG and transferred to a nitrocellulose membrane. (A and B) Immuno blots were probed with anti-His monoclonal antibody. (C) Immunoblots were probed with anti-DnaK monoclonal antibody, anti-SecY and anti-OmpA antisera to ensure appropriate separation of fractions. The OmpA* corresponds to a ~60 KDa protein detected by the anti-OmpA antisera in the outer membrane (130).

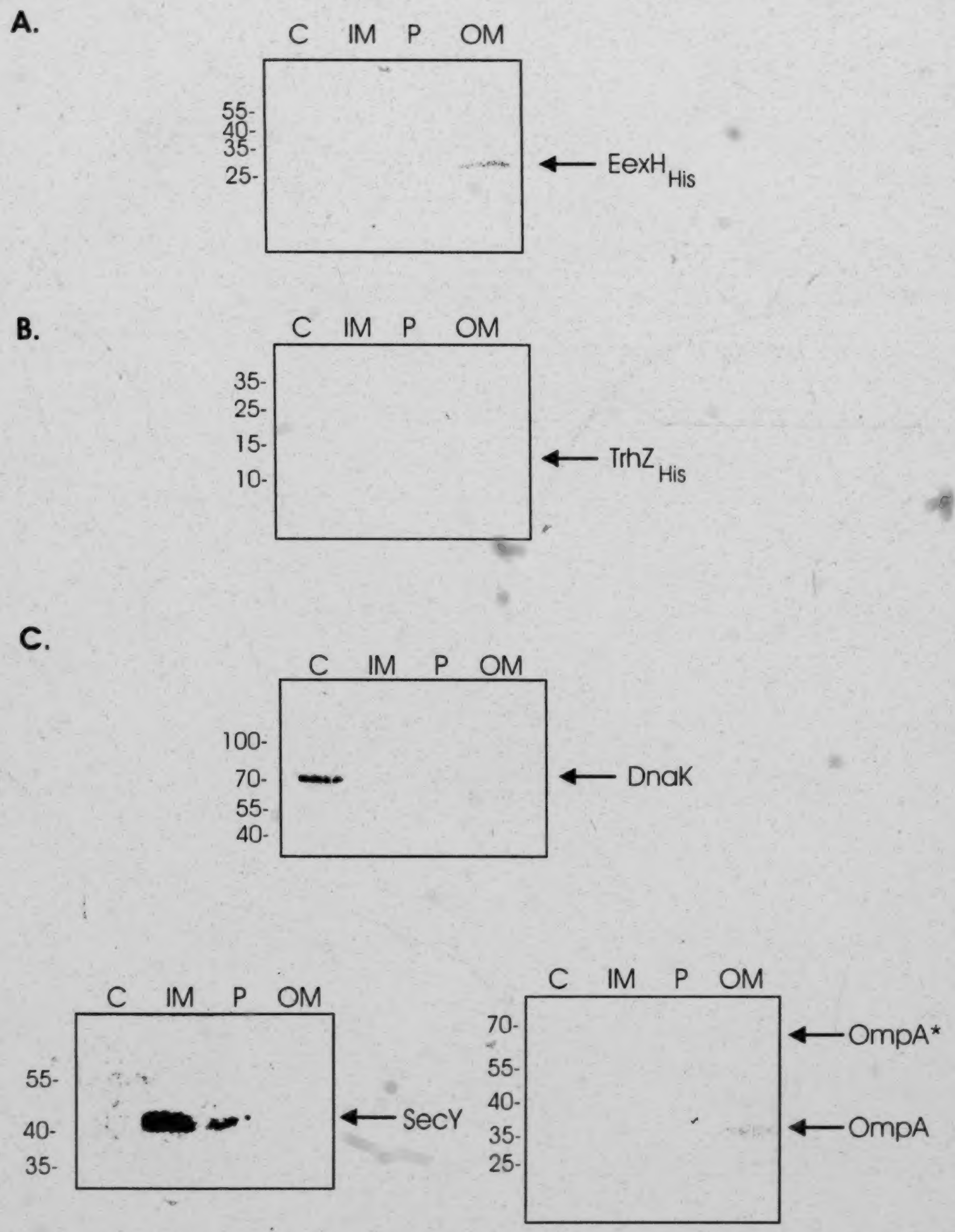
A.
C IM P OM
55-
40-
35-
25-
EexH His
B.
C IM P OM
35-
25-
15-
10-
TrhZ His
C.
C IM P OM
100-
70-
55-
40-
DnaK
C IM P OM
55-
40-
35-
SecY
C IM P OM
70-
55-
40-
35-
25-
OmpA*
OmpA

4.3.5 Do the R27 entry exclusion proteins interact with themselves?

We next sought to determine the mechanistic process of the R27-encoded Eex phenomenon. A possible mechanism of R27-encoded exclusion could be the interaction of the entry exclusion proteins in the donor and recipient cells; consequently, the donor cell and the recipient cell would each have to possess the Eex proteins to observe the exclusion phenotype. Functional and mutational analyses of the Tra2 region of R27 determined that the R27 Eex genes *trhZ* and *eexH* were not essential for the conjugative transfer of the IncHI1 plasmid (109). Cells harbouring drR27 plasmids with insertional mutations in the Eex genes were mixed with recipient cells containing an empty pMS119EH, or pMS119EH/HE expressing TrhZ or EexH. As an experimental control, donor drR27 with mutations in another gene encoded in the Z operon, *orf017*, and a gene in the proximal region of Tra2, *orf004*, were included in this study.

When donor cells harbouring drR27 plasmid with mutations in the *orf004* or *orf017* were mated with recipient cells expressing TrhZ, the resulting EI levels of 5525 and 2013 respectively were similar to the EI of 3001 obtained with WT drR27 (Table 4-6). Conversely, when the donor cells contained the drR27 mutant *eexH*, the EI level decreased to 125. Notably, only background levels of EI were observed when the do[illegible] cell harboured the drR27 mutant *trhZ* (Table 4-6). These data suggest that when the donor plasmid drR27 lacks the TrhZ protein, the IncH plasmid is not inhibited in conjugation with recipient cells expressing the R27 exclusion protein TrhZ; these Eex data support the possibility of a direct (or indirect) interaction of R27 Eex proteins which determines the efficacy of the Eex process. When the study was repeated with recipient cells expressing EexH, the Eex assay was only possible with donor cells harbouring the drR27 mutant *trhZ*. Again, a significant decrease in EI to background levels was observed (from 17483 to 8) when the R27 donor plasmid had an insertional mutation in the *trhZ* gene (Table 4-6). Unfortunately, when donor cells containing drR27 mutants

Table 4-6. Entry exclusion by TrhZ and EexH require that donor cells contain R27 exclusion protein for exclusion activity.

Plasmid in recipient cells [†]	Eex Indices[‡] when donor strain DY330R harbours:				
		drR27 with mutations in:			
	drR27	*orf004*	*eexH*	*orf017*	*trhZ*
Vector alone	5	5	5	3	2
TrhZ-EH	3001	5525	126	2013	5
EexH-HE	17483	N/A[§]	N/A[§]	N/A[§]	8

[†] *E.coli* RG11 served as the recipient cell.

[‡] EI is calculated by dividing the transfer frequency of cells harbouring an empty cosmid with the transfer frequency of cosmid clones containing R27 fragments.

[§] N/A corresponds to "not available" as the transconjugant colonies had a clumped morphology which made enumeration impossible.

orf004, *eexH*, and *orf017* were mated with recipient cells expressing EexH, the dilution plating required for the conjugation assay resulted in massive clumping of the transconjugant cells on the LB plates. The presence of EexH in the recipient cells consistently resulted in this cell morphology when mated with the three aforementioned drR27 mutants, even after repeated mating attempts. Electron microscopic analysis of transconjugant cells harbouring R27 mutants *orf 004* and *trhZ* revealed heavily negatively-stained regions on cell surfaces (Figure 4-4 B,C). The transconjugants cells harbouring the R27 mutant *orf 017* and a vector expressing TrhZ showed an elongated phenotype which was not observed when TrhZ was absent from the RG11 cells (Figure 4-4D and 4-5D). As TrhZ was determined to be an outer membrane, the presence of this entry exclusion protein on the cell surface appears to cause phenotypic changes in transconjugants with certain R27 mutants.

4.4 Discussion

Within large bacterial populations prokaryotic genomes are in a continuous state of flux due to a massive reservoir of DNA upon which to draw. The acquisition of foreign DNA via horizontal gene transfer rarely results in the insertion and stable maintenance of genes within a new host over multiple generations. Furthermore, mobile genetic elements-encode barriers that inhibit the initial entry of DNA into recipient cells (193). The entry exclusion process inhibits the transfer of conjugative elements into recipient cells harbouring isogenic or closely-related mobile elements (143). In addition to preventing the unnecessary energy expenditure of redundant conjugative transfer, entry exclusion determinants have been found to confer serum resistance on host cells (136) and have been proposed to break apart mating pairs releasing transconjugant cells to act as new donor cells (193).

Figure 4-4. Electon microscopic images of RG11 transconjugant cells expressing the entry exclusion protein TrhZ from pMS119HE. The RG11 TrhZ-HE cells were mated with DY330R cells containing (A) drR27 and the drR27 mutants (B) ORF 004, (C) *trhZ,* and (D) ORF 017.

(a) drR27 in RG11 EexH-HE

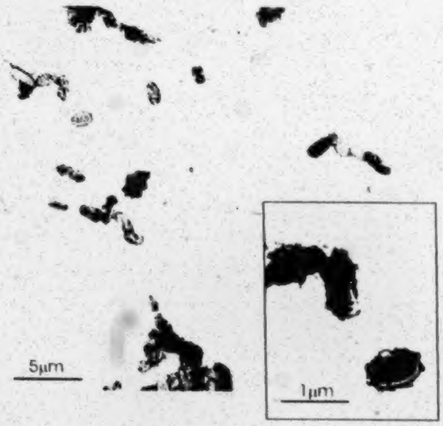

(b) drR27 orf004 in RG11 EexH-HE

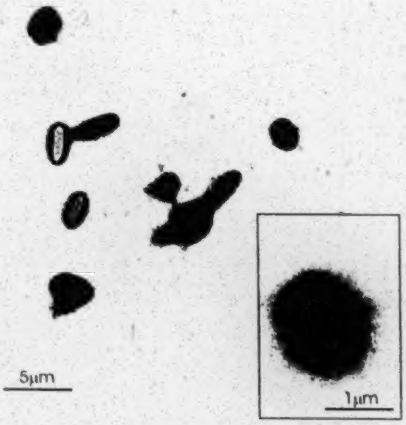

(c) drR27 *eexH* in RG11 EexH-HE

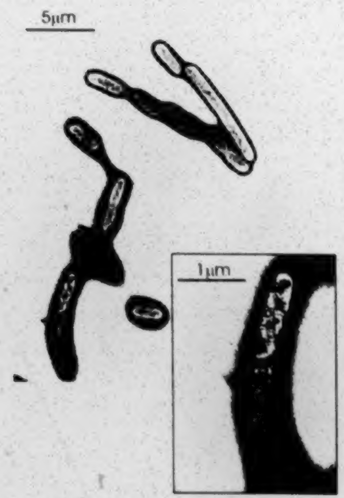

(d) drR27 orf017 in RG11 EexH-HE

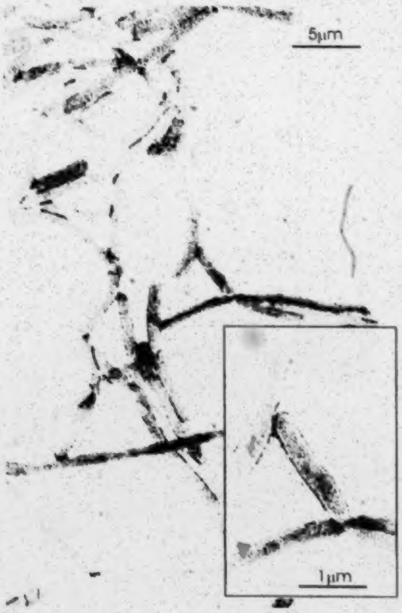

Figure 4-5. Electon microscopic images of RG11 transconjugant cells containing (A) drR27 and the drR27 mutants (B) ORF 004, (C) *trhZ*, and (D) ORF 017.

A. drR27 in RG11

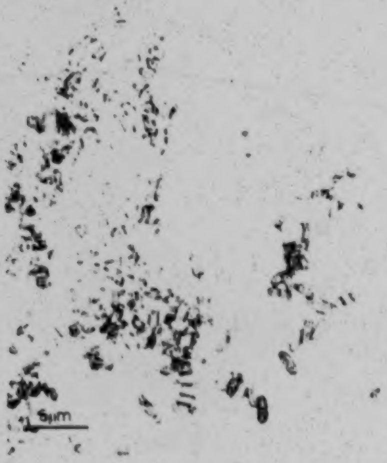

B. drR27 004 KO in RG11

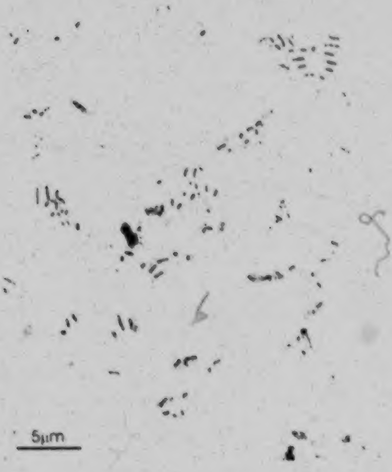

C. drR27 *trhZ* KO in RG11

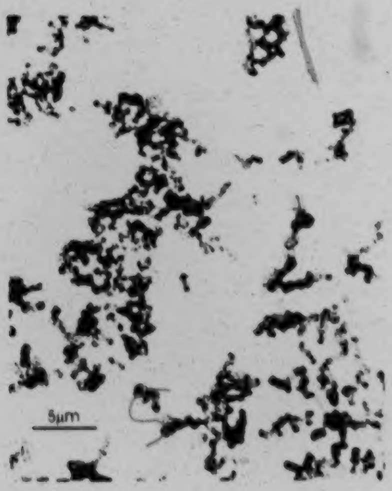

D. drR27 017 KO in RG11

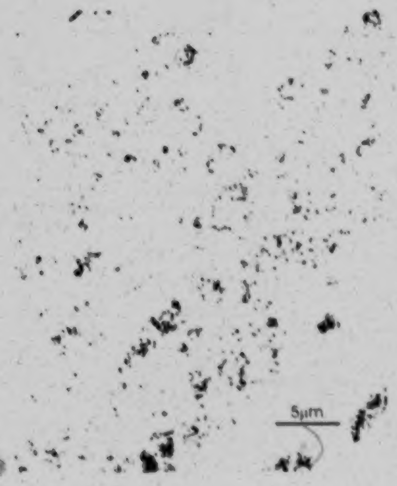

Here we describe two proteins that mediate entry exclusion within the prototypical IncHI plasmid R27. Although entry exclusion was initially documented within the IncHI family in 1977 (188), a cosmid screen of R27 has revealed that the entry exclusion (Eex) phenotype was conferred by TrhZ and EexH encoded within the Z operon located in the Tra2 region of this conjugative plasmid. The R27 cosmid library bank contained the majority of the R27 plasmid, however the presence of an *oriT* sequence within the Tra1 region resulted in difficulties with cloning adjacent regions (108, 140). The cosmid library did not include 10 orfs located within this section of the Tra1 region, of which six orfs have been assigned a functional role in conjugation (108). In the existing literature on Eex, no gene mediating Eex that was encoded outside of the defined transfer region has been reported (4, 81, 87, 121, 157). Nevertheless, we cannot exclude the possibility that one or more of the Tra1 orfs 115, 116, 118, or 121 may be involved in entry exclusion function of R27.

The functional and mutational characterization of the Tra2 region of R27 revealed that *trhZ* and *eexH* are not essential for the conjugative transfer of the IncHI1 plasmid (108). The non-essential nature of the R27 Eex proteins in conjugation is consistent with the Eex determinants that have been characterized (Table 4-5). A motif that has been associated with Eex determinants is the lipoprotein motif; neither EexH nor TrhZ contain this motif (Table 4-5) Notably, mutational analysis of the TrbK lipoprotein motif has identified that such a functional lipoprotein motif is not required for the Eex activity of the RP4 protein (80). The Eex proteins of the R27 plasmid both contain a transmembrane domain as part of a predicted signal sequencE. The majority of Eex determinants contain transmembrane domains and localization studies of the IncP and IncF Eex components have confirmed an association with the cellular envelope (Table 4-5)(2, 80, 97). Bacterial fractionation studies on the EexH and TrhZ proteins of R27 indicated that the TrhZ protein primarily associates with the inner membrane, whereas EexH was predominantly located in the outer membrane. The well-characterized TraT protein from the F plasmid was also identified as an outer membrane protein (2); the surface exposed TraT has been proposed to prevent the formation of mating aggregates. The TraT protein has been termed a surface exclusion protein. Although EexH mediates exclusion in the R27 plasmid and was localized to the outer membrane, we have employed the nomenclature proposed by Novick *et al.* in which all exclusion proteins are termed entry exclusion proteins (145).

Recent transcriptional studies on the R27 plasmid have determined that at 33-37°C (57), a temperature that is non-permissive for conjugative transfer of IncHI plasmids (189), there is global repression of essential transfer genes. This global repression can be mediated by plasmid or host-encoded Hha or H-NS (57). Transcriptional analysis of the Z operon, encoding the R27 entry exclusion proteins, revealed that the global repression induced by elevated temperatures reduced the expression of the Tra2 operon. The Z operon is flanked by the double partitioning modules of R27 and is transcribed in the opposite direction from the remaining two Tra2 operons. It is noteworthy that the Z operon, encoding proteins non-essential for the conjugative transfer of R27, appears to be regulated by the same mechanism as the operons encoding essential R27 transfer proteins.

An Eex assay was established to determine the levels of exclusion mediated by recipient cells expressing R27-encoded TrhZ or EexH, when mated with donor cells harbouring R27-related and non-related plasmids. It would be expected that a donor cell containing a closely-related IncH plasmid would elicit a high EI when mixed with recipient cells expressing the R27 exclusion proteins; conversely, donor cells harbouring non-related plasmids such as IncP or IncF plasmids could mate with the aforementioned recipient cells with minimal inhibition, thereby registering a low EI level. When recipient cells expressing TrhZ were mated with donor cells harbouring R27-related and non-related plasmids, there was a direct correlation between the increase in evolutionary distance from the R27 plasmid and the decrease in EI levels. Conversely, this trend was not apparent with the EexH protein. Surprisingly, when the donor cells harbouring the IncHI2 plasmid R478 were mated with recipient cells expressing EexH the EI levels of 95 were significantly lower than the EI level of 353 elicited by the F Factor a non-related IncFI plasmid.

A search of the NCBI database for homologues of the TrhZ and EexH identified orf016 and orf018 from the IncHI2 plasmid R478 (Figure 4-6). Whereas TrhZ is closely related to the orf016 from R478 (80.5% identity over an alignment length of 128 residues), EexH has only limited sequence similarity to the R478 orf018 (40.6% identity over an alignment length of 281). Moreover, the sequence similarity between EexH and 018 is lower in the C terminal region of the proteins (32.1% identity over an alignment length of 100 residues). The C terminal region of Eex proteins have been demonstrated to be the domain that determines the specificity of entry exclusion (80, 130). The limited sequence similarity in the C terminal region between EexH and orf018 from R27 and R478 respectively, may explain the inability of the EexH plasmid to exclude R478 during Eex activity assays.

Although a number of Eex determinants have been identified in a wide array of incompatibility groups, little is known about the mechanism by which the Eex proteins confer the exclusion phenotype to host cells. Studies on the TraS protein of the F plasmid, and Eex determinants from the conjugative elements SXT and R391 have revealed that these inner membrane proteins interact with the well-conserved mating pair formation protein TraG (8, 130). The TrbK protein from RP4 was also proposed to interact with a component of the mating pair formation complex (80). TrbK and the R391/SXT-encoded Eex proteins were not required in the donor cell to elicit an Eex event. Conversely, when donor cells containing an R27 *trhZ* mutant were mated with

Figure 4-6. Alignment of the R27 entry exclusion protein (A) TrhZ (GenBank accession no. NP_058232.1) with R478 protein orf 016 (GenBank accession no. CAE51546.1) and (B).R27 protein EexH (GenBank accession no. NP_058230.1) with the R478 protein orf 018 (GenBank accession no. CAE51548.1). Sequences were aligned using ClustalW and shaded in GeneDoc using the conservation mode at level two. Arrows indicate the predicted signal sequence cleavage site using SignalP.

(a)

```
TrhZ (R27) : MKYILTVLCTFFCQTASAYPYRIYTAPEGAIVKHILTMFVIGKTPTLVDV :  50
016 (R478) : MKQTLIVILLCFGHTALAYPYRIYTVPEGALVKNILTNEYLGKTPTVVLV :  50

TrhZ (R27) : SNTEAGSTFGILMYRHENVAIKIFTVMINAENNFTVSGPDVATMSLPGKA : 100
016 (R478) : SNTEAGSTFGILLFRHENVAIKIFTVMHSAENNFAVSGPDVATMSLPGKA : 100

TrhZ (R27) : PLNVTNLSNAAAVHIDLRFFLEEPANHEVQ : 130
016 (R478) : PLNVVNLGNGASVHIELRFYMSEPANTEY- : 129
```

(b)

```
EexH (R27) : MLKLELILLPLLAFLGPSNITNASTKTPIPSSQLSDAKTGVNYEFLTIAA :  50
018 (R478) : M-KINWKLISISTLLLHLHAAAAPHQEKEHRKDAFSSAAQKSDSLLSAKA :  49

EexH (R27) : NYVNGMALVDGRQRPVIKTSMTKRNYLQLENDSASTPLNLVIPKIEFSII : 100
018 (R478) : ELINGRAFINGKYRPVLKTEMTKTNFLEIMNVSNKESLFIVIPKLEYNII :  99

EexH (R27) : AKNGVFISKFISLDSDASGKRILVLEIGSSMTISIVNDLSSTPLQALVSV : 150
018 (R478) : AKNKILLNEKIALSEGTSGKSIVNVEEKSSLTISFIKDLANTPLQAIVSI : 149

EexH (R27) : IKQKFEVIAIFGPDQGKKFTLFLPSDSQNSSIDYVPSPEIALRIIAEKKL : 200
018 (R478) : IRNNKDILAIFGPDQGKGFTLLGNTSNDQVSVPDYSDLNIK-KLKIEQSV : 198

EexH (R27) : QPAIAIPEDASASLLPSHT-YKIRAAEKVRTFKFESFYWVGKFNKLLGGS : 249
018 (R478) : GNPVTINPKEKNYLLVGQGKYEILSLPKYQHLVFSEPVYIEKRKKILGCY : 248

EexH (R27) : DYFTKELKIYPGENFDISTIQKTTMKTENE : 279
018 (R478) : GYWTKETILYPGESLSFITSAKNNLKKRDE : 278
```

donors expressing TrhZ, there was minimal exclusion activity (EI=5) as the mating frequency was equivalent to that obtained with the R27 *trhZ* mutant mated with recipients containing empty vector (EI=2). Similar results were obtained when the *trhZ* mutant was utilized as a donor plasmid with recipient cells expressing EexH (EI=8). Further evidence to support the interaction between R27 Eex proteins is that the R27 *eexH* mutant was only minimally excluded from recipients expressing TrhZ (EI=126). These putative Eex interactions between R27 proteins may explain the major discrepancy in the EI levels elicited by TrhZ and EexH. When the entire Z operon was expressed from pMS119EH, EI levels of 2998 were obtained, similar to the EI level observed with donors expressing TrhZ alone (EI=3001). However, when the *trhZ* gene was excluded from the operon, the EI levels drastically increased to 13852, which is closer to the EI levels elicited by EexH alone (EI=17483). In future studies it is necessary to determine if the inner membrane-associated TrhZ regulates the expression, or perhaps localization, of EexH in the outer membrane when the two R27 Eex proteins are co-expressed.

Together, these data permit speculation on the mechanism involved in R27 entry exclusion. A successful interaction between the outer and inner membrane Eex components results in the exclusion of the incoming plasmid. A potential problem is that this model requires the inner membrane proteins of donor and recipient cells to interact. A similar problem exists with the proposed interaction between the inner membrane Eex and TraG proteins of the F and R391/SXT conjugative elements. The composition and architecture of the type IV secretion system (T4SS) remains elusive; there is increasing evidence that the conjugative pore enables proteins within the inner membrane to interact through translocation of certain conjugative proteins between mating cells (8). An alternative possibility is that the appressed donor and recipient membranes allow their respective inner membranes proteins to come into close proximity as there is evidence that an intermediate fraction representing both cytoplasmic and outer membrane components is formed by the T4SS (75, 166).

Chapter 5

General Discussion

5. Discussion

5.1 Bacterial Conjugation

Charles Darwin proposed the tree or coral of life to describe the history of all living and extinct organisms (38). Bifurcation of a branch of the tree represents a split and independent evolution of two species. Horizontal gene transfer (HGT) is a process that enables genetic exchange between independently evolved species (for a review see (70)). The result of this lateral exchange is the potential to turn the structured evolutionary tree into a tangled web (15).

Bacterial conjugation is a mechanism of HGT that is encoded by conjugative elements such as plasmids and integrative chromosomal elements. The bacterial envelope represents a formidable barrier for the entry or export of macromolecules. The majority of mobile genetic elements that are proficient at conjugative transfer encode a multiprotein complex, the type IV secretion system (T4SS), which spans the double membrane structure of Gram negative bacteria (34). Mobilizable plasmids such as the InQ plasmid RSF1010 do not encode a T4SS however these genetic elements are able to utilize the T4SS encoded by other self-transmissible plasmid families such as IncP plasmid, to facilitate lateral gene transfer (83).

Sequencing and mutational analysis of the IncHI1 plasmid, R27, has revealed that this Gram negative plasmid encodes a T4SS within two transfer regions, Tra1 and Tra2 (108, 109, 176). This thesis has characterized two Tra1-encoded proteins, TraJ and TraG, which are essential for R27 conjugative transfer, and thus these proteins have been termed "mediators" of R27 HGT (Chapter 2). A search of the R27 plasmid for proteins that inhibit IncH redundant transfer identified the Tra2-encoded proteins EexH and TrhZ; as these proteins prevent conjugative transfer they have been termed "inhibitors" of R27 HGT (Chapter 4).

The analysis of the mediators and inhibitors of an R27 HGT event will be described separately in sections 5.2 and 5.3, respectively.

5.2 Mediators of R27 HGT

Complete genomic sequence information is available for the IncHI1 plasmids R27 and pHCM1, as well as the IncHI2 plasmid R478 (69, 155, 176). The region of similarity among these IncHI plasmids encompasses the plasmid backbone determinants that encode replication, partitioning and conjugation functions. There were no genes within this minimal core that appeared to encode accessory functions such as resistance to antimicrobial agents (69). A closer examination of the conjugative genes of IncHI plasmids revealed that these large conjugative plasmids are a hybrid of genes that share homology with a variety of Inc groups. The IncH T4SS can be grouped with the IncF T4SS as significant homology exists within the proteins that are necessary for assembly of conjugative pili (112). Unlike the T4SS of the Ti plasmid or IncP plasmid, the F/H-type T4SS do not encode a third ATPase, VirB11. Conversely, the IncH relaxase protein which forms a covalent bond with the DNA substrate has greater similarity to the IncP relaxase than the relaxase encoded by the IncF plasmids. A final example of the hybrid nature of the IncH T4SS is the absence of the R27 accessory protein TraJ within the IncP, IncF or IncW plasmid families. TraJ homologues were identified in a number of H-type conjugative elements such as SXT and R391 (69).

An interaction has recently been identified between the R27 coupling protein TraG and a component of the T4SS, TrhB (66). The primary objective of this thesis was to extend the coupling protein interaction study by identifying interactions that may occur between TraG and the R27 relaxosome proteins. The bacterial two hybrid and immunoprecipitation techniques revealed that TraG could interact with TraJ (Chapter 2). Mutational analyses of the Tra1 region of R27 revealed that *traJ* encoded a protein that is essential for conjugative transfer of the R27 plasmid, but is not necessary for formation of conjugative pili on the cell surface (108). Our initial characterization of these data classified TraJ as a relaxosomal component (108). Further research, however, has indicated that TraJ is an accessory protein to the R27 coupling protein TraG (Chapter 2). One line of evidence that suggests that TraJ is not a relaxosome protein is the structural architecture of this R27 protein. The presence of multiple putative transmembrane domains within TraJ (69) is atypical of relaxosomal proteins which are normally associated with the cytoplasmic environment (124).

A second indication that TraJ is an accessory protein to the coupling protein was revealed upon a search of the NCBI databanks. Every genome containing a TraJ homologue also encodes a member of the coupling protein family (69). Moreover, the TraJ and TraG homologues are located within 1.5 kb of each another. Homologues of TraJ and TraG encoded within plasmid and chromosomal genomes were found to interact which suggests that this module of TraJ and TraG is evolutionarily related with respect to function (Chapter 2). Further evidence of the functional relatedness of TraJ and TraG is that TraJ shares sequence similarity with an N terminal, multiple transmembrane domain present in a family of DNA translocases, FtsK/SpoIIIE (Chapter 2). Sequence similarity has previously been documented between SpoIIIE and the coupling protein family (52); this sequence similarity is greatest in the NTP-binding domains located in the C terminal regions of these ATPases.

The shared similarity to a large DNA translocase family of proteins, in combination with the conserved interaction that exists between homologues of TraG and TraJ and the shared functional role in mediating R27 HGT, suggests that TraG and TraJ may have been fused together as a Rosetta stone protein sequence (129)(Chapter 2). According to the Rosetta Stone model, the progenitor of the IncH proteins TraG and TraJ would have been a single polypeptide similar to the FtsK/SpoIIIE DNA translocase family. An interesting observation is that within each genome encoding this TraJ-TraG module, the genetic organization is that *traG* is upstream of *traJ* (Figure 2-8). The R27 proteins TraJ and TraG share homology with the N and C terminal domains of the FtsK/SpoIIIE translocases, respectively (Chapter 2). There are two possible explanations for why the coupling protein is encoded upstream of the accessory protein. The first explanation is that a simple genetic rearrangement has occurred in the ancestral gene encoding for this fused polypeptide. While a second explanation is that the fused polypeptide had an atypical domain organization for an ATPase with transmembrane domains at both the N and C terminus.

The most pressing question regarding the proposed role of TraJ as an accessory to the R27 coupling protein is why this accessory protein is not a common feature of all members of the coupling protein family. Within the well-characterized coupling proteins of the IncF, and IncP plasmids, two transmembrane regions are sufficient for membrane localization and pore formation (169). A possible explanation is that in addition to the role as a stability factor for the coupling protein at the inner membrane, TraJ may play a role in delivering the single stranded DNA substrate to the hexameric pore of the coupling protein. One current model for conjugation, referred to as the "shoot and pump" model, involves the translocation of a relaxase bound to the processed DNA through the T4SS (122, 123). The second step of the model is that the coupling protein actively pumps the DNA across the conduit (122, 123). The TraJ-protein family contain two well-conserved, positively-charged residues between the second and third transmembrane domain (69). The cytoplasmic-association and close proximity to the coupling protein pore may facilitate the binding of processed DNA by these residues.

A schematic representation of the R27-encoded protein interactions identified in this thesis is presented in Figure 5-1. The positively-charged residues of TraJ have

Figure 5-1. A schematic representation of the interactions occurring between R27-encoded proteins studied in this thesis. The structural domains of the hexameric coupling protein TraG (dark blue) are indicated. The periplasmic interaction domain between TrhB (orange) and TraG is shown. The interaction between TrhB and TrhK (light blue) has not been demonstrated within the R27 Mpf, however there is evidence of such an interaction in related T4SS (see text). The two well conserved positively charge residues in TraJ (green) at the inner-membrane-cytoplasm interface are shown.

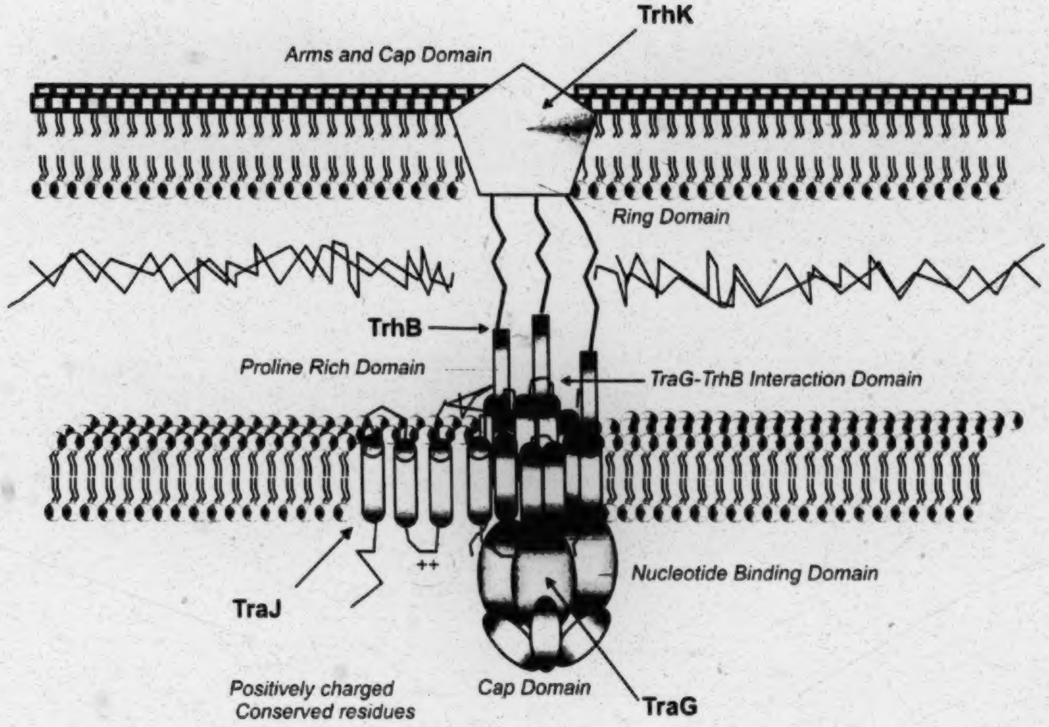
TrhK
Arms and Cap Domain
Ring Domain
TrhB
Proline Rich Domain
TraG-TrhB Interaction Domain
++
Nucleotide Binding Domain
TraJ
Positively charged
Conserved residues
Cap Domain
TraG

been represented. The TraJ domain that interacts with the coupling proteins has not yet been determined. Site-specific mutagenesis of the TraG periplasmic residues, flanked by transmembrane domains, was not sufficient to inhibit an interaction with TraJ suggesting that the TraJ-TraG interaction does not occur in the periplasmic space (Chapter 3). The periplasmic residues of the R27 coupling protein TraG have been found to be necessary for an interaction with the Mpf protein TrhB. Bacterial two hybrid analysis indicated that the coupling proteins from the IncP, IncW and IncF plasmids are also able to interact with the periplasmic-spanning TrhB protein. Notably, none of these non-cognate coupling proteins could complement a R27 *traG* mutant suggesting that these coupling proteins could not associate with the R27 relaxosome. Bacterial two hybrid analysis also revealed that non-cognate coupling proteins could not interact with the R27 TraJ protein (Chapter 3). If TraJ is involved in presenting the DNA to the conjugative pore, the inability to interact with TraJ may partially explain the inability of non-cognate coupling proteins to complement a R27 *traG* mutant.

Secretins are multimeric proteins that localize to the outer membrane and form pores enabling the secretion of macromolecules (190). An outer membrane pore has not been identified in the T4SS, however, the C terminal region of the R27 T4S protein TrhK (TraK from F plasmid) shares sequence similarity with secretins from the T2SS and T3SS (109). Figure 5-1 depicts the interaction between conjugative core proteins TrhB and TrhK. This is based on studies of the VirB/D4 T4SS of the Ti plasmid, which have presented immunoprecipitation data in which homologues of TrhB and TrhK, VirB10 and VirB9, respectively, form a complex in the presence of a functional coupling protein. Mutagenesis of the Ti plasmid coupling protein VirD4 prevented this association which led to the proposal that the periplasmic spanning-VirB10 protein is an ATP energy sensor (27).

The ATPase VirB4 of the *A. tumefaciens* VirB/D4 T4SS has recently been predicted to form a homohexamer and act as a inner membrane docking site during conjugation (133). The proposed hexameric configuration was based on sequence similarity to the prototypical R388 coupling protein TrwB. This conjugative model predicts that VirB4 binds to the hexameric VirB11 at the entrance to the conjugative pore and undergoes a conformational change in the presence of VirD4 such that VirD4 now docks with VirB11 (133). There are two major difficulties in incorporating the Ti conjugative model with the predicted R27 conjugative apparatus. The primary issue is that the H-type T4SS differs from the VirB/D4 T4SS in that it does not encode a VirB11 homologue. Secondly, bacterial two hybrid analysis and immunoprecipitation techniques demonstrate that the R27 coupling protein does not interact with the R27 VirB4 homologue TrhC (Chapter 2). As this interaction is central to the Ti conjugative model, it is likely that the conjugative mechanisms occurring at the inner membrane-cytoplasm interface are different for these two conjugative plasmids.

Characterization of the R27 T4S protein TrhC, a homologue of the ATPase VirB4, has indicated that GFP tagged-TrhC forms foci in the periphery of the cell membrane. This localization is dependent on the presence of essential Mpf proteins suggesting that these foci represent R27 Mpf complexes (67). Further studies indicated that conserved residues in the Walker A and B NTP binding motifs are not essential for the formation of foci but are essential for pilus formation and R27 conjugative transfer (68). These data suggest that ATP binding and hydrolysis by TrhC is not essential for assembly of Mpf complexes, however, ATPase activity is required for conjugative transfer following Mpf formation.

Immunofluorescent microscopic studies of the R27 coupling protein indicate that TraG also forms foci in the cell periphery (Chapter 3). Notably, the random distribution of coupling protein foci, and the average number of foci found per cell (~5-6) were similar to the results obtained from analysis of foci formed by the R27 Mpf complexes. A major difference between the foci formed by TraG and TrhC was that foci could be formed by the R27 coupling protein in the absence of other T4S proteins. Therefore the R27 coupling protein could be a docking site onto which the Mpf complex is assembled. An R27 *traG* mutant expressing TrhC-GFP, however, was still able to form fluorescent foci in the cell periphery indicating that Mpf complex formation occurs in the absence of the coupling protein (68). Together these results indicate that the R27 Mpf complex and coupling protein independently associate at discrete positions in the cellular membrane. It may be possible that a host-encoded protein is the docking site for the R27 conjugative proteins. The Mpf and coupling protein encoded by the Ti plasmid VirB/D4 T4SS also independently associate with a discrete cellular location, the pole of the host cell (99, 103). These Ti plasmid studies have not yet identified the membrane associated-protein or structure to which the T4S proteins bind.

5.2.1 Future Studies on the R27 Conjugative Apparatus

The "shoot and pump" model of conjugation proposes that the coupling protein has an active role in the secretion of the DNA substrate through the conjugative pore (122). Site-specific mutagenesis of the R27 coupling protein TraG has identified residues within the Walker A and B NTP-binding motifs that are essential for conjugative transfer of the IncH plasmid. Studies using mutagenesis of the periplasmic-spanning domain of TraG were instrumental in identifying the domain of the R27 coupling protein that interacts with the Mpf complex. Clearly, this technique is an effective tool in defining an R27 conjugative model. There are numerous R27 proteins with residues that are candidates for mutational analysis including the two well-conserved, positively charged residues of the R27 accessory protein TraJ. If a mutation within this region of TraJ inhibits conjugative transfer, DNA-binding studies with R27 DNA and non-specific DNA would be the next logical experiment to perform with TraJ.

A second candidate for mutational analysis is a well-conserved glutamine residue in TraG that is located distal to the Walker B motif (Figure 5-2). Structural predictions of the VirB4 ATPase from *A. tumefaciens* indicate that this glutamine residue (Q539 in TraG^{R27}) is structurally proximal to residues within the Walker A and B motifs that have been identified as essential for ATP binding (133). This glutamine residue may play a similar role in ATP hydrolysis as the Q loop motif of the ATP-binding cassette (ABC) transporters (98). Structural changes in the Q loop are essential for the hydrolytic activity of the ATPase; glutamine is the catalytic residue of the Q loop motif (98).

Mutation of the R27 coupling protein TraG periplasmic domain, which created the construct TraG:S4, prevented the association of the coupling protein with the Mpf protein, TrhB (Chapter 3). Interestingly, the TraG:S4 construct was still able to complement an R27 *traG* mutant, albeit with less than WT transfer frequency. As TraG:S4 is not able to interact with TrhB, the R27 coupling protein must interact with more than one component of the Mpf complex (Chapter 3). Future studies should include screening R27 Mpf proteins which putatively associate with the inner membrane for the ability to interact with the coupling protein.

Finally, the sequence similarity that exists between TrhK-like proteins and the secretins of the T2SS and T3SS may indicate that the T4SS does contain a member of the secretin family of proteins. A conjugative pore must contain a structure in the outer membrane that would mediate translocation. Attempts at isolating multimeric TrhK have to date been unsuccessful, even in the presence of additional conjugative proteins such as the lipoprotein TrhV. Purification and visualization of TrhK would represent a significant advancement in the study of conjugative plasmid biology. A renewed effort in isolating this SDS-resistant, multimeric structure may be a valuable enterprise.

Figure 5-2. Alignment of the Walker B motifs from coupling proteins from R27 (TraG; Gen Bank accession no. NP_058332), R478 (TraG; Gen Bank accession no.CAE5173). R391 (TraD; Gen Bank accession no. AAM08004), SXT (TraD; Gen Bank accession no. AAL59680), Ti (VirD4; Gen Bank accession no. NP_059816), R388 (TrwB; Gen Bank accession no. CAA44852), F (TraD; Gen Bank accession no.BVECAD), and RP4 (TraG; Gen Bank accession no.S22999). The numbers indicate the amino acids preceding the Walker B region. Sequences were aligned using ClustalW and shaded in GeneDoc using the conservation mode at level two. The Walker B motif of the coupling proteins is indicated (hhhhDE; where h is a hydrophobic residue (168)) Asterisks indicate the conserved glutamine residue which is a candidate for substitution mutagenesis.

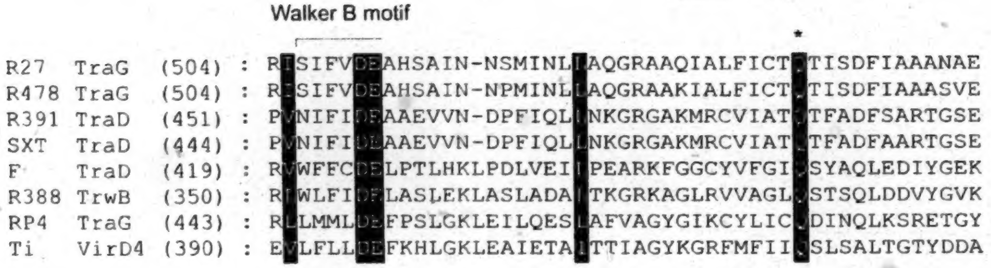
Walker B motif
*
R27 TraG (504) : RISIFVDEAHSAIN-NSMINLIAQGRAAQIALFICT[illegible]TISDFIAAANAE
R478 TraG (504) : RISIFVDEAHSAIN-NPMINLLAQGRAAKIALFICT[illegible]TISDFIAAASVE
R391 TraD (451) : PVNIFIDEAAEVVN-DPFIQLLNKGRGAKMRCVIAT[illegible]TFADFSARTGSE
SXT TraD (444) : PVNIFIDEAAEVVN-DPFIQLLNKGRGAKMRCVIAT[illegible]TFADFAARTGSE
F TraD (419) : RVWFFCDELPTLHKLPDLVEIIPEARKFGGCYVFGI[illegible]SYAQLEDIYGEK
R388 TrwB (350) : RIWLFIDELASLEKLASLADAITKGRKAGLRVVAGL[illegible]STSQLDDVYGVK
RP4 TraG (443) : RLLMMLDEFPSLGKLEILQESLAFVAGYGIKCYLIC[illegible]DINQLKSRETGY
Ti VirD4 (390) : EVLFLLDEFKHLGKLEAIETAITTIAGYKGRFMFII[illegible]SLSALTGTYDDA

5.3 Inhibitors of R27 HGT

Entry exclusion (Eex) prevents the redundant transfer of conjugative elements into recipients harbouring isogenic or closely-related mobile genetic elements (143). Exclusion activity has been documented in a number of conjugative plasmids, and recently in the integrative and conjugative chromosomal elements (ICEs) SXT and R39 (130). In 1977, Eex activity was documented in IncH1 and IncH2 plasmids, however the specific mediators of this exclusion event were not identified (188). An R27 cosmid library representing the majority of the IncHI1 plasmid was screened for the Eex ability. Three cosmids encoding the Tra2 region of R27 were determined to prevented the entry of the IncH plasmid, and sub-cloning of these cosmids identified that the R27 Eex activity was mediated by the Z operon. The Z operon contains four contiguous genes: *trhO, ORF 016, ORF 017,* and *trhZ*. When each gene was expressed in recipient cells and mated with donors harbouring the R27 plasmid, ORF016 and TrhZ reduced entry of the IncH plasmid. Accordingly, ORF016 was assigned the name EexH (Entry exclusion IncH).

A search of the NCBI databank for homologues of TrhZ and EexH revealed only ORF016 and ORF018, respectively, in the IncHI2 plasmid R478. These homology results are not unexpected as the conjugative transfer regions of R27 and R478 are well-conserved (69). However, there is very little sequence similarity among the other entry exclusion proteins encoded by conjugative elements from different incompatibility groups. The diversity of the entry exclusion proteins likely represents the specificity of the exclusion event; as the entry exclusion process prevents the redundant conjugative transfer of only related plasmids.

Transcriptional analysis of the Z operon revealed significantly repressed expression at 37 °C, a temperature that is non-permissive for the conjugative transfer of IncHI1 plasmids (Chapter 4). Temperature-dependent transcription has been demonstrated for a number of R27 transfer genes, including *traG* which encodes the R27 coupling protein (Chapter 2) (5, 57). Mutational analysis of the R27 Tra2 region determined that TrhZ and EexH are not essential for the conjugative transfer of the IncHI1 plasmid (109), and thus is therefore notable that transcription of the Z operon is also regulated in temperature-dependent manner. A logical explanation for this regulation is that expression of the IncHI1 Eex proteins is not necessary at 37 °C, as the large conjugative plasmids are unable to transfer at elevated temperatures (189).

Mutational analysis of the R27 Tra2 region revealed that a *trhZ* mutant had interesting phenotypic properties (109). H-gal is an H-pilus specific bacteriophage that induces lysis in host cells harbouring the R27 plasmid (126). Although the R27 *trhZ* mutant was proficient for conjugative transfer, cells harbouring this plasmid were resistant to H-gal infection (109). A similar result was observed with the IncP entry exclusion protein, TrbK. While propagation of bacteriophage required TrbK, conjugative transfer of the RP4 plasmid did not (81). Electron microscopy revealed that the IncP phage PRD1 were able to adsorb to the surface of cells harbouring a *trbK* mutant, however TrbK was required for subsequent entry of the phage into the cell (81). The inability of phage DNA to enter into cells in the absence of these entry exclusion proteins may provide insight into the mechanism of action of these exclusion determinants.

Bacterial fractionation studies on the R27 exclusion proteins revealed that TrhZ localizes to the inner membrane and EexH localizes predominantly to the outer membrane (Chapter 4). These results are similar to the localization of the two exclusion proteins encoded by the F plasmid; TraS localizes to the inner membrane whereas TraT functions in the outer membrane (3). Although the IncF and IncH plasmids encode two Eex proteins, the majority of the characterized conjugative elements encode only one Eex protein (Chapter 4). Moreover, available localization data from this class of conjugative elements indicate that the solitary Eex protein localize to the inner membrane (80, 130).

Eex studies on the IncP plasmid and ICEs SXT and R391 have determined that donor cells do not require a functional Eex protein to elicit exclusion from recipients harbouring isogenic conjugative elements (80, 130). Conversely, the R27 exclusion protein TrhZ is required in donor cells to mediate an exclusion event with recipients expressing either TrhZ or EexH. Minimal exclusion levels were observed when donor cells harbouring R27 *eexH* were mated with recipient cells expressing TrhZ (Figure 5-3). Although EexH and TrhZ can mediate entry exclusion independently in recipient cells, the Eex mutational studies indicate a dynamic interplay between the R27 exclusion proteins. These mutational studies also may explain the significant discrepancy in the exclusion indices (EI) levels elicited by TrhZ and EexH; the TrhZ and the entire Z operon mediate an EI level of ~3000 whereas EexH and TrhO-ORF017 elicit an EI of >10,000. These data suggest that the presence of TrhZ localized to the inner membrane represses the extreme EI levels exhibited by EexH found in the outer membrane.

The mechanistic details of the entry exclusion event have not yet been determined. Characterization of the F plasmid surface exclusion protein TraT has revealed that this outer membrane-associated protein destabilizes mating aggregates (2). There are now three studies on the inner-membrane associated exclusion proteins from IncF, IncP, and ICEs that have demonstrated an interaction with Mpf proteins of the donor cell (8, 80, 130). How this interaction translates into an exclusion event is not clear. An analogy between the action of inner membrane Eex proteins and the T4 phage protein Imm has been suggested (130). This inner membrane protein is involved in phage superinfection exclusion by binding a virion protein.

Figure 5-3. A schematic representation of Entry exclusion (Eex) activity mediated by the R27 proteins, TrhZ and EexH. Six mating-pair scenarios are illustrated with the Eex outcome indicated adjacent to the donor and recipient cells. The donor cells harbour either WT R27 plasmid, or R27 containing a mutation in *eexH* (R27:*eexH*) or *trhZ* (R27:*trhZ*). TrhZ is indicated as green boxes, whereas EexH is represented by blue circles, in the inner and outer membrane, respectively.

Donor **Recipient** **EEX** **Donor** **Recipient** **EEX**

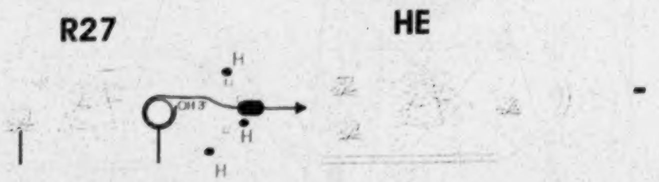
R27
HE
H
H
H
OH 3'
-

WT R27 is not excluded from recipients harbouring empty pMS119EH vector

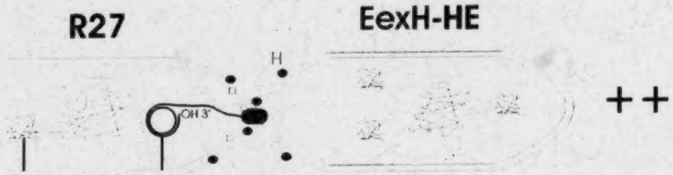
R27
EexH-HE
H
OH 3'
++

EexH is able to elicit an entry exclusion phenotype when mated with donor cells harbouring WT R27

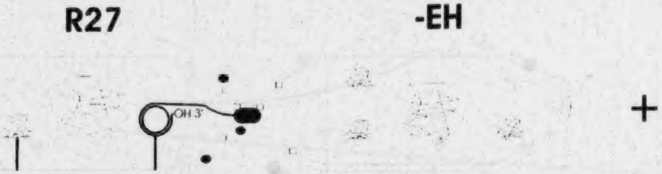

TrhZ is able to elicit an entry exclusion phenotype when mated with donor cells harbouring WT R27

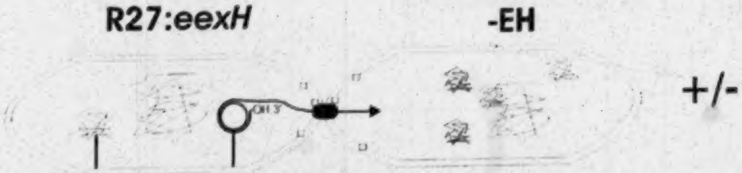
R27:eexH
-EH
OH 3'
+/-

Expression of TrhZ in the absence of EexH in donor and recipient cells is not sufficient to confer WT Eex activity

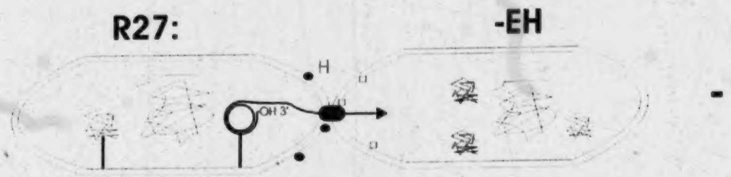

R27 requires TrhZ in the donor cell to mediate exclusion activity, implying that TrhZ may interact with itself

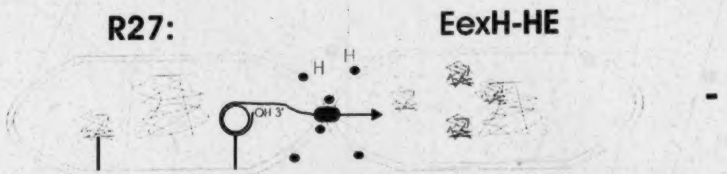
R27:
EexH-HE
H
H
OH 3'
-

Expression of EexH in donor and recipient cells is not sufficient to confer Eex activity. TrhZ is required for R27 exclusion

5.3.1 Future Studies on R27 Eex proteins.

A study of entry exclusion activity of the IncHI1 plasmid R27 showed that exclusion is mediated by TrhZ and EexH which are encoded within the Tra2 region of this conjugative element. The R27 cosmid library which was used to identify the exclusion proteins did not contain ~10 kb of the Tra1 region. Within this Tra1 region there are four ORFs (115, 116, 118 and 121) that are not required for conjugative transfer and have no identifiable homologues, both of which are characteristics of the entry exclusion family of proteins. These four genes should be screened for Eex activity to ensure that the R27 Eex activity is encoded exclusively within the Z operon. Based on existing Eex research in other plasmids, it seems unlikely that R27 encodes more than two Eex proteins.

A second way to ensure that the R27 Eex activity is mediated exclusively by TrhZ and EexH would be to generate an R27 plasmid with mutations in both *trhZ* and *eexH*. If a recipient cell harbouring this R27 double mutant is unable to exclude WT R27 in donor cells, this would provide further evidence that all the R27 exclusion proteins have been identified.

Surprisingly, recipient cells expressing EexH were found to minimally exclude the IncHI2 plasmid R478. This finding provides a perfect opportunity to detect R27 proteins that may interact with the outer membrane-associated EexH protein. A prime candidate would be the stabilization protein TrhG, which was proposed to interact with the ICE exclusion protein (130). If the R478 homologue *trhG* is able to complement a R27 *trhG* mutant, a complementation assay could be performed using recipient cells expressing EexH. As EexH does not appear to interact with components of the R478 conjugative apparatus, the R27 mutant complemented by R478 proteins should not be excluded when the EexH-interacting protein is screened. This assay was used effectively in the characterization of the ICE exclusion proteins (130).

A fascinating interplay seems to exist between TrhZ and EexH, with TrhZ exhibiting a dominant negative effect over EexH. Expression of just TrhZ and EexH within recipient cells would determine if the TrhZ repressive effect is mediated directly. EexH localization studies in the presence of TrhZ may indicate if the presence of the R27 inner membrane Eex protein affects the targeting of EexH to the outer membrane. Finally, a co-immunoprecipitation experiment may confirm that these proteins interact directly which would explain the dynamic exclusion process of the R27 plasmid.

In summary, the work presented in this thesis advances our understanding of the conjugative proteins encoded by the IncH plasmid R27 that mediate or inhibit the exchange of DNA in mating aggregates. An interaction between the R27 coupling protein and an accessory protein may represent evidence that these proteins are descendants of a DNA translocase of the FtsK/SpoIIIE family. Furthermore, essential domains within the R27 coupling protein that facilitate ATP binding and/or hydrolysis, and an interaction with the Mpf complex have been identified through site-specific mutagenesis. The location of the R27 coupling protein within the cell was determined through immunofluorescent microscopic studies. The association of this hexameric protein with random positions in the cell periphery resembled the distribution of R27 Mpf complexes. The R27 determinants that prevent the redundant transfer of IncHI plasmids have been identified and initially characterized. A mechanistic process for the exclusion event has yet to be determined, however studies on the R27 Eex genes *trhZ* and *eexH* should be instrumental in furthering our knowledge of the exclusion phenomenon.

Bibliography

1. **Abrahams, J. P., A. G. Leslie, R. Lutter, and J. E. Walker.** 1994. Structure at 2.8 A resolution of F1-ATPase from bovine heart mitochondria. Nature **370:**621-8.
2. **Achtman, M., N. Kennedy, and R. Skurray.** 1977. Cell--cell interactions in conjugating *Escherichia coli*: role of traT protein in surface exclusion. Proc Natl Acad Sci U S A **74:**5104-8.
3. **Achtman, M., P. A. Manning, C. Edelbluth, and P. Herrlich.** 1979. Export without proteolytic processing of inner and outer membrane proteins encoded by F sex factor tra cistrons in *Escherichia coli* minicells. Proc Natl Acad Sci U S A **76:**4837-41.
4. **Achtman, M., P. A. Manning, B. Kusecek, S. Schwuchow, and N. Willetts.** 1980. A genetic analysis of F sex factor cistrons needed for surface exclusion in *Escherichia coli*. J Mol Biol **138:**779-95.
5. **Alonso, G., Baptista,K, Ngo,T. and Taylor,D.E.** 2005. Transcriptional organization of the temperature-sensitive transfer system from the IncHI1 plasmid R27. Microbiology **151**.
6. **Anderson, E. S., and H. R. Smith.** 1972. Chloramphenicol resistance in the typhoid bacillus. Br Med J **3:**329-31.
7. **Anthony, K. G., P. Kathir, D. Moore, K. Ippen-Ihler, and L. S. Frost.** 1996. Analysis of the traLEKBP sequence and the TraP protein from three F-like plasmids: F, R100-1 and ColB2. J Bacteriol **178:**3194-200.
8. **Anthony, K. G., W. A. Klimke, J. Manchak, and L. S. Frost.** 1999. Comparison of proteins involved in pilus synthesis and mating pair stabilization from the related plasmids F and R100-1: insights into the mechanism of conjugation. J Bacteriol **181:**5149-59.

9. **Arrondo, J. L., I. Echabe, I. Iloro, M. A. Hernando, F. de la Cruz, and F. M. Goni.** 2003. A bacterial TrwC relaxase domain contains a thermally stable alpha-helical core. J Bacteriol **185:**4226-32.

10. **Atmakuri, K., E. Cascales, and P. J. Christie.** 2004. Energetic components VirD4, VirB11 and VirB4 mediate early DNA transfer reactions required for bacterial type IV secretion. Mol Microbiol **54:**1199-211.

11. **Austin, S., and K. Nordstrom.** 1990. Partition-mediated incompatibility of bacterial plasmids. Cell **60:**351-4.

12. **Avery, O. T., C. M. MacLeod, and M. McCarty.** 1949. Studies on the chemical nature of the substance inducing transformation of pneumococcal types. Inductions of transformation by a desoxyribonucleic acid fraction isolated from pneumococcus type III. J Exp Med **149:**297-326.

13. **Bacon, D. J., R. A. Alm, D. H. Burr, L. Hu, D. J. Kopecko, C. P. Ewing, T. J. Trust, and P. Guerry.** 2000. Involvement of a plasmid in virulence of *Campylobacter jejuni* 81-176. Infect Immun **68:**4384-90.

14. **Balzer, D., W. Pansegrau, and E. Lanka.** 1994. Essential motifs of relaxase (TraI) and TraG proteins involved in conjugative transfer of plasmid RP4. J Bacteriol **176:**4285-95.

15. **Bapteste, E., Y. Boucher, J. Leigh, and W. F. Doolittle.** 2004. Phylogenetic reconstruction and lateral gene transfer. Trends Microbiol **12:**406-11.

16. **Bath, J., L. J. Wu, J. Errington, and J. C. Wang.** 2000. Role of *Bacillus subtilis* SpoIIIE in DNA transport across the mother cell-prespore division septum. Science **290:**995-7.

17. **Beranek, A., M. Zettl, K. Lorenzoni, A. Schauer, M. Manhart, and G. Koraimann.** 2004. Thirty-eight C-terminal amino acids of the coupling protein TraD of the F-like conjugative resistance plasmid R1 are required and sufficient

to confer binding to the substrate selector protein TraM. J Bacteriol **186:**6999-7006.

18. **Bolland, S., M. Llosa, P. Avila, and F. de la Cruz.** 1990. General organization of the conjugal transfer genes of the IncW plasmid R388 and interactions between R388 and IncN and IncP plasmids. J Bacteriol **172:**5795-802.

19. **Bordo, D., and P. Argos.** 1991. Suggestions for "safe" residue substitutions in site-directed mutagenesis. J Mol Biol **217:**721-9.

20. **Bradley, D. E., V. M. Hughes, H. Richards, and N. Datta.** 1982. R plasmids of a new incompatibility group determine constitutive production of H pili. Plasmid **7:**230-8.

21. **Bradley, D. E., D. E. Taylor, and D. R. Cohen.** 1980. Specification of surface mating systems among conjugative drug resistance plasmids in *Escherichia coli* K-12. J Bacteriol **143:**1466-70.

22. **Branda, S. S., S. Vik, L. Friedman, and R. Kolter.** 2005. Biofilms: the matrix revisited. Trends Microbiol **13:**20-6.

23. **Burns, D. L.** 2003. Type IV transporters of pathogenic bacteria. Curr Opin Microbiol **6:**29-34.

24. **Burrus, V., and M. K. Waldor.** 2004. Shaping bacterial genomes with integrative and conjugative elements. Res Microbiol **155:**376-86.

25. **Cabezon, E., E. Lanka, and F. de la Cruz.** 1994. Requirements for mobilization of plasmids RSF1010 and ColE1 by the IncW plasmid R388: trwB and RP4 traG are interchangeable. J Bacteriol **176:**4455-8.

26. **Cabezon, E., J. I. Sastre, and F. de la Cruz.** 1997. Genetic evidence of a coupling role for the TraG protein family in bacterial conjugation. Mol Gen Genet **254:**400-6.

27. **Cascales, E., and P. J. Christie.** 2004. Agrobacterium VirB10, an ATP energy sensor required for type IV secretion. Proc Natl Acad Sci U S A **101:**17228-33.

28. **Cascales, E., and P. J. Christie.** 2004. Definition of a bacterial type IV secretion pathway for a DNA substrate. Science **304:**1170-3.

29. **Cascales, E., and P. J. Christie.** 2003. The versatile bacterial type IV secretion systems. Nat Rev Microbiol **1:**137-49.

30. **Censini, S., C. Lange, Z. Xiang, J. E. Crabtree, P. Ghiara, M, Borodovsky, R. Rappuoli, and A. Covacci.** 1996. cag, a pathogenicity island of *Helicobacter pylori*, encodes type I-specific and disease-associated virulence factors. Proc Natl Acad Sci U S A **93:**14648-53.

31. **Chen, I., and D. Dubnau.** 2004. DNA uptake during bacterial transformation. Nat Rev Microbiol **2:**241-9.

32. **Christie, P. J.** 2001. Type IV secretion: intercellular transfer of macromolecules by systems ancestrally related to conjugation machines. Mol Microbiol **40:**294-305.

33. **Christie, P. J.** 2004. Type IV secretion: the Agrobacterium VirB/D4 and related conjugation systems. Biochim Biophys Acta **1694:**219-34.

34. **Christie, P. J., K. Atmakuri, V. Krishnamoorthy, S. Jakubowski, and E. Cascales.** 2005. Biogenesis, architecture, and function of bacterial type iv secretion systems. Annu Rev Microbiol **59:**451-85.

35. **Christie, P. J., and J. P. Vogel.** 2000. Bacterial type IV secretion: conjugation systems adapted to deliver effector molecules to host cells. Trends Microbiol **8:**354-60.

36. **Costerton, J. W., P. S. Stewart, and E. P. Greenberg.** 1999. Bacterial biofilms: a common cause of persistent infections. Science **284:**1318-22.

37. **Crago, A. M., and V. Koronakis.** 1998. Salmonella InvG forms a ring-like multimer that requires the InvH lipoprotein for outer membrane localization. Mol Microbiol **30:**47-56.

38. **Darwin, C.** 1987. Charles Darwin's Notebooks 1836-1844. Cornell University Press, Ithaca.

39. **Das, A., and Y. H. Xie.** 1998. Construction of transposon Tn3phoA: its application in defining the membrane topology of the *Agrobacterium tumefaciens* DNA transfer proteins. Mol Microbiol **27:**405-14.

40. **Datta, N.** 1975. Epidemiology and classification of plasmids, p. 9-15. *In* D. Schlessinger (ed.), Microbiology. American Society of Microbiology, Washington.

41. **Davies, D.** 2003. Understanding biofilm resistance to antibacterial agents. Nat Rev Drug Discov **2:**114-22.

42. **Davies, J.** 1994. Inactivation of antibiotics and the dissemination of resistance genes. Science **264:**375-82.

43. **de la Cruz, F., and J. Davies.** 2000. Horizontal gene transfer and the origin of species: lessons from bacteria. Trends Microbiol **8:**128-33.

44. **De Mot, R., P. Proost, J. Van Damme, and J. Vanderleyden.** 1992. Homology of the root adhesin of *Pseudomonas fluorescens* OE 28.3 with porin F of P. aeruginosa and P. syringae. Mol Gen Genet **231:**489-93.

45. **Dillard, J. P., and H. S. Seifert.** 2001. A variable genetic island specific for *Neisseria gonorrhoeae* is involved in providing DNA for natural transformation and is found more often in disseminated infection isolates. Mol Microbiol **41:**263-77.

46. **Disque-Kochem, C., and B. Dreiseikelmann.** 1997. The cytoplasmic DNA-binding protein TraM binds to the inner membrane protein TraD in vitro. J Bacteriol **179:**6133-7.

47. **Doolittle, R. F.** 2005. Evolutionary aspects of whole-genome biology. Curr Opin Struct Biol **15:**248-53.

48. **Doolittle, R. F.** 2000. Searching for the common ancestor. Res Microbiol **151:**85-9.

49. **Doolittle, W. F., Y. Boucher, C. L. Nesbo, C. J. Douady, J. O. Andersson, and A. J. Roger.** 2003. How big is the iceberg of which organellar genes in nuclear genomes are but the tip? Philos Trans R Soc Lond B Biol Sci **358:**39-57; discussion 57-8.

50. **Dubnau, D.** 1999. DNA uptake in bacteria. Annu Rev Microbiol **53:**217-44.

51. **Durrenberger, M. B., W. Villiger, and T. Bachi.** 1991. Conjugational junctions: morphology of specific contacts in conjugating *Escherichia coli* bacteria. J Struct Biol **107:**146-56.

52. **Errington, J., J. Bath, and L. J. Wu.** 2001. DNA transport in bacteria. Nat Rev Mol Cell Biol **2:**538-45.

53. **Faruque, S. M., M. J. Albert, and J. J. Mekalanos.** 1998. Epidemiology, genetics, and ecology of toxigenic *Vibrio cholerae*. Microbiol Mol Biol Rev **62:**1301-14.

54. **Fekete, R. A., and L. S. Frost.** 2000. Mobilization of chimeric oriT plasmids by F and R100-1: role of relaxosome formation in defining plasmid specificity. J Bacteriol **182:**4022-7.

55. **Fica, A., M. E. Fernandez-Beros, L. Aron-Hott, A. Rivas, K. D'Ottone, J. Chumpitaz, J. M. Guevara, M. Rodriguez, and F. Cabello.** 1997. Antibiotic-resistant *Salmonella typhi* from two outbreaks: few ribotypes and IS200 types harbor Inc HI1 plasmids. Microb Drug Resist **3:**339-43.

56. **Filip, C., G. Fletcher, J. L. Wulff, and C. F. Earhart.** 1973. Solubilization of the cytoplasmic membrane of *Escherichia coli* by the ionic detergent sodium-lauryl sarcosinate. J Bacteriol **115:**717-22.

57. **Forns, N., R. C. Banos, C. Balsalobre, A. Juarez, and C. Madrid.** 2005. Temperature-Dependent Conjugative Transfer of R27: Role of Chromosome- and Plasmid-Encoded Hha and H-NS Proteins. J Bacteriol **187:**3950-9.

58. **Frank, A. C., C. M. Alsmark, M. Thollesson, and S. G. Andersson.** 2005. Functional divergence and horizontal transfer of type IV secretion systems. Mol Biol Evol **22:**1325-36.

59. **Frost, L. S., K. Ippen-Ihler, and R. A. Skurray.** 1994. Analysis of the sequence and gene products of the transfer region of the F sex factor. Microbiol Rev **58:**162-210.

60. **Frost, L. S., R. Leplae, A. O. Summers, and A. Toussaint.** 2005. Mobile genetic elements: the agents of open source evolution. Nat Rev Microbiol **3:**722-32.

61. **Furste, J. P., W. Pansegrau, G. Ziegelin, M. Kroger, and E. Lanka.** 1989. Conjugative transfer of promiscuous IncP plasmids: interaction of plasmid-encoded products with the transfer origin. Proc Natl Acad Sci U S A **86:**1771-5.

62. **Fux, C. A., J. W. Costerton, P. S. Stewart, and P. Stoodley.** 2005. Survival strategies of infectious biofilms. Trends Microbiol **13:**34-40.

63. **Gauthier, A., J. L. Puente, and B. B. Finlay.** 2003. Secretin of the enteropathogenic *Escherichia coli* type III secretion system requires components of the type III apparatus for assembly and localization. Infect Immun **71:**3310-9.

64. **Geisenberger, O., A. Ammendola, B. B. Christensen, S. Molin, K. H. Schleifer, and L. Eberl.** 1999. Monitoring the conjugal transfer of plasmid RP4 in

activated sludge and in situ identification of the transconjugants. FEMS Microbiol Lett **174:**9-17.

65. **Ghigo, J. M.** 2001. Natural conjugative plasmids induce bacterial biofilm development. Nature **412:**442-5.

66. **Gilmour, M. W., J. E. Gunton, T. D. Lawley, and D. E. Taylor.** 2003. Interaction between the IncHI1 plasmid R27 coupling protein and type IV secretion system: TraG associates with the coiled-coil mating pair formation protein TrhB. Mol Microbiol **49:**105-16.

67. **Gilmour, M. W., T. D. Lawley, M. M. Rooker, P. J. Newnham, and D. E. Taylor.** 2001. Cellular location and temperature-dependent assembly of IncHI1 plasmid R27-encoded TrhC-associated conjugative transfer protein complexes. Mol Microbiol **42:**705-15.

68. **Gilmour, M. W., and D. E. Taylor.** 2004. A subassembly of R27-encoded transfer proteins is dependent on TrhC nucleoside triphosphate-binding motifs for function but not formation. J Bacteriol **186:**1606-13.

69. **Gilmour, M. W., N. R. Thomson, M. Sanders, J. Parkhill, and D. E. Taylor.** 2004. The complete nucleotide sequence of the resistance plasmid R478: defining the backbone components of incompatibility group H conjugative plasmids through comparative genomics. Plasmid **52:**182-202.

70. **Gogarten, J. P., and J. P. Townsend.** 2005. Horizontal gene transfer, genome innovation and evolution. Nat Rev Microbiol **3:**679-87.

71. **Gomis-Ruth, F. X., G. Moncalian, F. de la Cruz, and M. Coll.** 2002. Conjugative plasmid protein TrwB, an integral membrane type IV secretion system coupling protein. Detailed structural features and mapping of the active site cleft. J Biol Chem **277:**7556-66.

72. **Gomis-Ruth, F. X., G. Moncalian, R. Perez-Luque, A. Gonzalez, E. Cabezon, F. de la Cruz, and M. Coll.** 2001. The bacterial conjugation protein TrwB resembles ring helicases and F1-ATPase. Nature **409:**637-41.

73. **Gomis-Ruth, F. X., M. Sola, F. de la Cruz, and M. Coll.** 2004. Coupling factors in macromolecular type-IV secretion machineries. Curr Pharm Des **10:**1551-65.

74. **Goodman, S. D., and J. J. Scocca.** 1988. Identification and arrangement of the DNA sequence recognized in specific transformation of *Neisseria gonorrhoeae*. Proc Natl Acad Sci U S A **85:**6982-6.

75. **Grahn, A. M., J. Haase, D. H. Bamford, and E. Lanka.** 2000. Components of the RP4 conjugative transfer apparatus form an envelope structure bridging inner and outer membranes of donor cells: implications for related macromolecule transport systems. J Bacteriol **182:**1564-74.

76. **Grahn, A. M., J. Haase, E. Lanka, and D. H. Bamford.** 1997. Assembly of a functional phage PRD1 receptor depends on 11 genes of the IncP plasmid mating pair formation complex. J Bacteriol **179:**4733-40.

77. **Grohmann, E., G. Muth, and M. Espinosa.** 2003. Conjugative plasmid transfer in gram-positive bacteria. Microbiol Mol Biol Rev **67:**277-301, table of contents.

78. **Gunton, J. E., Gilmour,M.W., Alonso,G., and Taylor, D.E.** 2005. Subcellular localization and functional domains of the coupling protein, TraG, from IncHI1 plasmid R27. Microbiology **151:**3549-3561.

79. **Guzman, L. M., D. Belin, M. J. Carson, and J. Beckwith.** 1995. Tight regulation, modulation, and high-level expression by vectors containing the arabinose PBAD promoter. J Bacteriol **177:**4121-30.

80. **Haase, J., M. Kalkum, and E. Lanka.** 1996. TrbK, a small cytoplasmic membrane lipoprotein, functions in entry exclusion of the IncP alpha plasmid RP4. J Bacteriol **178:**6720-9.

81. **Haase, J., R. Lurz, A. M. Grahn, D. H. Bamford, and E. Lanka.** 1995. Bacterial conjugation mediated by plasmid RP4: RSF1010 mobilization, donor-specific phage propagation, and pilus production require the same Tra2 core components of a proposed DNA transport complex. J Bacteriol **177:**4779-91.

82. **Hacker, J., G. Blum-Oehler, I. Muhldorfer, and H. Tschape.** 1997. Pathogenicity islands of virulent bacteria: structure, function and impact on microbial evolution. Mol Microbiol **23:**1089-97.

83. **Hamilton, C. M., H. Lee, P. L. Li, D. M. Cook, K. R. Piper, S. B. von Bodman, E. Lanka, W. Ream, and S. K. Farrand.** 2000. TraG from RP4 and TraG and VirD4 from Ti plasmids confer relaxosome specificity to the conjugal transfer system of pTiC58. J Bacteriol **182:**1541-8.

84. **Harnett, N., S. McLeod, Y. AuYong, J. Wan, S. Alexander, R. Khakhria, and C. Krishnan.** 1998. Molecular characterization of multiresistant strains of *Salmonella typhi* from South Asia isolated in Ontario, Canada. Can J Microbiol **44:**356-63.

85. **Harris, R. L., V. Hombs, and P. M. Silverman.** 2001. Evidence that F-plasmid proteins TraV, TraK and TraB assemble into an envelope-spanning structure in *Escherichia coli*. Mol Microbiol **42:**757-66.

86. **Hartman, H.** 1984. The origin of the eukaryotic cell. Speculations Sci Technol **7:**77-81.

87. **Hartskeerl, R., P. Overduin, W. Hoekstra, and J. Tommassen.** 1986. Nucleotide sequence of the exclusion-determining locus of IncI plasmid R144. Gene **42:**107-11.

88. **Hartskeerl, R. A., and W. P. Hoekstra.** 1984. Exclusion in IncI-type *Escherichia coli* conjugations: the stage of conjugation at which exclusion operates. Antonie Van Leeuwenhoek **50:**113-24.

89. **Hausner, M., and S. Wuertz.** 1999. High rates of conjugation in bacterial biofilms as determined by quantitative in situ analysis. Appl Environ Microbiol **65:**3710-3.

90. **Heilpern, A. J., and M. K. Waldor.** 2000. CTXphi infection of *Vibrio cholerae* requires the tolQRA gene products. J Bacteriol **182:**1739-47.

91. **Hoffman, L. R., D. A. D'Argenio, M. J. MacCoss, Z. Zhang, R. A. Jones, and S. I. Miller.** 2005. Aminoglycoside antibiotics induce bacterial biofilm formation. Nature **436:**1171-5.

92. **Hofreuter, D., S. Odenbreit, G. Henke, and R. Haas.** 1998. Natural competence for DNA transformation in *Helicobacter pylori*: identification and genetic characterization of the comB locus. Mol Microbiol **28:**1027-38.

93. **Horiike, T., K. Hamada, and T. Shinozawa.** 2002. Origin of eukaryotic cell nuclei by symbiosis of Archaea in Bacteria supported by the newly clarified origin of functional genes. Genes Genet Syst **77:**369-76.

94. **Hormaeche, I., I. Alkorta, F. Moro, J. M. Valpuesta, F. M. Goni, and F. De La Cruz.** 2002. Purification and properties of TrwB, a hexameric, ATP-binding integral membrane protein essential for R388 plasmid conjugation. J Biol Chem **277:**46456-62.

95. **Huber, K. E., and M. K. Waldor.** 2002. Filamentous phage integration requires the host recombinases XerC and XerD. Nature **417:**656-9.

96. **Jakubowski, S. J., V. Krishnamoorthy, E. Cascales, and P. J. Christie.** 2004. *Agrobacterium tumefaciens* VirB6 domains direct the ordered export of a DNA substrate through a type IV secretion System. J Mol Biol **341:**961-77.

97. **Jalajakumari, M. B., A. Guidolin, H. J. Buhk, P. A. Manning, L. M. Ham, A. L. Hodgson, K. C. Cheah, and R. A. Skurray.** 1987. Surface exclusion genes traS

and traT of the F sex factor of *Escherichia coli* K-12. Determination of the nucleotide sequence and promoter and terminator activities. J Mol Biol **198:**1-11.

98. **Jones, P. M., and A. M. George.** 2002. Mechanism of ABC transporters: a molecular dynamics simulation of a well characterized nucleotide-binding subunit. Proc Natl Acad Sci U S A **99:**12639-44.

99. **Judd, P. K., R. B. Kumar, and A. Das.** 2005. The type IV secretion apparatus protein VirB6 of *Agrobacterium tumefaciens* localizes to a cell pole. Mol Microbiol **55:**115-24.

100. **Kado, C. I.** 2000. The role of the T-pilus in horizontal gene transfer and tumorigenesis. Curr Opin Microbiol **3:**643-8.

101. **Karimova, G., J. Pidoux, A. Ullmann, and D. Ladant.** 1998. A bacterial two-hybrid system based on a reconstituted signal transduction pathway. Proc Natl Acad Sci U S A **95:**5752-6.

102. **Kingsman, A., and N. Willetts.** 1978. The requirements for conjugal DNA synthesis in the donor strain during flac transfer. J Mol Biol **122:**287-300.

103. **Kumar, R. B., and A. Das.** 2002. Polar location and functional domains of the *Agrobacterium tumefaciens* DNA transfer protein VirD4. Mol Microbiol **43:**1523-32.

104. **Kumar, S., K. Tamura, and M. Nei.** 2004. MEGA3: Integrated software for Molecular Evolutionary Genetics Analysis and sequence alignment. Brief Bioinform **5:**150-63.

105. **Kurland, C. G.** 2005. What tangled web: barriers to rampant horizontal gene transfer. Bioessays **27:**741-7.

106. **Lanka, E., and B. M. Wilkins.** 1995. DNA processing reactions in bacterial conjugation. Annu Rev Biochem **64:**141-69.

107. **Lawley, T. D.** 2003. The lifecycle of the conjugative plasmid. University of Alberta, Edmonton.

108. **Lawley, T. D., M. W. Gilmour, J. E. Gunton, L. J. Standeven, and D. E. Taylor.** 2002. Functional and mutational analysis of conjugative transfer region 1 (Tra1) from the IncHI1 plasmid R27. J Bacteriol **184:**2173-80.

109. **Lawley, T. D., M. W. Gilmour, J. E. Gunton, D. M. Tracz, and D. E. Taylor.** 2003. Functional and mutational analysis of conjugative transfer region 2 (Tra2) from the IncHI1 plasmid R27. J Bacteriol **185:**581-91.

110. **Lawley, T. D., W. A. Klimke, M. J. Gubbins, and L. S. Frost.** 2003. F factor conjugation is a true type IV secretion system. FEMS Microbiol Lett **224:**1-15.

111. **Lawley, T. D., and D. E. Taylor.** 2003. Characterization of the double-partitioning modules of R27: correlating plasmid stability with plasmid localization. J Bacteriol **185:**3060-7.

112. **Lawley, T. D., Wilkins,B.M., and Frost, L.S.** 2004. Bacterial Conjugation in Gram-Negative Bacteria. *In* B. E. Funnell, and Philips, G. (ed.), The Biology of Plasmids. American Society of Microbiology Press, Washington.

113. **Lawrence, J. G.** 2002. Gene transfer in bacteria: speciation without species? Theor Popul Biol **61:**449-60.

114. **Lederberg, J. a. T., E.L.** 1946. Gene recombination in *Escherichia coli.* Nature **158:**558.

115. **Lederberg, J. L., Lino,T.** 1956. Phase variation in Salmonella. Genetics **41:**743-757.

116. **Lee, M. H., N. Kosuk, J. Bailey, B. Traxler, and C. Manoil.** 1999. Analysis of F factor TraD membrane topology by use of gene fusions and trypsin-sensitive insertions. J Bacteriol **181:**6108-13.

117. **Lee, S. J., M. C. Gray, L. Guo, P. Sebo, and E. L. Hewlett.** 1999. Epitope mapping of monoclonal antibodies against *Bordetella pertussis* adenylate cyclase toxin. Infect Immun **67:**2090-5.

118. **Lessl, M., D. Balzer, K. Weyrauch, and E. Lanka.** 1993. The mating pair formation system of plasmid RP4 defined by RSF1010 mobilization and donor-specific phage propagation. J Bacteriol **175:**6415-25.

119. **Li, P. L., I. Hwang, H. Miyagi, H. True, and S. K. Farrand.** 1999. Essential components of the Ti plasmid trb system, a type IV macromolecular transporter. J Bacteriol **181:**5033-41.

120. **Liberek, K., C. Georgopoulos, and M. Zylicz.** 1988. Role of the *Escherichia coli* DnaK and DnaJ heat shock proteins in the initiation of bacteriophage lambda DNA replication. Proc Natl Acad Sci U S A **85:**6632-6.

121. **Llosa, M., S. Bolland, and F. de la Cruz.** 1994. Genetic organization of the conjugal DNA processing region of the IncW plasmid R388. J Mol Biol **235:**448-64.

122. **Llosa, M., and F. de la Cruz.** 2005. Bacterial conjugation: a potential tool for genomic engineering. Res Microbiol **156:**1-6.

123. **Llosa, M., F. X. Gomis-Ruth, M. Coll, and F. de la Cruz Fd.** 2002. Bacterial conjugation: a two-step mechanism for DNA transport. Mol Microbiol **45:**1-8.

124. **Llosa, M., S. Zunzunegui, and F. de la Cruz.** 2003. Conjugative coupling proteins interact with cognate and heterologous VirB10-like proteins while exhibiting specificity for cognate relaxosomes. Proc Natl Acad Sci U S A **100:**10465-70.

125. **Lorenz, M. G., and W. Wackernagel.** 1994. Bacterial gene transfer by natural genetic transformation in the environment. Microbiol Rev **58:**563-602.

126. **Maher, D., R. Sherburne, and D. E. Taylor.** 1991. Bacteriophages for incompatibility group H plasmids: morphological and growth characteristics. Plasmid **26:**141-6.

127. **Maher, D., R. Sherburne, and D. E. Taylor.** 1993. H-pilus assembly kinetics determined by electron microscopy. J Bacteriol **175:**2175-83.

128. **Maneewannakul, K., P. Kathir, S. Endley, D. Moore, J. Manchak, L. Frost, and K. Ippen-Ihler.** 1996. Construction of derivatives of the F plasmid pOX-tra715: characterization of traY and traD mutants that can be complemented in trans. Mol Microbiol **22:**197-205.

129. **Marcotte, E. M., M. Pellegrini, H. L. Ng, D. W. Rice, T. O. Yeates, and D. Eisenberg.** 1999. Detecting protein function and protein-protein interactions from genome sequences. Science **285:**751-3.

130. **Marrero, J., and M. K. Waldor.** 2005. Interactions between inner membrane proteins in donor and recipient cells limit conjugal DNA transfer. Dev Cell **8:**963-70.

131. **Mazel, D., and J. Davies.** 1999. Antibiotic resistance in microbes. Cell Mol Life Sci **56:**742-54.

132. **McLeod, S. M., H. H. Kimsey, B. M. Davis, and M. K. Waldor.** 2005. CTXphi and *Vibrio cholerae*: exploring a newly recognized type of phage-host cell relationship. Mol Microbiol **57:**347-56.

133. **Middleton, R., K. Sjolander, N. Krishnamurthy, J. Foley, and P. Zambryski.** 2005. Predicted hexameric structure of the Agrobacterium VirB4 C terminus suggests VirB4 acts as a docking site during type IV secretion. Proc Natl Acad Sci U S A **102:**1685-90.

134. **Miller, J. H.** 1972. Experiments in molecular genetics. Cold Spring Harbor Laboratory, Cold Spring Harbor, N.Y.

135. **Mira, A., H. Ochman, and N. A. Moran.** 2001. Deletional bias and the evolution of bacterial genomes. Trends Genet **17:**589-96.

136. **Moll, A., P. A. Manning, and K. N. Timmis.** 1980. Plasmid-determined resistance to serum bactericidal activity: a major outer membrane protein, the traT gene product, is responsible for plasmid-specified serum resistance in *Escherichia coli*. Infect Immun **28:**359-67.

137. **Moncalian, G., E. Cabezon, I. Alkorta, M. Valle, F. Moro, J. M. Valpuesta, F. M. Goni, and F. de La Cruz.** 1999. Characterization of ATP and DNA binding activities of TrwB, the coupling protein essential in plasmid R388 conjugation. J Biol Chem **274:**36117-24.

138. **Moncalian, G., and F. de la Cruz.** 2004. DNA binding properties of protein TrwA, a possible structural variant of the Arc repressor superfamily. Biochim Biophys Acta **1701:**15-23.

139. **Mori, H., and K. Ito.** 2001. The Sec protein-translocation pathway. Trends Microbiol **9:**494-500.

140. **Newnham, P. J., and D. E. Taylor.** 1990. Genetic analysis of transfer and incompatibility functions within the IncHI plasmid R27. Plasmid **23:**107-18.

141. **Nikaido, H.** 1994. Isolation of outer membranes. Methods Enzymol **235:**225-34.

142. **Normark, B. H., and S. Normark.** 2002. Evolution and spread of antibiotic resistance. J Intern Med **252:**91-106.

143. **Novick, R. P.** 1969. Extrachromosomal inheritance in bacteria. Bacteriol Rev **33:**210-63.

144. **Novick, R. P.** 1987. Plasmid incompatibility. Microbiol Rev **51:**381-95.

145. **Novick, R. P., R. C. Clowes, S. N. Cohen, R. Curtiss, 3rd, N. Datta, and S. Falkow.** 1976. Uniform nomenclature for bacterial plasmids: a proposal. Bacteriol Rev **40:**168-89.

146. **O'Callaghan, D., C. Cazevieille, A. Allardet-Servent, M. L. Boschiroli, G. Bourg, V. Foulongne, P. Frutos, Y. Kulakov, and M. Ramuz.** 1999. A homologue of the *Agrobacterium tumefaciens* VirB and Bordetella pertussis Ptl type IV secretion systems is essential for intracellular survival of Brucella suis. Mol Microbiol **33:**1210-20.

147. **Ochman, H., J. G. Lawrence, and E. A. Groisman.** 2000. Lateral gene transfer and the nature of bacterial innovation. Nature **405:**299-304.

148. **Ochman, H., and R. K. Selander.** 1984. Evidence for clonal population structure in *Escherichia coli*. Proc Natl Acad Sci U S A **81:**198-201.

149. **Ochman, H., T. S. Whittam, D. A. Caugant, and R. K. Selander.** 1983. Enzyme polymorphism and genetic population structure in *Escherichia coli* and Shigella. J Gen Microbiol **129:**2715-26.

150. **Odenbreit, S., J. Puls, B. Sedlmaier, E. Gerland, W. Fischer, and R. Haas.** 2000. Translocation of *Helicobacter pylori* CagA into gastric epithelial cells by type IV secretion. Science **287:**1497-500.

151. **Okamoto, S., A. Toyoda-Yamamoto, K. Ito, I. Takebe, and Y. Machida.** 1991. Localization and orientation of the VirD4 protein of *Agrobacterium tumefaciens* in the cell membrane. Mol Gen Genet **228:**24-32.

152. **Pansegrau, W., D. Balzer, V. Kruft, R. Lurz, and E. Lanka.** 1990. In vitro assembly of relaxosomes at the transfer origin of plasmid RP4. Proc Natl Acad Sci U S A **87:**6555-9.

153. **Pansegrau, W., E. Lanka, P. T. Barth, D. H. Figurski, D. G. Guiney, D. Haas, D. R. Helinski, H. Schwab, V. A. Stanisich, and C. M. Thomas.** 1994. Complete nucleotide sequence of Birmingham IncP alpha plasmids. Compilation and comparative analysis. J Mol Biol **239:**623-63.

154. **Pansegrau, W., G. Ziegelin, and E. Lanka.** 1990. Covalent association of the traI gene product of plasmid RP4 with the 5'-terminal nucleotide at the relaxation nick site. J Biol Chem **265:**10637-44.

155. **Parkhill, J., G. Dougan, K. D. James, N. R. Thomson, D. Pickard, J. Wain, C. Churcher, K. L. Mungall, S. D. Bentley, M. T. Holden, M. Sebaihia, S. Baker, D. Basham, K. Brooks, T. Chillingworth, P. Connerton, A. Cronin, P. Davis, R. M. Davies, L. Dowd, N. White, J. Farrar, T. Feltwell, N. Hamlin, A. Haque, T. T. Hien, S. Holroyd, K. Jagels, A. Krogh, T. S. Larsen, S. Leather, S. Moule, P. O'Gaora, C. Parry, M. Quail, K. Rutherford, M. Simmonds, J. Skelton, K. Stevens, S. Whitehead, and B. G. Barrell.** 2001. Complete genome sequence of a multiple drug resistant *Salmonella enterica* serovar Typhi CT18. Nature **413:**848-52.

156. **Perumal, N. B., and E. G. Minkley, Jr.** 1984. The product of the F sex factor traT surface exclusion gene is a lipoprotein. J Biol Chem **259:**5357-60.

157. **Pohlman, R. F., H. D. Genetti, and S. C. Winans.** 1994. Entry exclusion of the IncN plasmid pKM101 is mediated by a single hydrophilic protein containing a lipid attachment motif. Plasmid **31:**158-65.

158. **Prasadarao, N. V., C. A. Wass, J. N. Weiser, M. F. Stins, S. H. Huang, and K. S. Kim.** 1996. Outer membrane protein A of *Escherichia coli* contributes to invasion of brain microvascular endothelial cells. Infect Immun **64:**146-53.

159. **Redfield, R. J., A. D. Cameron, Q. Qian, J. Hinds, T. R. Ali, J. S. Kroll, and P. R. Langford.** 2005. A novel CRP-dependent regulon controls expression of competence genes in *Haemophilus influenzae*. J Mol Biol **347:**735-47.

160. **Redfield, R. J., M. R. Schrag, and A. M. Dean.** 1997. The evolution of bacterial transformation: sex with poor relations. Genetics **146:**27-38.

161. **Reisner, A., J. A. Haagensen, M. A. Schembri, E. L. Zechner, and S. Molin.** 2003. Development and maturation of *Escherichia coli* K-12 biofilms. Mol Microbiol **48:**933-46.

162. **Richaume, A., J. S. Angle, and M. J. Sadowsky.** 1989. Influence of soil variables on in situ plasmid transfer from *Escherichia coli* to Rhizobium fredii. Appl Environ Microbiol **55:**1730-4.

163. **Rochelle, P. A., J. C. Fry, and M. J. Day.** 1989. Factors affecting conjugal transfer of plasmids encoding mercury resistance from pure cultures and mixed natural suspensions of epilithic bacteria. J Gen Microbiol **135:**409-24.

164. **Rooker, M. M., C. Sherburne, T. D. Lawley, and D. E. Taylor.** 1999. Characterization of the Tra2 region of the IncHI1 plasmid R27. Plasmid **41:**226-39.

165. **Sambrook, J., E. F. Fritsch, and T. Maniatis.** 1989. Molecular cloning : a laboratory manual, 2nd ed. Cold Spring Harbor Laboratory Press, Cold Spring Harbor, N.Y.

166. **Samuels, A. L., E. Lanka, and J. E. Davies.** 2000. Conjugative junctions in RP4-mediated mating of *Escherichia coli*. J Bacteriol **182:**2709-15.

167. **Schmiederer, M., and B. Anderson.** 2000. Cloning, sequencing, and expression of three *Bartonella henselae* genes homologous to the Agrobacterium tumefaciens VirB region. DNA Cell Biol **19:**141-7.

168. **Schneider, E., and S. Hunke.** 1998. ATP-binding-cassette (ABC) transport systems: functional and structural aspects of the ATP-hydrolyzing subunits/domains. FEMS Microbiol Rev **22:**1-20.

169. **Schroder, G., S. Krause, E. L. Zechner, B. Traxler, H. J. Yeo, R. Lurz, G. Waksman, and E. Lanka.** 2002. TraG-like proteins of DNA transfer systems and

of the *Helicobacter pylori* type IV secretion system: inner membrane gate for exported substrates? J Bacteriol **184:**2767-79.

170. **Schroder, G., and E. Lanka.** 2005. The mating pair formation system of conjugative plasmids-A versatile secretion machinery for transfer of proteins and DNA. Plasmid **54:**1-25.

171. **Schroder, G., and E. Lanka.** 2003. TraG-like proteins of type IV secretion systems: functional dissection of the multiple activities of TraG (RP4) and TrwB (R388). J Bacteriol **185:**4371-81.

172. **Shanahan, P. M., M. V. Jesudason, C. J. Thomson, and S. G. Amyes.** 1998. Molecular analysis of and identification of antibiotic resistance genes in clinical isolates of *Salmonella typhi* from India. J Clin Microbiol **36:**1595-600.

173. **Shanahan, P. M., K. A. Karamat, C. J. Thomson, and S. G. Amyes.** 2000. Characterization of multi-drug resistant *Salmonella typhi* isolated from Pakistan. Epidemiol Infect **124:**9-16.

174. **Sharp, M. D., and K. Pogliano.** 2003. The membrane domain of SpoIIIE is required for membrane fusion during *Bacillus subtilis* sporulation. J Bacteriol **185:**2005-8.

175. **Sherburne, C. K.** 2000. Conjugal and Genetic Analysis of R27. University of Alberta, Edmonton.

176. **Sherburne, C. K., T. D. Lawley, M. W. Gilmour, F. R. Blattner, V. Burland, E. Grotbeck, D. J. Rose, and D. E. Taylor.** 2000. The complete DNA sequence and analysis of R27, a large IncHI plasmid from *Salmonella typhi* that is temperature sensitive for transfer. Nucleic Acids Res **28:**2177-86.

177. **Sisco, K. L., and H. O. Smith.** 1979. Sequence-specific DNA uptake in Haemophilus transformation. Proc Natl Acad Sci U S A **76:**972-6.

178. **Smith, H. R., N. D. Grindley, G. O. Humphreys, and E. S. Anderson.** 1973. Interactions of group H resistance factors with the F factor. J Bacteriol **115:**623-8.

179. **Smith, H. W.** 1974. Letter: Thermosensitive transfer factors in chloramphenicol-resistant strains of *Salmonella typhi*. Lancet **2:**281-2.

180. **Sorensen, S. J., M. Bailey, L. H. Hansen, N. Kroer, and S. Wuertz.** 2005. Studying plasmid horizontal transfer in situ: a critical review. Nat Rev Microbiol **3:**700-10.

181. **Strack, B., M. Lessl, R. Calendar, and E. Lanka.** 1992. A common sequence motif, -E-G-Y-A-T-A-, identified within the primase domains of plasmid-encoded I- and P-type DNA primases and the alpha protein of the *Escherichia coli* satellite phage P4. J Biol Chem **267:**13062-72.

182. **Sukupolvi, S., and C. D. O'Connor.** 1990. TraT lipoprotein, a plasmid-specified mediator of interactions between gram-negative bacteria and their environment. Microbiol Rev **54:**331-41.

183. **Sutherland, I.** 2001. Biofilm exopolysaccharides: a strong and sticky framework. Microbiology **147:**3-9.

184. **Sutherland, I. W.** 2001. The biofilm matrix--an immobilized but dynamic microbial environment. Trends Microbiol **9:**222-7.

185. **Szpirer, C. Y., M. Faelen, and M. Couturier.** 2000. Interaction between the RP4 coupling protein TraG and the pBHR1 mobilization protein Mob. Mol Microbiol **37:**1283-92.

186. **Tato, I., S. Zunzunegui, F. de la Cruz, and E. Cabezon.** 2005. TrwB, the coupling protein involved in DNA transport during bacterial conjugation, is a DNA-dependent ATPase. Proc Natl Acad Sci U S A **102:**8156-61.

187. **Taylor, D. E.** 1983. Transfer-defective and tetracycline-sensitive mutants of the incompatibility group HI plasmid R27 generated by insertion of transposon 7. Plasmid **9:**227-39.

188. **Taylor, D. E., and R. B. Grant.** 1977. Incompatibility and surface exclusion properties of H1 and H2 plasmids. J Bacteriol **131:**174-8.

189. **Taylor, D. E., and J. G. Levine.** 1980. Studies of temperature-sensitive transfer and maintenance of H incompatibility group plasmids. J Gen Microbiol **116:**475-84.

190. **Thanassi, D. G.** 2002. Ushers and secretins: channels for the secretion of folded proteins across the bacterial outer membrane. J Mol Microbiol Biotechnol **4:**11-20.

191. **Thanassi, D. G., and S. J. Hultgren.** 2000. Multiple pathways allow protein secretion across the bacterial outer membrane. Curr Opin Cell Biol **12:**420-30.

192. **Thomas, C. M.** 2000. Paradigms of plasmid organization. Mol Microbiol **37:**485-91.

193. **Thomas, C. M., and K. M. Nielsen.** 2005. Mechanisms of, and barriers to, horizontal gene transfer between bacteria. Nat Rev Microbiol **3:**711-21.

194. **Thompson, J. D., D. G. Higgins, and T. J. Gibson.** 1994. CLUSTAL W: improving the sensitivity of progressive multiple sequence alignment through sequence weighting, position-specific gap penalties and weight matrix choice. Nucleic Acids Res **22:**4673-80.

195. **Thorsted, P. B., D. P. Macartney, P. Akhtar, A. S. Haines, N. Ali, P. Davidson, T. Stafford, M. J. Pocklington, W. Pansegrau, B. M. Wilkins, E. Lanka, and C. M. Thomas.** 1998. Complete sequence of the IncPbeta plasmid R751: implications for evolution and organisation of the IncP backbone. J Mol Biol **282:**969-90.

196. **Torsvik, V., J. Goksoyr, and F. L. Daae.** 1990. High diversity in DNA of soil bacteria. Appl Environ Microbiol **56:**782-7.

197. **van Schaik, E. J., C. L. Giltner, G. F. Audette, D. W. Keizer, D. L. Bautista, C. M. Slupsky, B. D. Sykes, and R. T. Irvin.** 2005. DNA binding: a novel function of *Pseudomonas aeruginosa* type IV pili. J Bacteriol **187:**1455-64.

198. **Vogel, J. P., H. L. Andrews, S. K. Wong, and R. R. Isberg.** 1998. Conjugative transfer by the virulence system of *Legionella pneumophila*. Science **279:**873-6.

199. **Wain, J., and C. Kidgell.** 2004. The emergence of multidrug resistance to antimicrobial agents for the treatment of typhoid fever. Trans R Soc Trop Med Hyg **98:**423-30.

200. **Walden, R., B. Reiss, C. Koncz, and J. Schell.** 1997. The impact of Ti-plasmid-derived gene vectors on the study of the mechanism of action of phytohormones. Annu Rev Phytopathol **35:**45-66.

201. **Waldor, M. K., and J. J. Mekalanos.** 1996. Lysogenic conversion by a filamentous phage encoding cholera toxin. Science **272:**1910-4.

202. **Walker, J. E., M. Saraste, M. J. Runswick, and N. J. Gay.** 1982. Distantly related sequences in the alpha- and beta-subunits of ATP synthase, myosin, kinases and other ATP-requiring enzymes and a common nucleotide binding fold. Embo J **1:**945-51.

203. **Wang, L., and J. Lutkenhaus.** 1998. FtsK is an essential cell division protein that is localized to the septum and induced as part of the SOS response. Mol Microbiol **29:**731-40.

204. **Watanabe, T.** 1963. Infective heredity of multiple drug resistance in bacteria. Bacteriol Rev **27:**87-115.

205. **Waters, V. L.** 2001. Conjugation between bacterial and mammalian cells. Nat Genet **29:**375-6.

206. **Waters, V. L.** 1999. Conjugative transfer in the dissemination of beta-lactam and aminoglycoside resistance. Front Biosci **4:**D433-56.

207. **Weinbauer, M. G., and F. Rassoulzadegan.** 2004. Are viruses driving microbial diversification and diversity? Environ Microbiol **6:**1-11.

208. **Weiss, D. S.** 2004. Bacterial cell division and the septal ring. Mol Microbiol **54:**588-97.

209. **Welch, R. A., V. Burland, G. Plunkett, 3rd, P. Redford, P. Roesch, D. Rasko, E. L. Buckles, S. R. Liou, A. Boutin, J. Hackett, D. Stroud, G. F. Mayhew, D. J. Rose, S. Zhou, D. C. Schwartz, N. T. Perna, H. L. Mobley, M. S. Donnenberg, and F. R. Blattner.** 2002. Extensive mosaic structure revealed by the complete genome sequence of uropathogenic *Escherichia coli*. Proc Natl Acad Sci U S A **99:**17020-4.

210. **Welkos, S., M. Schreiber, and H. Baer.** 1974. Identification of Salmonella with the O-1 bacteriophage. Appl Microbiol **28:**618-22.

211. **Whitchurch, C. B., T. Tolker-Nielsen, P. C. Ragas, and J. S. Mattick.** 2002. Extracellular DNA required for bacterial biofilm formation. Science **295:**1487.

212. **Whiteley, M., and D. E. Taylor.** 1983. Identification of DNA homologies among H incompatibility group plasmids by restriction enzyme digestion and Southern transfer hybridization. Antimicrob Agents Chemother **24:**194-200.

213. **Wilhelm, S. W. a. S., C.A.** 1999. Viruses and nutrient cycles in the sea. Bioscience **49:**781-788.

214. **Willetts, N., and R. Skurray.** 1980. The conjugation system of F-like plasmids. Annu Rev Genet **14:**41-76.

215. **Woese, C. R.** 2002. On the evolution of cells. Proc Natl Acad Sci U S A **99:**8742-7.

216. **Woese, C. R., O. Kandler, and M. L. Wheelis.** 1990. Towards a natural system of organisms: proposal for the domains Archaea, Bacteria, and Eucarya. Proc Natl Acad Sci U S A **87:**4576-9.

217. **Wu, L. J., and J. Errington.** 1994. *Bacillus subtilis* spoIIIE protein required for DNA segregation during asymmetric cell division. Science **264:**572-5.

218. **Wu, L. J., P. J. Lewis, R. Allmansberger, P. M. Hauser, and J. Errington.** 1995. A conjugation-like mechanism for prespore chromosome partitioning during sporulation in *Bacillus subtilis.* Genes Dev **9:**1316-26.

219. **Wuertz, S., L. Hendrickx, M. Kuehn, K. Rodenacker, and M. Hausner.** 2001. In situ quantification of gene transfer in biofilms. Methods Enzymol **336:**129-43.

220. **Yamada, Y., M. Yamada, and A. Nakazawa.** 1995. A ColE1-encoded gene directs entry exclusion of the plasmid. J Bacteriol **177:**6064-8.

221. **Yeo, H. J., S. N. Savvides, A. B. Herr, E. Lanka, and G. Waksman.** 2000. Crystal structure of the hexameric traffic ATPase of the *Helicobacter pylori* type IV secretion system. Mol Cell **6:**1461-72.

222. **Yu, D., H. M. Ellis, E. C. Lee, N. A. Jenkins, N. G. Copeland, and D. L. Court.** 2000. An efficient recombination system for chromosome engineering in *Escherichia coli.* Proc Natl Acad Sci U S A **97:**5978-83.

223. **Zechner, E. L., de la Cruz, F., Eisenbrandt, R., Grahn, A.M., Koraimann, G., Lanka, E., Muth, G.,Pansegrau, W., Thomas, C.M., Wilkins, B.M., and Ztayka, M.** 2000. Conjugative-DNA processes, p. 87-174. *In* C. M. Thomas (ed.), The Horizontal Gene Pool. Harwood Academic Publishers, Amsterdam.

224. **Ziegelin, G., W. Pansegrau, R. Lurz, and E. Lanka.** 1992. TraK protein of conjugative plasmid RP4 forms a specialized nucleoprotein complex with the transfer origin. J Biol Chem **267:**17279-86.